

HORIZON EUROPE PROGRAMME – TOPIC HORIZON-CL5-2021-D3-03-05

Wind energy in the natural and social environment

Research and Innovation action (RIA)



wimby
WIND IN MY BACKYARD

WIMBY

Wind in My Backyard: Using holistic modelling tools to advance social awareness and engagement on large wind power installations in the EU

Grant Agreement No. 101083460

Starting date: 1st January 2023 – Duration: 36 months

Deliverable D4.5

Augmented open source highRES-Europe, JRC-EU-TIMES and micro-level model and scenario dataset around social and ecological impacts

DOCUMENT INFORMATION

| | |
|----------------------------|--|
| Deliverable number | D4.5 |
| Deliverable title | Augmented open source highRES-Europe, JRC-EU-TIMES and micro-level model and scenario dataset around social and ecological impacts |
| Work Package | WP4 |
| Deliverable type | R |
| Dissemination level | P |
| Due date | 30.06.2025 (Month 30) |
| Pages | 91 |
| Document version | 4.0 |
| Lead author(s) | James Price, UCL |
| Contributors | Guillermo Valenzuela-Venegas, UiO; Oskar Vågerö, UiO; Marianne Zeyringer, UiO; Meixi Zhang, PSI; Evangelos Panos, PSI; Alena Lohrmann, ETH; Wendy Reyes-Calle, ETH; Ruihong Chen, ETH; |

The WIMBY project has received funding from the European Union’s research and innovation programme Horizon Europe under the grant agreement No. 101083460. This document reflects only the author’s view, and the Commission is not responsible for any use that may be made of the information it contains.



DOCUMENT CHANGE HISTORY

| Version | Date | Author | Description |
|-----------------------------|------------|---|--|
| DRAFT | | | |
| 0.1 | 14.03.2025 | Oskar Vågerö, UiO | Creation |
| 0.2 | 06.06.2025 | James Price, UCL; Guillermo Valenzuela-Venegas, UiO; Oskar Vågerö, UiO | Consolidation of input from contributors |
| FIRST PEER REVIEW | | | |
| 1.0 | 12.06.2025 | Russell McKenna, PSI/ETH | Proofreading and peer review |
| 1.1 | 20.06.2025 | James Price, UCL; Guillermo Valenzuela-Venegas, UiO; Oskar Vågerö, UiO; Marianne Zeyringer, UiO; Meixi Zhang, PSI; Evangelos Panos, PSI; Alena Lohrmann, ETH; Wendy Reyes-Calle, ETH; Ruihong Chen, ETH | Consolidation of input from reviewers |
| SECOND PEER REVIEW | | | |
| 2.0 | 16.06.2025 | Andrea N. Hahmann, DTU | Second peer review |
| 2.1 | 20.06.2025 | James Price, UCL; Guillermo Valenzuela-Venegas, UiO; Oskar Vågerö, UiO; Marianne Zeyringer, UiO; Meixi Zhang, PSI; Evangelos Panos, PSI; Alena Lohrmann, ETH; Wendy Reyes-Calle, ETH; Ruihong Chen, ETH | Consolidation of input from reviewers |
| COORDINATOR APPROVAL | | | |
| 3.0 | 25.06.2025 | Luis Ramirez, UU | Coordinator review |



| | | | |
|-----|------------|---|---|
| 3.1 | 27.06.2025 | James Price, UCL; Guillermo Valenzuela-Venegas, UiO; Oskar Vågerö, UiO; Marianne Zeyringer, UiO; Meixi Zhang, PSI; Evangelos Panos, PSI; Alena Lohrmann, ETH; Wendy Reyes-Calle, ETH; Ruihong Chen, ETH | Consolidation of input from coordinator |
| 3.2 | 27.06.2025 | Luis Ramirez, UU | Coordinator approval |

FINAL VERSION

| | | | |
|-----|------------|------------------------|---|
| 4.0 | 30.06.2025 | Stella Arapoglou (VUB) | Format review, version ready for submission |
|-----|------------|------------------------|---|



SHORT ABSTRACT FOR DISSEMINATION PURPOSES

Abstract

This report describes the development and application of energy systems modelling across multiple spatial scales to generate a set of scenarios which quantitatively assess the system level implications of key local factors that shape wind power siting. At the macro-scale (European continent) this includes the further development, linking and application of two models, JRC-EU-TIMES and highRES-Europe, to assess these implications for Europe's transition to net-zero. This is combined with a local or micro-scale modelling approach which is developed and applied to a case study for the Styria region of Austria, to capture details the former models cannot. Where possible we make a concerted effort to ensure model transparency and result reproducibility. Initial insights from the scenario modelling show that greater prioritisation of social and environmental protections in wind siting can lead to a vastly different role for onshore wind across Europe and systems that are potentially up to nearly 15% more costly in 2050. We demonstrate that the decade 2025-2035 is crucial for scaling up renewable deployment in the electricity supply to help decarbonise the demand and meet the intermediate climate change mitigation targets. Our micro-scale analysis highlights a clear trade-off between land availability and economic efficiency, where greater energy production potential may come at the expense of substantially higher infrastructure investment, depending on the scenario. The intention is that these scenarios are further analysed in WIMBY Deliverable 4.6.



TABLE OF CONTENTS

| | |
|--|-----------|
| EXECUTIVE SUMMARY | 14 |
| 1. INTRODUCTION | 16 |
| 2. THE MODELS | 17 |
| 2.1 highRES-Europe | 17 |
| 2.1.1 Spatial disaggregation..... | 18 |
| 2.1.2 Existing electricity system infrastructure | 19 |
| 2.1.3 Bias-correction | 21 |
| 2.1.4 Solar PV advancements | 23 |
| 2.1.5 Wind energy related employment | 24 |
| 2.1.6 Advancements in transparency and reproducibility | 25 |
| 2.1.7 International interconnection updates..... | 28 |
| 2.2 JRC-EU-TIMES..... | 28 |
| 2.2.1 Granularity in wind technology modelling | 30 |
| 2.2.2 Model extension in PtX conversion sectors | 31 |
| 2.2.3 Improvements in end-use consumer sector modelling | 32 |
| 2.2.4 Comprehensive policy implementation | 33 |
| 2.2.5 Model Transparency and Reproducibility | 35 |
| 2.3 Micro-scale modelling | 35 |
| 2.3.1 Wind farm layout generation | 36 |
| 2.3.2 External grid connection model..... | 41 |
| 3. SCENARIO MODELLING | 42 |
| 3.1 Model linkage | 42 |
| 3.2 Land availability scenarios | 44 |
| 3.2.1 Technical exclusions..... | 45 |
| 3.2.2 Environmental exclusions | 47 |
| 3.2.3 Social exclusions | 50 |
| 3.2.4 Land availability in the spatial scenario combinations | 53 |
| 3.3 Macro-scale scenario development | 54 |
| 3.3.1 Whole energy system scenarios..... | 54 |
| 3.3.1 Additional boundary conditions applied to highRES-Europe | 56 |
| 3.4 Micro-scale scenario development | 57 |
| 4. RESULTS | 59 |
| 4.1 Macro-scale modelling scenario results..... | 59 |
| 4.1.1 JRC-EU-TIMES results serve as boundary conditions for highRES-Europe | 59 |
| 4.1.2 Scenario Variations in energy supply and Power Conversion Sector | 62 |
| 4.1.3 National-level cumulative new wind capacities trajectories and near-term challenges..... | 65 |





















| | | |
|-------------------------|--|-----------|
| 4.1.4 | Cost and design implications for Europe’s electricity system in 2050 | 68 |
| 4.2 | Micro-scale modelling scenario results | 74 |
| 5. | SUMMARY AND CONCLUSIONS..... | 77 |
| 5.1 | Macro-scale | 77 |
| 5.1.1 | The pathway to a carbon-free Europe-wide energy system..... | 77 |
| 5.1.2 | Cost and design implications for Europe’s electricity system in 2050 | 78 |
| 5.2 | Micro-scale..... | 79 |
| REFERENCES | | 81 |
| ANNEX..... | | 88 |



LIST OF PARTNERS

| No | Logo | Name | Short Name | Country |
|----|---|---|------------|----------------|
| 1 |  | VRIJE UNIVERSITEIT BRUSSEL | VUB | Belgium |
| 2 |  | DANMARKS TEKNISKE UNIVERSITET | DTU | Denmark |
| 3 |  | INTERNATIONALES INSTITUT FÜR ANGEWANDTE SYSTEMANALYSE | IIASA | Austria |
| 4 |  | UNIVERSITÄT FÜR BODENKULTUR WIEN | BOKU | Austria |
| 5 |  | UNIVERSITETET I OSLO | UiO | Norway |
| 6 |  | NAZKA MAPPS BVBA | NAZKA | Belgium |
| 7 |  | KELSO INSTITUTE EUROPE GEMEINNÜTZIGE GMBH | KIE | Germany |
| 8 |  | DEEP BLUE SRL | DEEP BLUE | Italy |
| 9 |  | UNIVERSITEIT UTRECHT | UU | Netherlands |
| 10 |  | POLITECNICO DI TORINO | POLITO | Italy |
| 11 |  | UNIVERSITÀ DEGLI STUDI DI PALERMO | UNIPA | Italy |
| 12 |  | APREN-ASSOCIAÇÃO PORTUGUESA DE ENERGIAS RENOVAVEIS | APREN | Portugal |
| 13 |  | MULTICONSULT NORGE AS | MCN | Norway |
| 14 |  | EIDGENOESSISCHE TECHNISCHE HOCHSCHULE ZÜRICH | ETH Zürich | Switzerland |
| 15 |  | PAUL SCHERRER INSTITUT | PSI | Switzerland |
| 16 |  | UNIVERSITY COLLEGE LONDON | UCL | United Kingdom |



ABBREVIATIONS

| Acronym | Description |
|-----------------------|---|
| AEP | Annual Energy Production |
| BECCS | Bioenergy with Carbon Capture and Storage |
| BtL | Biomass-to-Liquids |
| CCS | Carbon Capture and Storage |
| CDDA | Common Database on Designed Areas |
| CLC | Corine Land Cover |
| COPs | Coefficients of Performance |
| DAG | Directed Acyclic Graph |
| DC | Direct Current |
| DEM | Digital Elevation Model |
| EEA | The European Economic Area |
| EED | Energy Efficiency Directive |
| EF | Emission Factor |
| ENTSO-E | European Network of Transmission System Operators for Electricity |
| EPBD | Energy Performance of Buildings Directive |
| ES | Emission Standards |
| ETS | European Trading System |
| ERA5 | ECMWF Reanalysis Version 5 |
| FT | Fischer-Tropsch |
| GA | Genetic Algorithm |
| GEM | Global Energy Monitor |
| GHG | Greenhouse Gases |
| GIS | Geographical Information Systems |
| GWA | Global Wind Atlas |
| highRES-Europe | the high temporal and spatial Resolution Electricity System model |
| IUCN | The International Union for Conservation of Nature |
| LULUCF | Land Use, Land-Use Change and Forestry |
| MCDA | Multi-Criteria Decision Analysis |
| MUSA | MULTi-criteria Satisfaction Analysis |
| NECPs | National Energy and Climate Plans |
| NUTS | Nomenclature of territorial units for statistics |
| OSM | Open Street Map |



| | |
|----------------|---------------------------------------|
| O&G | Oil and Gas |
| O&M | Operation and Maintenance |
| PtX | Power-to-X |
| RED | Renewable Energy Directive |
| StL | Sun-to-Liquids |
| TYNDP | The Ten-Year Network Development Plan |
| WTG | Wind Turbine Generators |

LIST OF FIGURES

Figure 1: Spatial coverage of countries (delineated by different colours) and NUTS2 regions (thin black lines) modelled in highRES-Europe..... 19

Figure 2: Estimated existing capacity by technology in 2050.....21

Figure 3: Difference between the mean ERA5 wind speed (m/s) corrected by GWA ratios and the original ERA5 data at 0.25°×0.25° resolution. The red colour highlights areas where the wind speed from ERA5 is underestimated, and the blue colour indicates where it is overestimated. 23

Figure 4: Simplified Directed Acyclic Graph (DAG) of the highRES-Europe workflow. Each shape represents a rule, with the name listed first. Below the name are the wildcards (scenario variables), if applicable.27

Figure 5: Schematic representation of JRC-EU-TIMES energy system model. 30

Figure 6: Graphic representation of the processes for each type of synthetic fuel. 32

Figure 7: Methodology of the spatial wind farm design and internal grid integration. DEM: digital elevation model [16], CLC: CORINE Land Cover 2018 [21], WS: wind speed data [35] with hourly resolution for a year.....37

Figure 8: Schematic overview of the linkage between the models. 43

Figure 9: Geospatial overview of eligible and excluded land areas for wind power deployment based on technical aspects only. 47

Figure 10: Geospatial overview of eligible areas for wind onshore deployment based on the three environmental scenarios.49

Figure 11: Geospatial overview of eligible areas for wind onshore deployment based on the three social scenarios. 53

Figure 12: Overview of the resulting land availability and how large a share of the total area is available for onshore wind deployment for the nine scenarios..... 54



Figure 13: Feasible areas for wind energy deployment in Styria, Austria, across three land-use scenarios. Figure A represents the location of the Styria region in Austria, Figures B, C, and D show the three scenarios: high-high, med-med, and low-low, respectively. Blue arrows point to the Leibniz district. 58

Figure 14: Feasible areas for wind energy deployment in Leibnitz, Styria, Austria, across three land-use scenarios. Figure A represents the location of the Leibnitz district in Styria, Figures B, C, and D show the three scenarios: high-high, med-med, and low-low, respectively..... 59

Figure 15: Total greenhouse gas emissions in CO₂ equivalent for CLIMM scenario. 60

Figure 16: Electricity consumption for each end-use sector in JRC-EU-TIMES. Min-Max range refers to the difference between the scenario with the minimum and the one with the maximum..... 61

Figure 17: Final energy consumption in the CLIMM scenario for the EU-27+. 62

Figure 18: Changes in the hydrogen and synthetic fuels supply from JRC-EU-TIMES..... 63

Figure 19: Scenario variations of renewable electricity deployment for total Europe deviating from the mean of all scenarios. The black dotted line is the arithmetic mean of the values from all 9 scenarios from JRC-EU-TIMES. 64

Figure 20: (a) Installed wind capacity in 2020 and 2035; (b) cumulative wind capacity installation for 2025; (c) cumulative wind capacity for 2030 on a national European level. The ranking of the countries is based on the largest to smallest of wind capacity for scenario CLIHH. The figures (b) and (c) serve to observe the ranking..... 67

Figure 21: Spatial (NUTS2) distribution of onshore wind capacities for the nine scenarios from highRES-Europe modelling. The colorbar is capped at 15 GW to keep the lower end of the scale visible; some NUTS2 areas have installed capacity in excess of this limit..... 68

Figure 22: Installed electricity system capacities for the low-low (social-environmental) scenario (left) as well as the relative difference for the remaining eight scenarios, compared to the low-low scenario. The upper panel of the figure shows electricity generation technologies while the lower panel shows energy storage. All results from highRES-Europe modelling... 69

Figure 23: Comparison of installed onshore wind power capacity in the high-high scenario from highRES-Europe and 2024 levels, based on data from ENTSO-E [73] and U.K. Department for Energy Security and Net Zero [74]... 70



Figure 24: System-wide annual electricity generation for the low-low scenario (left), as well as the relative difference to the low-low scenario for the remaining eight scenarios (right) from highRES-Europe.....71

Figure 25: Share of annual generation across the 28 modelled countries for the diagonal scenarios of low-low (L-L), medium-medium (M-M) and high-high (H-H) from highRES-Europe modelling.....72

Figure 26: Total annualised system cost increase relative to the low-low scenario for the whole of Europe (all 28 countries modelled in highRES-Europe combined).....73

Figure 27: Spatial distribution of eligible wind farm areas and substation infrastructure under the three land-use scenarios in the selected district. Blue markers represent the location of existing MV/HV substations obtained from OpenStreetMap (OSM) [75]. Green dashed areas indicate regions eligible for wind farm deployment. Red arrows point at specific polygons selected for detailed analysis; each associated with an internal substation (black dot). 74

Figure 28: An illustrative example of the internal grid connection model output. The wind farm boundary is provided as a feasible area from Section 3. The location of wind turbine generators (WTG) is determined by the wind farm layout model described in Section 2.3.1. The figure shows n_{max} = Maximum number of cables that can be connected to the substation, N = Number of WTG, α = Number of sharp cables turning angles along with the percentage increase, I = Total length in meters of all cables in the layout, ϵ = Total estimated internal cabling cost in euros. The legend in the top-right corner indicates the cable cross-sections, OSS = Onshore substation, WTG, and wind farm boundary..... 75

Figure 29: An illustrative example of the external grid connection model output. 76

Figure 30: Geospatial overview of eligible and excluded land areas for offshore wind power deployment based on technical aspects only.....88

Figure 31: Geospatial overview of eligible areas for wind offshore deployment based on the three environmental scenarios.89

Figure 32: Geospatial overview of eligible areas for wind offshore deployment based on the three social scenarios.....89

LIST OF TABLES

Table 1: Employment factors for wind energy related jobs, based on Bucha et al. [23]..... 24



| | |
|---|----|
| Table 2: Simplified representation of policy implementation targeting Greenhouse Gas Emissions..... | 33 |
| Table 3: Simplified representation of policy implementation targeting Energy Supply..... | 34 |
| Table 4: Conductors used in the internal topology design [42], [43], [44], [45]. | 40 |
| Table 5: Weights for wind farm connection cost modelling [49], [50]..... | 41 |
| Table 6: Electricity system boundary conditions for 2050. These boundaries are generated by JRC-EU-TIMES and input to highRES-Europe..... | 43 |
| Table 7: Technical exclusion zones applied throughout all scenarios..... | 45 |
| Table 8: Environmental exclusions applied in each scenario..... | 50 |
| Table 9: Social exclusions applied in each scenario..... | 50 |
| Table 10: The major EU directives included in the CLI scenario..... | 55 |
| Table 11: Scenario name alignment between the two macro-models..... | 55 |
| Table 12: Scenarios considered in micro-level analysis..... | 57 |
| Table 13: Summary of results of the chosen polygon in each scenario..... | 76 |
| Table 14: Major data sources used in the recalibration of the JRC-EU-TIMES model to the 2019 statistics..... | 90 |



EXECUTIVE SUMMARY

This report describes the development and application of energy systems modelling across multiple spatial scales to quantitatively assess the system level implications and trade-offs of the social and environmental factors that shape wind power deployment and its role in Europe's energy system achieving net-zero. At the macro-scale (European continent), this includes the further development, linking, and application of two models, JRC-EU-TIMES and highRES-Europe. Additionally, a micro-scale modelling approach is also developed, linked with highRES-Europe and applied to the Styria region of Austria to capture details that the former models cannot.

To undertake the ambitious objective described above, the modelling draws on and leverages earlier work from WIMBY Work Packages (WPs) 1 and 2, as well as their deliverables produced by DTU, UU, IIASA, BOKU, and ETH. This report also marks the culmination of extensive collaboration between the partners of WIMBY WP4 in developing and linking their models.

The core outputs described in this report are two fold: i) the augmented open source macro energy system models and the newly developed micro scale model and ii) the scenario datasets which capture the implications for the energy system of different levels of prioritisation of the social and environmental dimensions that determine where wind power is sited.

Initial insights from our continental scale modelling demonstrate that the decade 2025–2035 is crucial for scaling up renewable deployment in the electricity supply to help decarbonise the demand and meet the intermediate climate change mitigation targets. In this context, wind has a central role requiring a doubling of its capacity from today. Beyond 2035, wind deployment needs to maintain this momentum and accelerate further to meet the net-zero target, with at least a quadrupling of the installed capacity compared to 2025. We find that greater social and environmental protections can lead to a vastly different role for onshore wind power across Europe and systems that are potentially up to nearly 15% more costly in 2050.

Additionally, our micro-scale analysis highlights a clear trade-off between land availability and economic efficiency, where greater energy production



potential may come at the expense of substantially higher infrastructure investment, depending on the scenario.

The scenario datasets will feed into WIMBY Deliverable 4.6, which will detail synergies, best practice and trade-offs, to enable a more detailed analysis of the trade-offs between key system planning objectives. Furthermore, using the micro-scale modelling results, a multi-criteria decision analysis (MCDA) will be carried out. The spatially explicit results from the macro-scale modelling will also be integrated into the WIMBY interactive map (Deliverable 5.2) to help users understand the outcomes of their particular planning preferences at the continental scale.



1. INTRODUCTION

As of 2022, wind power already supplies almost 14% of Europe's electricity generation [1]. Some countries go well beyond this figure, with, for example, 57% of electricity generation in Denmark [2], 29% in the UK [3], and 27% in Germany [4] coming from wind in 2023. Going forward, given its cost competitiveness and maturity, wind is expected to play a key role in Europe achieving its goal of climate neutrality by enabling the deep decarbonisation of electricity generation. Indeed, the importance of net-zero carbon electricity is only set to grow with the drive to electrify more of the energy system, such as transport and heat.

However, the growth of wind power across Europe faces many challenges, see [5] for a detailed review. Many of these challenges stem from the concerns of local stakeholders regarding the potential impacts of wind development on, for example, landscape aesthetics, human wellbeing (i.e., due to noise or shadow flicker), and wildlife. It is the relative prioritisation amongst stakeholders and policymakers of these local, granular factors, balanced with the national and continent-wide objectives of mitigating climate change in a cost effective and secure manner, that will ultimately determine the role wind will play in helping to deliver net-zero.

One of the primary objectives of WIMBY is to understand the system level implications of these trade-offs by assessing their impact on the integration of wind power across the European energy system. The goal of this report is to respond to this challenge by coupling a set of energy planning models across local (micro) to continental (macro) scales that capture key social and environmental factors that shape wind resource availability. We aim to elaborate the system cost and design trade-offs across these scenarios and quantify the contribution of wind to Europe's net-zero future.

At the macro level we bring together the high spatial and temporal resolution electricity model for Europe (highRES-Europe) and the whole energy system model JRC-EU-TIMES. We frame our analysis using land availability scenarios for wind deployment which reflect a range of potential futures where stakeholder's priorities vary with respect to the social and environmental aspects of wind power. The Geographical Information System (GIS) part of highRES-Europe quantitatively models these land



availability constraints and provides them to JRC-EU-TIMES which optimises the transition of the whole European energy system to net-zero. Boundary conditions for the electricity system in 2050 are then used to constrain highRES-Europe, together with the land availability scenarios, to design spatially detailed net-zero electricity systems. In addition, the land scenarios are also used to set boundary conditions for the micro-scale modelling, which here focuses on a case study for the Austrian region of Styria. Where possible we make a concerted effort to ensure model transparency and result reproducibility.

This report is structured as follows: the next section provides a description of the micro- and macro-scale models and their development undertaken as part of WIMBY. Section 3 describes the scenario modelling approach that we take and the model coupling. Finally, we highlight a selection of results in Section 4 and provide some brief conclusions in Section 5.

2. THE MODELS

In this section we describe the models used in this Deliverable and detail the further augmentations made to them as part of WIMBY. These improvements serve to both facilitate the scenario implementation described in Section 3 as well as improve transparency and reproducibility.

2.1 highRES-Europe

The high spatial and temporal Resolution Electricity System model for Europe (highRES-Europe) is an electricity systems modelling framework specifically designed for modelling high shares of variable renewable electricity generation in Europe [6], [7]. The model simultaneously makes planning decisions, i.e., location and capacity, for a snapshot year and hourly operational decisions within that year, i.e., dispatch, for electricity generation, storage, and transmission, ensuring that supply meets demand at least cost (for a more detailed overview of the model equations, see Supplementary Information in [7]). This optimisation is usually constrained to meet deep decarbonisation objectives such as net-zero. The version of highRES-Europe used in this project models 25 EU countries (excluding Cyprus and Malta) plus Norway, Switzerland, and the UK.



As part of WIMBY, the teams at UCL and UiO have made significant improvements to highRES-Europe (see the base version in [6] for more details). These include the integration of the social and environmental constraints from WIMBY WP1 and WP2, enhancements to the transparency and reproducibility of the framework, and improvements to the model's spatial resolution. These augmentations, detailed in what follows, serve to enable and enhance the delivery of the overall objective of assessing the implications of social and environmental restrictions on the role of wind power in Europe achieving net-zero¹.

2.1.1 Spatial disaggregation

A key aspect of capturing the location specific factors that shape where wind power can be sited and, in turn, their implications on overall system design is being able to model deployment with sufficient spatial granularity. Furthermore, modelling variable renewables like wind and solar at higher spatial detail also helps better represent the variation in weather conditions across a country, thereby capturing whether specific regions offer more preferential conditions for renewables. With this in mind, the one node per country representation of the European electricity system in highRES-Europe [6] has been significantly improved, particularly for onshore/offshore wind and solar PV siting. All other generation, storage and transmission planning remains at the one node per country level.

Following the testing of highRES-Europe at various resolutions and considering the trade-offs between gains in planning fidelity (and the usefulness to stakeholders) and computational expense, we concluded that a good balance is struck by modelling wind and solar deployment at the Nomenclature of Territorial Units for Statistics (NUTS) 2 level.

¹ The enhanced version of the highRES-Europe used in this report is publicly available in: <https://github.com/highRES-model/highRES-Europe-WF/releases/tag/WIMBYD4.5>
<https://github.com/highRES-model/highRES-Europe-GAMS/releases/tag/WIMBYD4.5>.



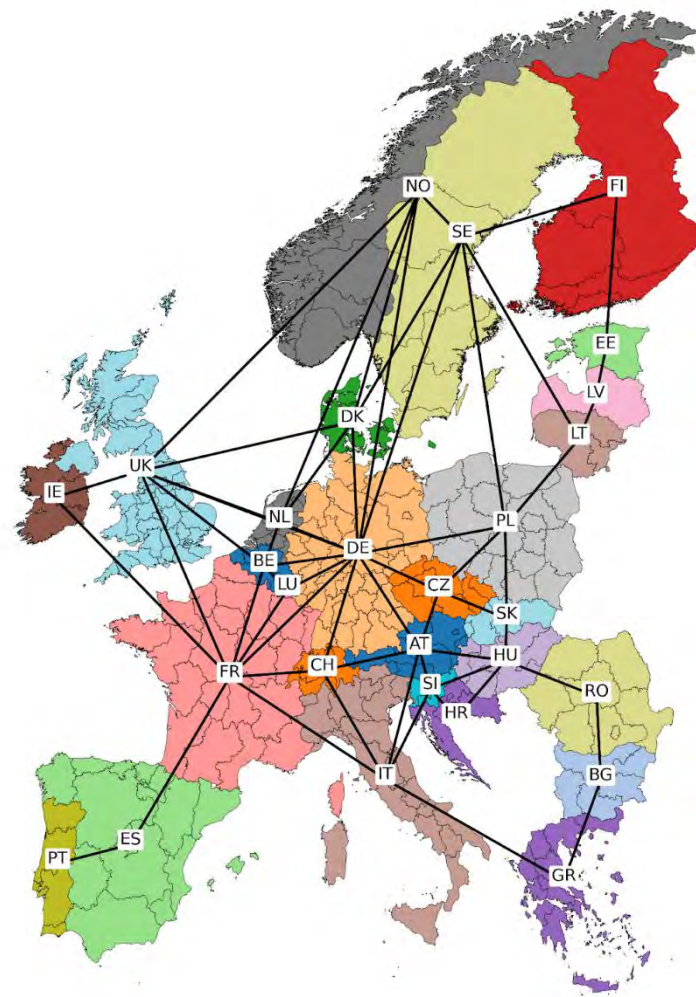


Figure 1: Spatial coverage of countries (delineated by different colours) and NUTS2 regions (thin black lines) modelled in highRES-Europe.

Figure 1 shows the spatial coverage of the European power system modelled in highRES-Europe, complete with the reference transmission network topology taken from ENTSO-E’s Ten Year Network Development plan from 2024 [8]. Subject to land availability, onshore wind and solar PV deployment can take place in any of the ~280 NUTS2 regions shown.

2.1.2 Existing electricity system infrastructure

To enhance the model’s representation of the future electricity system, we implemented improvements that incorporate the existing capacity infrastructure in 2050 for renewable sources at the NUTS2 level and for nuclear at the country level. This approach enables the model to differentiate between existing and new installed capacity when making

investment decisions, resulting in a system configuration more aligned with reality.

We estimate the existing capacity based on the Global Energy Monitor (GEM) [9], [10], [11]: an open-access platform, which provides detailed information on power generation facilities worldwide. This database contains information on onshore wind, offshore wind, solar, and nuclear installations, including project names, operational status, precise locations (latitude and longitude), and commissioning and decommissioning dates.

To determine the existing facilities in 2050, we first extract the power plant data for the 28 European countries included in the model (25 EU countries plus Norway, Switzerland, and the UK). We then apply a projection approach to these entries based on their commissioning dates and expected operational lifetimes. The commissioning date is directly obtained from the provided information in the GEM database. The technology-specific lifetime is defined depending on the technology being considered. For renewable technologies, we set a lifetime of 30 years, while for nuclear infrastructures, we define a lifetime of 41 years based on the 75th percentile of the retired plant lifetime from GEM. Using these values, we estimate the retirement dates for the power plants currently in operation and under construction, as listed in GEM, by adding the expected lifetime to their commissioning dates. Lastly, we filter out all plants projected to retire before 2050.

To aggregate the estimated existing infrastructure to the NUTS2 level, we allocate each plant to its corresponding NUTS2 region by overlaying latitude and longitude coordinates in GEM with the appropriate region. For onshore plants, we directly use the NUTS2 region that coincides with their specific locations, while for offshore plants, we associate the nearest coastal NUTS2 region as their reference area. With this information, we aggregate the filtered capacities by NUTS2 regions, except nuclear capacities, which are aggregated at the country level.

Figure 2 illustrates the spatial distribution of existing capacity projected to remain operational in 2050. Although onshore wind capacity is present throughout Europe, Nordic countries exhibit a higher concentration. Solar capacity is predominantly located in southern regions, with Spain showing the highest concentration. Offshore wind installations are mainly sited in the



North Sea region, whereas nuclear facilities are limited to a few countries, notably Finland, France, Slovakia, and the UK.

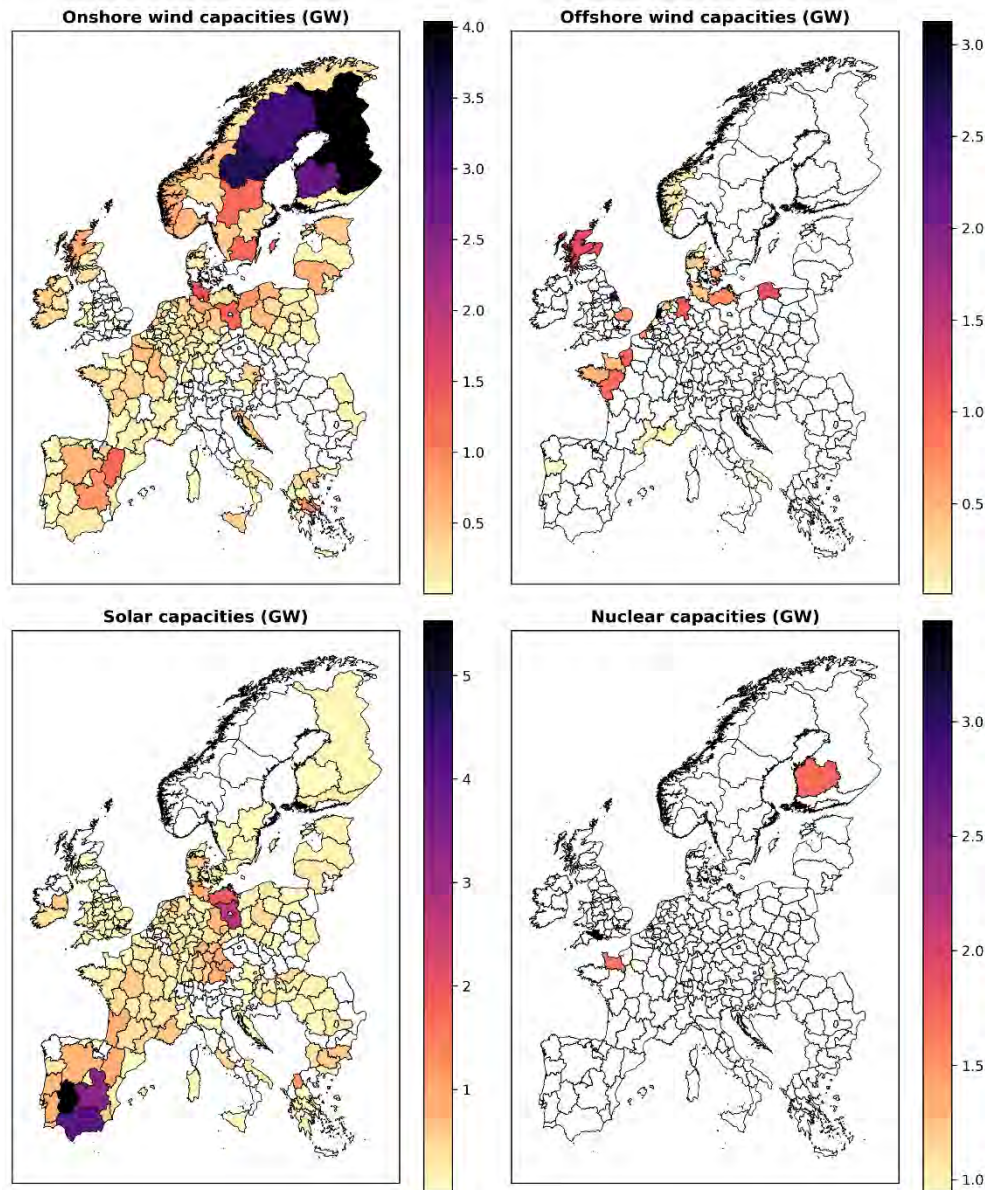


Figure 2: Estimated existing capacity by technology in 2050.

2.1.3 Bias-correction

Accurate representation of wind potential across NUTS2 regions requires a reliable dataset that correctly estimates the wind speeds. For this purpose, highRES-Europe employs ERA5 reanalysis data to calculate the wind potential at the required height of the wind turbines. This dataset provides high-resolution weather data ($0.25^\circ \times 0.25^\circ$, roughly 31 km) [12], such as wind speed at 100 m, amongst others, that are used to calculate the renewable energy potential at the grid cell level, followed by an aggregation step of this data to the corresponding NUTS2 regions.

Although this dataset provides a good representation of the wind speed, it is well known to contain bias in specific areas, particularly in regions with complicated topography [13]. To mitigate this issue, bias-correction ratios derived from WIMBY Deliverable 1.1 are utilised on the ERA5 wind speed data [14]. These ratios were developed by averaging microscale wind speed values from the Global Wind Atlas (GWA) [15] over a $0.025^\circ \times 0.025^\circ$ grid and then dividing them by the corresponding ERA5 values (see Deliverable 1.1 for further details). Then, by applying these ratios, the ERA5 wind speeds are corrected and downscaled to a resolution of $0.025^\circ \times 0.025^\circ$. To ensure consistency with other weather variables used in highRES-Europe, the resulting values are resampled back to the original $0.25^\circ \times 0.25^\circ$ resolution.

Figure 3 shows the differences between the bias-corrected wind speed at 100 m using GWA ratios and the original ERA5 data. Grid cells coloured red highlight where ERA5 underestimates wind speed, while grid cells coloured blue highlight where wind speed is overestimated. The figure reveals that ERA5 tends to underestimate the wind speed throughout most of Europe, with particularly significant underestimations noted in mountainous regions, such as Norway and the Alps [13].



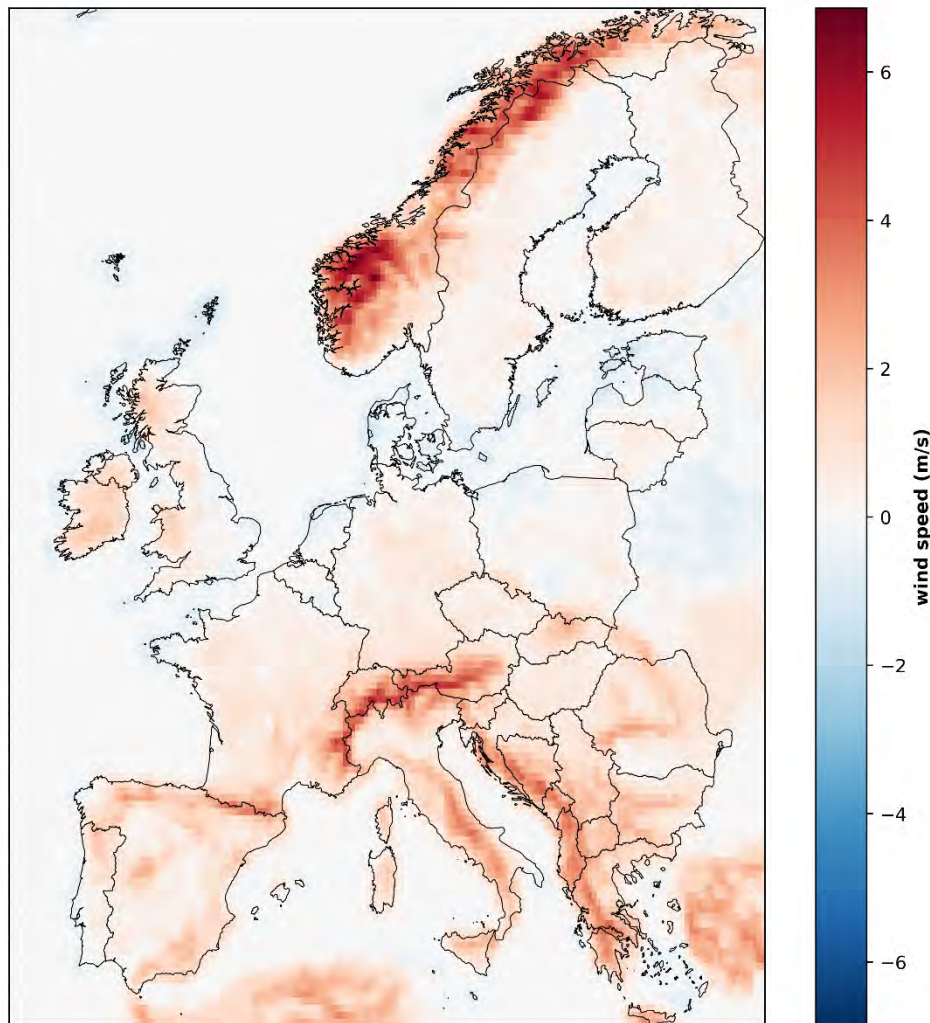


Figure 3: Difference between the mean ERA5 wind speed (m/s) corrected by GWA ratios and the original ERA5 data at 0.25°×0.25° resolution. The red colour highlights areas where the wind speed from ERA5 is underestimated, and the blue colour indicates where it is overestimated.

2.1.4 Solar PV advancements

While not the specific focus of this project and deliverable, solar PV is expected to play a critical role in enabling a net-zero emission European electricity and energy system. As part of WIMBY, we have sought to improve the representation of solar PV in highRES-Europe.

Firstly, similar to wind power, solar PV also faces a range of technical, social, and environmental challenges related to its siting. On the technical side, we implemented a slope restriction using the Copernicus Digital Elevation Model at 90 m resolution [16], thus aligning our elevation model with that used elsewhere in WIMBY. We set the slope restriction such that ground-

mounted solar PV can be built in areas with a slope less than or equal to 11% or 6.3 degrees based on [17].

In terms of environmental protection, we have set ground-mounted solar PV so it is restricted from The International Union for Conservation of Nature (IUCN) category Ia-IV (taken from the Common Database of Designed Areas for Europe from 2023 [18] and for the UK from 2020 [19]) and Natura 2000 areas from 2020 [20]. For the former dataset, the European and UK data years differ because of the UK leaving the EU and ceasing to contribute to the database. This restriction is aligned with the medium level of the environmental restrictions for wind power, as explained later in this deliverable.

For social restrictions, we have utilised the CORINE land cover 2018 [21] dataset at a 100 m resolution to exclude land covered by select urban areas, forests and semi-natural areas, water bodies, and wetlands. To account for concerns regarding food production, we use novel data [22] on agricultural intensity for Europe to restrict deployment from medium and high intensity crops and grasslands.

2.1.5 Wind energy related employment

Although wind energy come with certain negative impacts, motivating the social and environmental exclusions in Section 3.2, it can also have positive effects, such as new employment opportunities both locally and nationally. Part of the work conducted in WIMBY D2.10 [23] included assessing the impact of wind energy deployment on job creation in the wind energy industry. To study this, a job creation model was developed, based on existing literature on the topic. The model considers three types of jobs (direct, indirect, and induced) created from wind power activities in five different stages of its lifespan (development, construction, manufacturing, operation and maintenance (O&M), as well as decommissioning). The resulting employment factors in the different lifecycle stages can be coupled to energy system models, such as highRES-Europe.

Table 1: Employment factors for wind energy related jobs, based on Bucha et al. [23]

| Stage | Direct | Indirect | Induced | Total | Geographical scope of jobs |
|--------------------|--------|----------|---------|-------|----------------------------|
| Development | 0.69 | 0.59 | 0.59 | 1.87 | local / national |

| | | | | | |
|------------------------|----------|------|-------|--|------------------|
| Manufacturing | α | 5.68 | 3.65 | | international |
| Construction | β | 3.08 | 4.16 | | local / national |
| O&M | γ | 9.36 | 12.53 | | local / national |
| Decommissioning | δ | 0.9 | 1.01 | | local / national |

Wind energy related jobs are calculated as a function of the number of projects, and the employment factors are shown in Table 1. The employment factor for direct jobs related to manufacturing, construction, O&M, and decommissioning is a function of the turbine size and whether it is an onshore or offshore turbine.

$$\alpha = 13.37 - 9.5 \cdot OS \quad (1)$$

$$\beta = 9.46 - 3.65 \cdot OS - 4.07 \quad (2)$$

$$\gamma = 19.38 + 0.92 \cdot TC - 15.74 \quad (3)$$

$$\delta = 2.82 - 2.11 \cdot OS \quad (4)$$

Equations 1-4 present the resulting direct employment factors, where OS equals to one for an offshore wind turbine and zero for an onshore wind turbine, and TC represents the turbine capacity in MW.

The number of jobs generated in the wind energy sector is hence derived from turbines of different sizes and scales very poorly when aggregated to a larger geographic area. An increase from 3 MW to 6 MW for an onshore turbine only generates an additional 2.5 job-years (+5%). Energy system model output on capacity deployment is typically presented for a larger geographical region (e.g. NUTS2 or country-level). Applying the values in Table 1 therefore needs to include assumptions on how many wind power plants of a certain size is present in the geographical region. To account for this, we take the same turbine sizes used when generating the capacity factors (for onshore: 3 MW and for offshore: 15 MW) and estimate the number of turbines per NUTS2 region. The wind energy employment estimation is calculated after the model results have been generated and provides additional information on the implications of the results, without being part of the model optimisation.

The resulting wind energy related employment, based on the modelled scenarios described in Section 3 will be presented in deliverable 4.6.

2.1.6 Advancements in transparency and reproducibility



The highRES-Europe modelling framework is open-source and publicly available on GitHub². Although the model itself is available, there have been considerable advancements to the transparency and openness of the model, particularly concerning the workflow for producing the input data required for highRES-Europe. The new and updated preprocessing workflow is now also publicly available³.

The highRES-Europe workflow is built using the workflow management system Snakemake [24], which is based on the programming language Python and is openly available. Building the highRES-Europe workflow with Snakemake comes with a number of benefits in terms of automation, scalability, and portability, making it reproducible.

² <https://github.com/highRES-model/highRES-Europe-GAMS>

³ <https://github.com/highRES-model/highRES-Europe-WF>



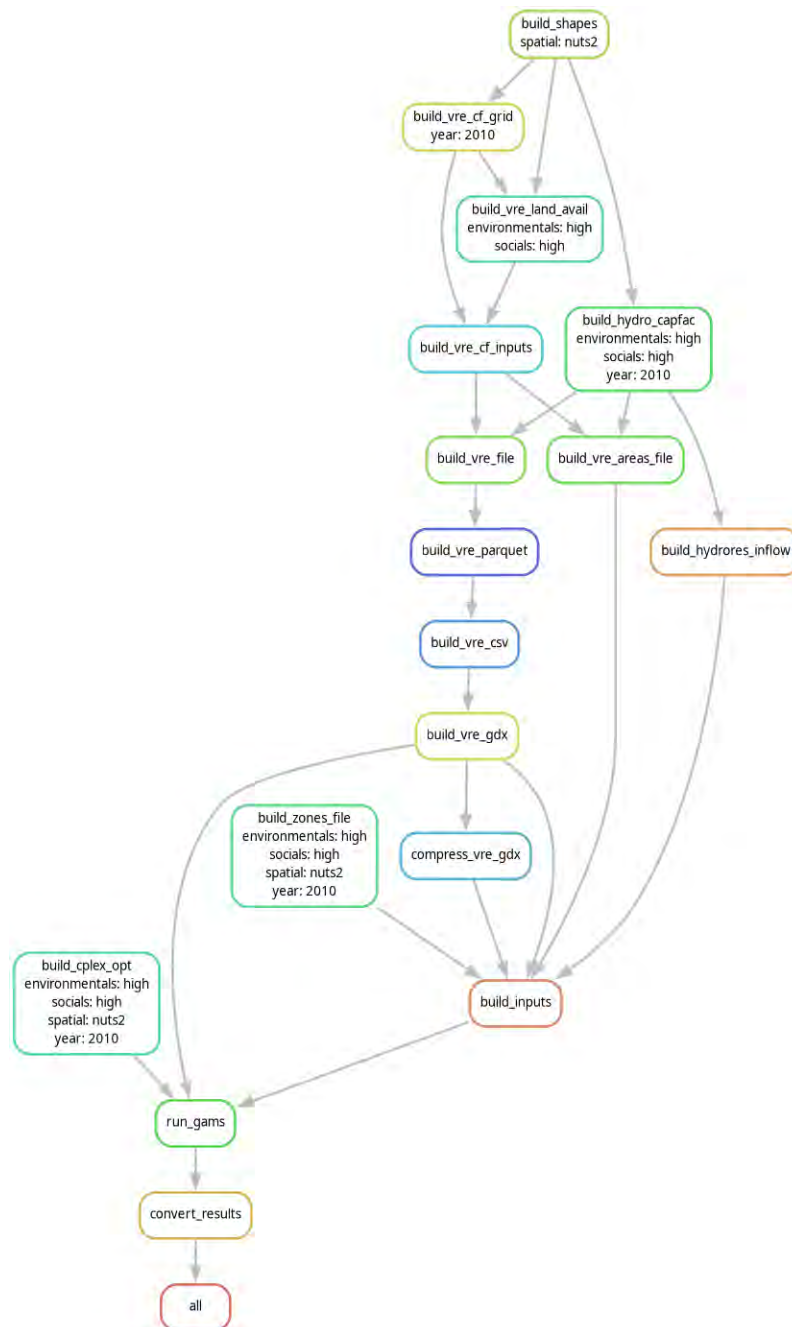


Figure 4: Simplified Directed Acyclic Graph (DAG) of the highRES-Europe workflow. Each shape represents a rule, with the name listed first. Below the name are the wildcards (scenario variables), if applicable.

A Snakemake workflow consists of different rules that typically have inputs, outputs and shell commands or scripts to produce the outputs from the inputs. Rules are connected, and the output of one rule is often the input of another rule. A simplified workflow (single wildcards) is illustrated in Figure 4. The workflow begins with the rule `build_shapes`, which takes some inputs (shapefiles of Europe) and processes them into reduced shapes of the

regions of interest. The reduced processed shapes are then used as input to rule `build_vre_cf_grid`, `build_vre_land_avail` and `build_hydro_capfac`.

Whereas code and data availability are crucial for openness and transparency in modelling, there is a need for readability, traceability, and documentation to fully achieve transparency [24]. Documentation for both the model (highRES-Europe-GAMS) and the workflow (highRES-Europe-WF) is available via a newly created ReadTheDocs⁴.

With access to the model structure and workflow via GitHub, the documentation describing the Snakemake rules and GAMS modules, as well as the data used in the workflow, is available via Zenodo [25], anyone is able to set up and modify the highRES modelling framework, to verify results or conduct their own analysis.

2.1.7 International interconnection updates

The reinforcement of interconnection between European countries is likely to play a key role in enabling a highly renewable energy system. As such, we have updated the reference grid modelled in highRES-Europe based on data from ENTSO-E TYNDP 2024 [8]. Furthermore, we have also included all potential network candidates described in TYNDP 2024 to constrain new network investment in the model. This enhancement ensures that network development in our modelled scenarios is aligned with the best available data on the real-world buildout of the European electricity network.

2.2 JRC-EU-TIMES

JRC-EU-TIMES is a linear optimization bottom-up technology model that minimizes the total energy system cost, including investments in technologies, operational and decommissioning costs of plants, and other costs. Resource potentials for energy extraction/production are, and policy targets can be implemented as constraints. Technologies' learning curves, costs, and basic macroeconomic assumptions serve as inputs to the model. As illustrated in Figure 5, the model, being a multi-sector and multi-carrier energy systems model, encompasses all steps from primary resources to

⁴ <https://highres-europe-wf.readthedocs.io/en/latest/>

end-use consumption, such as transformation, transport, and distribution. It covers all end-use sectors in great detail, by representing 7 industrial sectors, 6 services sectors, residential and services buildings by age and type, and 18 transport modes. Its temporal resolution ranges from daily to annually, with a geographical coverage of all 27 EU countries, Switzerland, Norway, and the United Kingdom. It has a time horizon until 2050 with 5-year time steps. The model output presents a comprehensive view of the European energy system configuration. Its mathematical approach as a linear optimization problem ensures maximum cost-effectiveness of the energy services to satisfy demand, and the emission reduction constraints mitigate negative environmental impact.

Among its unique characteristics are the endogenous trade of energy carriers such as electricity, gas, and hydrogen, the endogenous trade of carbon permits and green certificates, and a DC power flow approximation of the electricity transmission grid in Europe. It also has a detailed representation of other backbone European energy infrastructures, such as storage, pipelines, and terminals. In addition, the model tracks the vintages of energy technologies, including the option for early retirement of existing capacities.



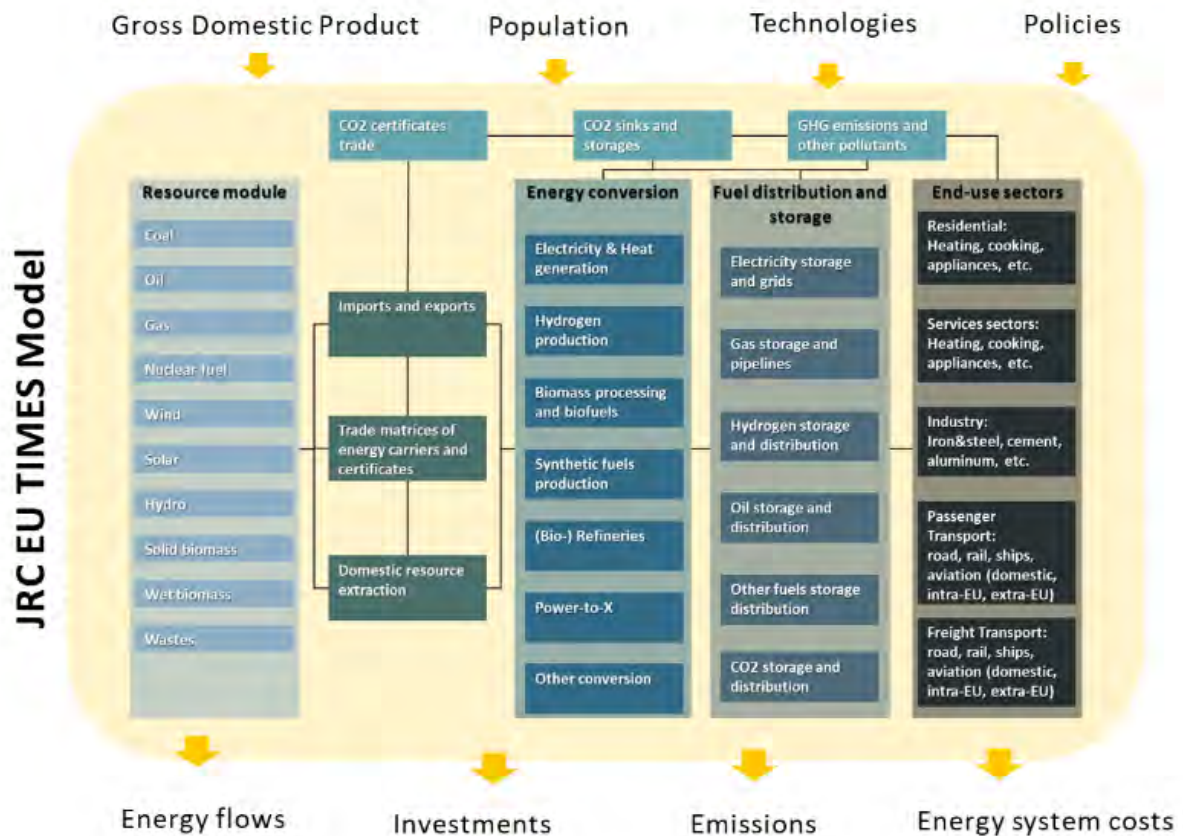


Figure 5: Schematic representation of JRC-EU-TIMES energy system model.

The model has been significantly improved through a thorough re-calibration from base year of 2010 to year 2019 in terms of energy and emissions statistics within the WIMBY project. This process required consolidating data from multiple sources to ensure consistency across sectors and regions. As part of the re-calibration, the model structure was refined to reduce computational complexity—for example, by excluding years prior to 2019 from the optimisation process. The updated version of the model includes 2020 as a milestone year to account for the impacts of the COVID-19 pandemic. While 2024 has been roughly calibrated, full integration of that year was limited due to the unavailability of complete energy and emissions data at the time. A range of major databases was used for this calibration effort, with the most relevant sources summarized in Table 14 in the Annex. All statistical inputs were aligned to reflect 2019 as the new base year for the model.

2.2.1 Granularity in wind technology modelling

Wind turbines have been disaggregated from four types in the previous version of the model into 14 types in the WIMBY version of the model based on more granular categorization of capacity factors. Leveraging the link with

highRES-Europe, and sharing the same techno-economic characterisation of the wind technology, this model development includes onshore wind turbines with capacity factors ranging from 15% to >45%, and offshore wind turbines from 25% to >55%. The representation of more granular capacity factors for wind turbines reflects spatial differentiation of the resource quality and enables a more realistic selection of turbines in scenarios with strong exclusion constraints. The temporal resolution for wind is at a time slice level, with distinctions of day, night and peak times for each typical day (one typical day per season). In this regard, JRC-EU-TIMES retains its aggregated temporal resolution but the availability factors for wind technology are based on the new capacity factors are derived from the spatial analysis performed by highRES-Europe and mapped to the timeslice resolution of JRC-EU-TIMES.

Furthermore, the capacity potentials are updated for each of the newly implemented turbine technologies based on highRES-Europe database, considering in this way the links of WP4 with WP1 and WP2. These new potentials are given as cumulative new capacities allowed to be installed from 2020 to 2050. To ensure that the starting installed capacities align with highRES-Europe assumptions, JRC-EU-TIMES has also adapted the decommissioning profile of existing wind capacities from the highRES-Europe database based on the assumed profile from 2020 to 2050 [9].

2.2.2 Model extension in PtX conversion sectors

With the foreseen penetration of renewable electricity in the energy system [26]. and focus on decarbonizing hard-to-abate end-use consumer sectors (e.g. aviation, industry), the consideration of the conversion sector becomes important. Wind can be considered as one of the candidate renewable technologies for synthetic fuels production [26]. The improved JRC-EU-TIMES incorporates increased granularity in Power-to-X (PtX) technologies, whereby three main low-carbon fuel production pathways were chosen as shown in Figure 6; containing both electrochemical and thermochemical processes [27]; Biomass-to-liquids (BtL), Sun-to-Liquids (StL) [28] and Power-to-Liquids (PtL). More specifically, for BtL, we select vegetable oil as feedstock for either transesterification or hydrotreating. For StL, we select a syngas pathway, produced through a thermochemical reactor using solar heat that is further fed into the Fischer-Tropsch (FT) process. For PtL, syngas produced through hydrogenation of CO₂ using renewable electricity is fed

into the FT synthesis or methanol produced using renewable electricity or steam to be converted and refined further to produce crude oil.

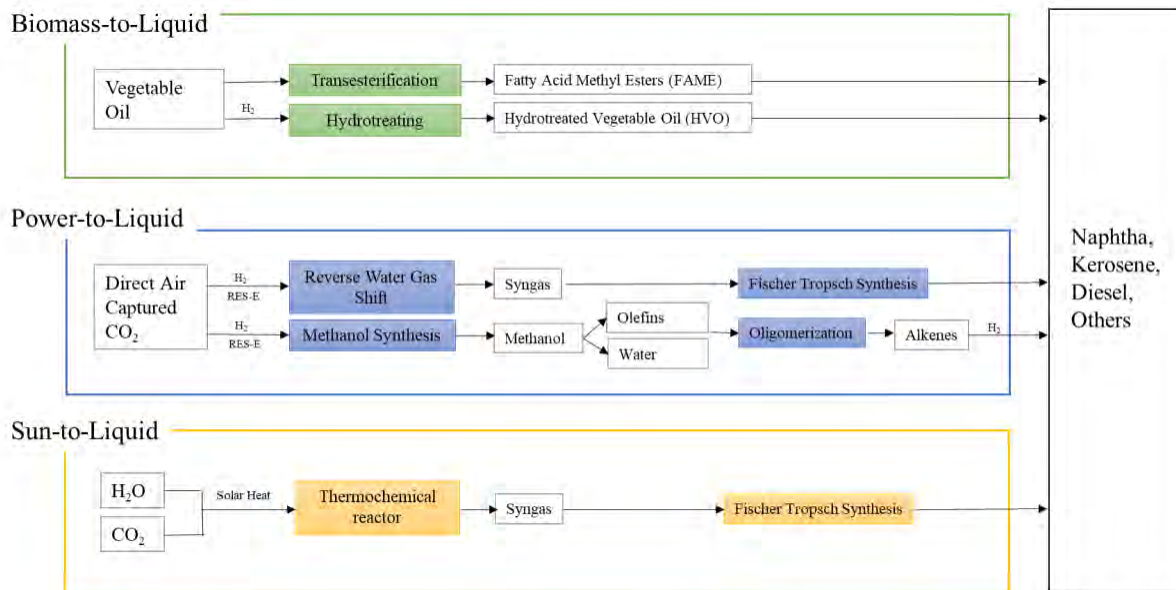


Figure 6: Graphic representation of the processes for each type of synthetic fuel.

The implementation also reflects updated cost assessments and the integration of emerging technologies in electrolysis and e-fuel production. Furthermore, the model now includes endogenous trade of hydrogen (H_2) and PtX energy carriers, allowing for a more dynamic representation of global energy flows. Additionally, the resource potentials for and respective levelized cost of hydrogen and PtX imports from outside the EU have been revised based on the latest data from the PtX Atlas [29], [30], enhancing the reliability of cross-border supply projections.

2.2.3 Improvements in end-use consumer sector modelling

The end-use consumer sectors drive the demand for energy consumption requirements, hence is a crucial factor in projection of the necessity for renewable electricity and the contribution of wind.

The updated model features extensive improvements across all major sectors. In the industry sector, enhancements include detailed material flow tracking, revised metal scrap costs, modelling of iron pellet trade within and beyond Europe, and expanded technology granularity. New options for hydrogen use in process heat and updates in primary and secondary aluminium production pathways are also included, alongside refined cost and potential estimates for CO_2 capture technologies—bringing the total

number of modelled industrial technologies to over 400. In the buildings sector, the model now includes a more granular representation of electrical appliances, a new endogenous building stock evolution submodule, and geographically differentiated coefficients of performance (COPs) for heat pumps. Corrections were also made to address inconsistencies in technology characterizations. For the transport sector, the model reflects a more detailed treatment of aviation technologies based on travel distances and separates demand into national, intra-EU, and extra-EU segments.

2.2.4 Comprehensive policy implementation

JRC-EU-TIMES also takes into consideration the spectrum of current EU directives and regulations on energy and climate. Structural changes were implemented to account for policy instruments such as bans, mandates, standards, and financial support mechanisms embedded in the EU legislation, including the introduction of ETS2 for the buildings and transport sectors. Table 2 includes legislations implemented until 1.1.2024 and are foreseen as pillars of legislation from the EU Green Deal, ReFuel Aviation, and REPower EU Plan (EU2023/435) which would alter the trajectory of the energy system. Though this subsection will not dive into the specificities of the legislation, which can be referred to in the citations, it will shortly elaborate on the method of policy implementations in a bottom-up technology-rich model.

Table 2: Simplified representation of policy implementation targeting Greenhouse Gas Emissions.

| # | Directive | Simplified Representation |
|---|---|--|
| 1 | ETS and ETS2 Directives (EC2003/87 to EU2023/959) | $\sum_{r \in R} ETSCO2_{r,t,s} \leq CAP_s$ |
| 2 | GHG effort sharing (EU2018/842, EU2023/857) until ETS2 is operational | $E_{r,t} - ETSCO2_{r,t,ETS} \leq CAP_{r,t}$ |
| 3 | CO ₂ standards cars (EU2019/631, EU2023/851) | $\sum_{i=1}^n F_{i,t} \cdot EF_i \leq ES_t \cdot V_t$ |
| 4 | CO ₂ standards heavy duty vehicles (EU2019/1242) | $\sum_{i=1}^n F_{i,t} \cdot EF_i \leq ES_t \cdot HV_t$ |

Overarching indices are *r* as region/country, *t* as time/year. Variables *E* stands for the Greenhouse Gas Emissions, *ETSCO2* as CO₂ covered within the ETS, *F* as the consumption of a certain fuel type, *EF* as the emission factor, *ES* as emission standards (in gCO₂/km) and *V* and *HV* as stock of standard

passenger vehicles (in passenger kilometre) and heavy-duty vehicles (in passenger kilometre) respectively.

An example is the vehicles' emissions standards (Eq. 3 and Eq. 4). The emissions of the vehicles are dependent on their fuel efficiencies; thus the constraint cannot be directly on the efficiency as these are hard technical data. Instead of constraining individual vehicles, we apply an overall emission constraint on the whole stock. This approach leaves flexibility for the model to choose the vehicle type so long as it fulfils the overall emission constraint.

Table 3: Simplified representation of policy implementation targeting Energy Supply.

| # | Directive | Simplified Representation |
|---|---|---|
| 1 | EED energy efficiency (EU2023/1791) | $\sum_{s \in S} \sum_{f \in F} F_{r,s,f,t} \leq (1 - R) \cdot \sum_{s \in S} \sum_{f \in F} F_{r,s,f,t-1}$ |
| 2 | EPBD buildings energy performance (EU2018/844) | $\sum_{s \in B} \sum_{f \in F} F_{r,s,f,t} \leq (1 - R) \cdot \sum_{s \in B} \sum_{f \in F} F_{r,s,f,t-1}$ |
| 3 | EU RED III renewable energy (EU2018/2001 & 2023/2413) | $GC_{r,t} \geq p_{r,t} \cdot (E_{r,t} - H_{r,t})$ |
| 4 | Coal phase out | $E_{r,t} = 0$ $\forall r \in DK, FI, EL, HU, IE, IT, NL, PT, SK, ES, \forall t \geq 2030$ $E_{r,t} = 0, \forall r \in DE, SI \forall t \geq 2050$ |

New indices shown in Table 3 are *s* for end-use consumer sectors, *B* for the building sector. *F* represents fuel consumption and *f* for the type of fuel. *GC* states for Green Certificates produced by renewable energy generation. *R* for the reduction factor stipulated by the directives. *p* as the percentage of renewable energy generation demanded by the directive. *E* as renewable electricity generated, and *H* as renewable electricity generated for hydrogen production.

It is worth noting, that in order to ensure that the additionality principle [31] is considered for green hydrogen production, a new parameter is created, serving as a form of certificate (*GC* in Eq. 3) to explicitly account for the renewable portion of heat or electricity production. Such a parameter ensures that when constructing the model constraints for renewable electricity or hydrogen production, they are for direct end-use instead of conversion or transformation purposes.

Finally, the individual countries' emissions mitigation targets and renewable energy targets are collected from the latest National Energy and Climate Plans (NECPs) [32].

The projections for new nuclear power plants planned or under construction follow the national plans declared and collected by the World Nuclear Association [33].

Other major policies implemented in the model include buildings standards, appliances standards, and efficiency directives. We also consider Directives related to the use sustainable fuels in aviation and maritime transport.

2.2.5 Model Transparency and Reproducibility

JRC-EU-TIMES has been an open-source model [34], which is based on the TIMES framework developed within the Energy Technology Systems Analysis Program (ETSAP) by the International Energy Agency (IEA) and extensively used by the EU Commission. The TIMES framework lays a solid foundation for the representation of Europe's energy system.

The input files with the new data for calibration are listed in the Annex Table 14, and changes in model structure can be found in form of dmp.files on *Gitea*. With a valid GAMS/CPLEX license, the dmp.files can be solved by running the command scripts to produce.gdx files. The.gdx files are then processed with a gms. script to output the desired results from the model to be printed on the format of a result template in form of excel sheets. The graphs made uses a python script to further visualizes the results from the excel sheets. For a more detailed and specified description of the model, please refer to the *Gitea* repository⁵.

2.3 Micro-scale modelling

In this section, the development of a micro-scale model of wind farm deployment is detailed. For this analysis, ETH has previously proposed contributing with the existing municipal energy system model, RE³ASON.

⁵ [WIMBY/JRC-EU-TIMES - JRC-EU-TIMES - PSI GIT Service](#)

However, we decided to develop a more comprehensive model that advances the micro-scale analysis with wind farm deployment. This model incorporates an integrated approach for wind farm design and a grid integration model – both developed on a very high spatial resolution. Compared to our new approach, the RE³ASON model has a lower spatial resolution and considerably lower complexity regarding the wind technology development. Moreover, our new approach can be applied to any location of interest. The new approach was tested for the areas identified as feasible for wind farm deployment. The scope of the analysis is oriented toward the technical feasibility of individual wind farm deployment; therefore, the internal and external cable costs are included in the analysis.

The developed micro-scale model includes four stages: i) an optimal wind farm layout is generated for a given area, for which the theoretical annual energy production (AEP) and internal wind farm connection costs are estimated. ii) Dijkstra's algorithm is applied to determine the most cost-effective path to connect the wind farm to the power grid. iii) A multi-criteria decision analysis is conducted to exclude wind turbines with the highest perceived negative impact. iv) AEP and the grid connection costs are recalculated using the remaining wind turbines for the adjusted wind farm layout.

2.3.1 Wind farm layout generation

The wind farm layout model combines spatial wind-oriented random layout generation, wake effect modelling, and multi-objective evolutionary optimisation. The methodology of the layout model, together with the grid connection model, is illustrated in Figure 7. The following sections describe the implementation of the model in more detail.



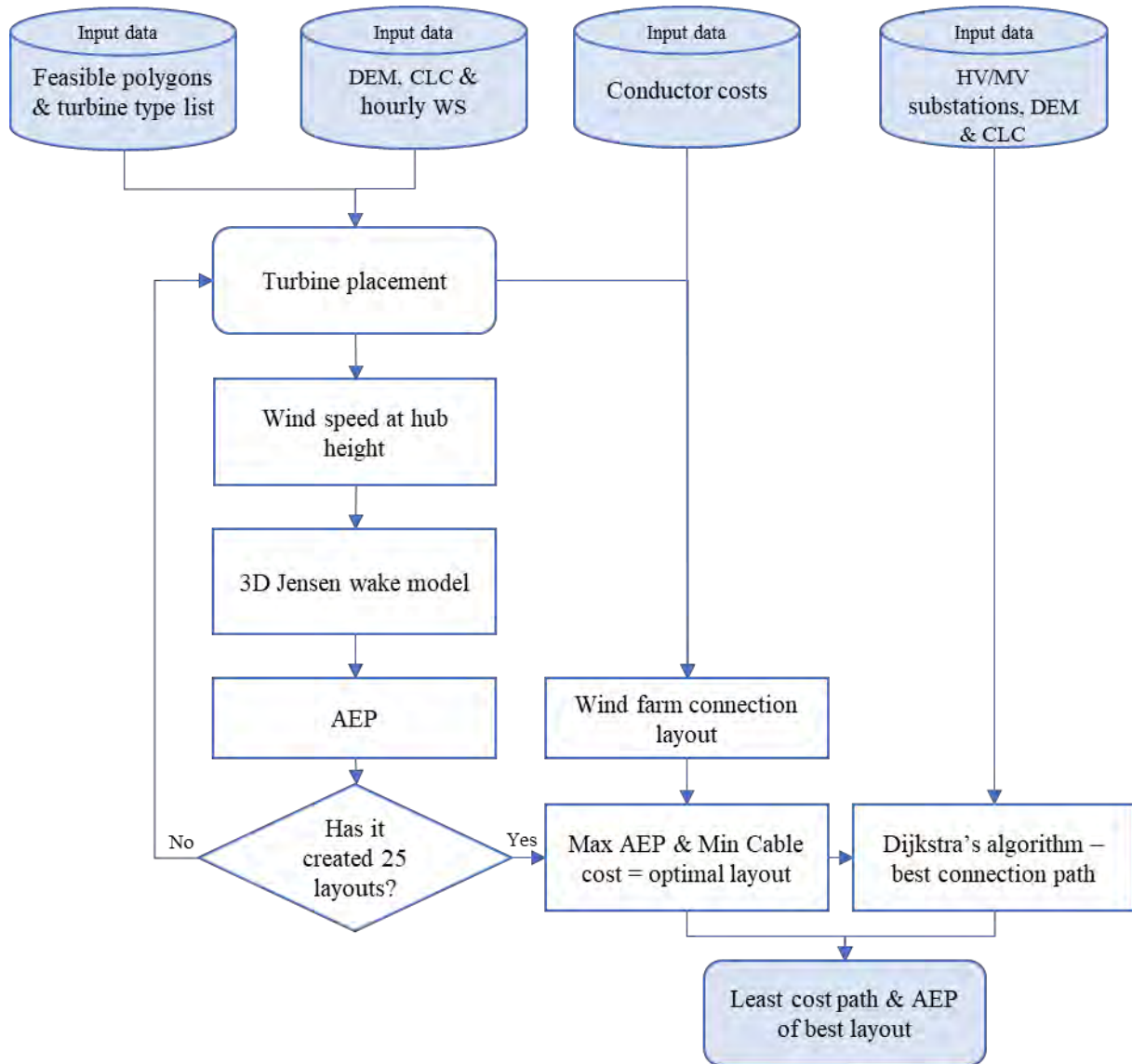


Figure 7: Methodology of the spatial wind farm design and internal grid integration. DEM: digital elevation model [16], CLC: CORINE Land Cover 2018 [21], WS: wind speed data [35] with hourly resolution for a year.

Spatial wind-oriented random layout generation

The initial layout is generated using a wind-oriented heuristic method to generate the initial layout of a wind farm for a given feasible area. After extracting the wind data, the dominant wind direction θ_ω is determined from the site-specific wind rose. The first turbine is positioned upwind in alignment with θ_ω , and the remaining turbines $N_t - 1$ are placed pseudo-randomly while constrained by a minimum spacing criterion as:

$$d_{ij}^{downwind} \geq 4D \text{ and } d_{ij}^{crosswind} \geq 4,$$

where D is the rotor diameter and d_{ij} is the distance between turbines i and j in the respective directions. In this study, a minimum turbine spacing of 4 rotor diameters ($4D$) was adopted based on a balance between spatial constraints and acceptable wake interaction. Although previous optimisation studies [36] suggest that optimal efficiency is typically achieved at larger spacings ($7D$ – $11D$), using a $4D$ minimum reflects common industry practice in land-constrained settings and enables the evaluation of denser layout scenarios and therefore is the value using for our analysis [37], [38].

To ensure suitability for different wind conditions and terrain, the model automatically selects a suitable wind turbine type from a list of 10 turbines with varying power ratings, selected from the Wind Power Dataset [39]. This selection is based on the potential AEP, the required initial investment, and the site’s mean wind speed site \bar{v}_{site} . Each turbine has two potential hub heights, which are selected according to the local elevation of its siting position.

Finally, the extrapolation of the wind speed at hub height $v_i(h_i)$ is calculated using the logarithmic wind profile as:

$$v_i(h_i) = v_{ref} \cdot \frac{\ln\left(\frac{h_k}{z_{0,k}}\right)}{\ln\left(\frac{h_{ref}}{z_{0,k}}\right)},$$

where $z_{0,k}$ is the site-specific surface roughness, and v_{ref} is the wind speed at the reference height h_{ref} .

Wake effect modelling and calculation of AEP

Estimating the wake deficit is crucial in quantifying the reduction in power output caused by the spatial arrangement of wind turbines—a phenomenon known as the wake effect. In complex terrain, variations in elevation can intensify the wake deficit, making precise calculation even more critical. The effective wind speed for each turbine v_{eff_i} is therefore recalculated by accounting for the upstream deficits $\Delta v_{j \rightarrow i}$ caused by other turbines, as demonstrated in the equation below:

$$v_{eff_i} = v_i(h_i) - \sum_{j \in u(i)} \Delta v_{j \rightarrow i},$$

where $u(i)$ is the set of upstream turbines affecting turbine i . Upstream deficits $\Delta v_{j \rightarrow i}$ are calculated using the 3D Jensen wake model, which assumes linear wake expansion and momentum deficit [40]. The Jensen

wake model, known as the park model, is a widely used model for simulating wind turbine wake effects. Initially formulated for flat terrain, it assumes a linearly expanding, top-hat shape wake with uniform velocity deficit inside the wake cone. This has been expanded to complex terrain, in which the wake follows the symmetry of the terrain at a constant height above the ground. This allows the wake to be aligned with the local topography and wind direction.

The velocity $\Delta v_{j \rightarrow i}$ at a point i caused by an upstream turbine j is computed as:

$$\Delta v_{j \rightarrow i} = v_{\infty} \left[\frac{2a_j}{\left(1 + k \cdot \frac{S_{ji}}{R_j}\right)^2} \right],$$

where v_{∞} is the free-stream wind speed, a_j is the axial induction factor of turbine j , S_{ji} is the downwind distance from turbine j to point i , R_j is the rotor radius of turbine j , and k is the wake decay constant, typically ranging from 0.04 to 0.075 [40], dependent on the ambient turbulence intensity. Additionally, when multiple wakes overlap, the total velocity deficit at turbine i is calculated using the quadratic sum of individual deficits.

The resulting values of effective wind speed are used to calculate the total power output at each time step and the AEP as:

$$AEY = \sum_{i=1}^{N_t} \sum_{\theta, v} f(v, \theta) \cdot P_i(v_i^{eff}(\theta)),$$

where $f(v, \theta)$ is the joint probability distribution of wind speed and its direction.

Internal connection costs

To calculate internal cable connection costs, we first compute internal cabling design using EDWIN from the TOPFARM toolkit [41]. The layout is generated using a heuristic algorithm that leverages Delaunay triangulation to form a graph and interactively connect turbines in a tree structure toward a local substation node. The algorithm seeks to minimise the total cost by considering factors such as cable length, type, and size, as well as the number of junctions, turning angles, and substation connections. The substation node is located at the centroid of the polygon, and each edge in

the tree is assigned to a conductor cross-section. The cross-section and prices are adjusted based on values from the literature, as shown in Table 4

The cable cost is calculated using the resulting cable lengths l_{ij} and the corresponding conductor sizes A_{ij} , which are then used for the calculation of internal cabling costs, according to the equation:

$$C_{cable} = \sum l_{ij} \cdot c_{ij}(A_{ij}),$$

where $c_{ij}(A_{ij})$ is the cost function dependent on the conductor cross-section size. An illustrative example is shown in Section 4.2.

Table 4: Conductors used in the internal topology design [42], [43], [44], [45].

| Cross-Section (mm ²) | Material | Rated Current (A) | Resistance (Ω/km) | CAPEX (k€/km) |
|----------------------------------|----------|-------------------|-------------------|---------------|
| 150 | Aluminum | 270 | 0.206 | 133 |
| 240 | Aluminum | 360 | 0.125 | 196 |
| 400 | Aluminum | 490 | 0.078 | 294 |
| 800 | Aluminum | 700 | 0.040 | 490 |
| 1000 | Aluminum | 810 | 0.032 | 560 |

Multi-objective evolutionary optimisation

All the previously mentioned steps are repeated 25 times for each polygon to identify the optimal wind farm layout in this final step, as shown in Figure 7. This number was selected as an upper limit. In most cases, the optimal layout was identified well below the 25th candidate. To determine the optimal wind farm layout, we apply a metaheuristic multi-objective optimisation, which aims to:

- Maximise AEP: $\max f_1 = AEP$
- Minimise internal cable cost: $\min f_2 = C_{cable}$

The multi-objective genetic algorithm (GA) is based on an evolutionary machine learning algorithm, which is implemented in the DEAP library of the Python interface [46]. The result of this stage is the site-specific optimal layout of the wind farm, including its characteristics (exact location, type of wind turbines, specific hub height for each turbine, estimated AEP, total internal cabling costs, and substation location). The following section describes the methodology of the external grid connection of the wind farm.



2.3.2 External grid connection model

We have implemented an innovative algorithm for identifying the shortest path between two points, which, unlike the approach used in WP2, takes into account land cover and terrain constraints. The WP2 model was limited to straight-line connections between points, without considering deviations required by land use or environmental factors, making it less suitable for realistic routing in our context.

A spatially explicit Dijkstra’s algorithm identifies the most cost-effective route between each wind farm centroid and the nearest medium- or high-voltage (MV/HV) substation. The algorithm identifies the least-cost path using weights that reflect the relative constructability and ecological impact. It follows the raster-based cost used in spatial planning, as presented in Table 5. The model incorporates slope and elevation in routing decisions using DEM [16]. Furthermore, the model includes structure (tangent, running angle, angled deadend, and non-angled deadend) costs and voltage-specific conductors adapted from real-world transmission planning guidelines [47], [48].

Table 5: Weights for wind farm connection cost modelling [49], [50].

| Weights | CLC code range | Land Cover Type | Description |
|---------|----------------|-----------------------------------|---|
| 10 | 6 – 10 | Industrial, infrastructure, roads | Low cost if corridors exist |
| 20 | 11 – 15 | Cultivated farmland | Moderate cost for trenching and accessibility |
| 25 | 22 – 25 | Semi-natural areas, grassland | Lower ecological impact |
| 35 | 26 – 29 | Shrubland | Slightly higher ecological impact than grassland |
| 45 | 16 – 21 | Forest | Higher cost due to clearing and restricted access |
| 100 | 30 – 34 | Wetland | High cost due to ecological sensitivity |
| 150 | 1 – 5 | Urban areas | Very expensive due to construction limitations |
| 1000 | 35 – 44 | Water bodies | Considered impassable |

The cable types are dynamically assigned based on power capacity and voltage level. Section 4.2 shows an example of the grid connection model result. As mentioned, the model calculates the connection costs to the

nearest substation from the wind farm centroid. This centroid-based approach improves scalability and reduces computational load, but it also introduces a limitation by oversimplifying the actual spatial layout of the turbines.

3. SCENARIO MODELLING

To understand how the key social and environmental factors that shape wind power deployment at the local level contribute to guiding its role in achieving net-zero across Europe, we have developed a scenario modelling framework. Our approach involves the coupling of the three models described in Section 2 to quantitatively elaborate the implications for the energy system of a set potential futures in which stakeholders express different levels of prioritisation for these factors. In this section we describe how the models are linked, the land availability scenarios which represent wind siting preferences and other details relevant to our scenario modelling.

3.1 Model linkage

At the macro-scale, we bi-directionally couple JRC-EU-TIMES and highRES-Europe. The former model provides insights on the transition of the whole European energy system to net-zero, while highRES-Europe explores the spatially detailed implications for the electricity system in 2050. In addition, the case study for Styria uses three of the land availability scenarios as boundary conditions for its modelling, representing a uni-directional link with highRES-Europe. Figure 8 provides a schematic of the linkage between the three models.

The bi-directional coupling between JRC-EU-TIMES and highRES-Europe involves a number of steps. Firstly, a harmonisation of key input data between the models takes place. The land availability scenarios, covering social, environmental and technical dimensions, are processed by highRES-Europe's GIS code. This computes the land available in km² per ERA5 grid cell (and determines which NUTS2 and country that grid cell is in) for all nine exclusion scenarios, i.e., all permutations of low, medium, and high across the social and environmental dimensions. It also provides annual capacity factors for wind at the grid cell level.



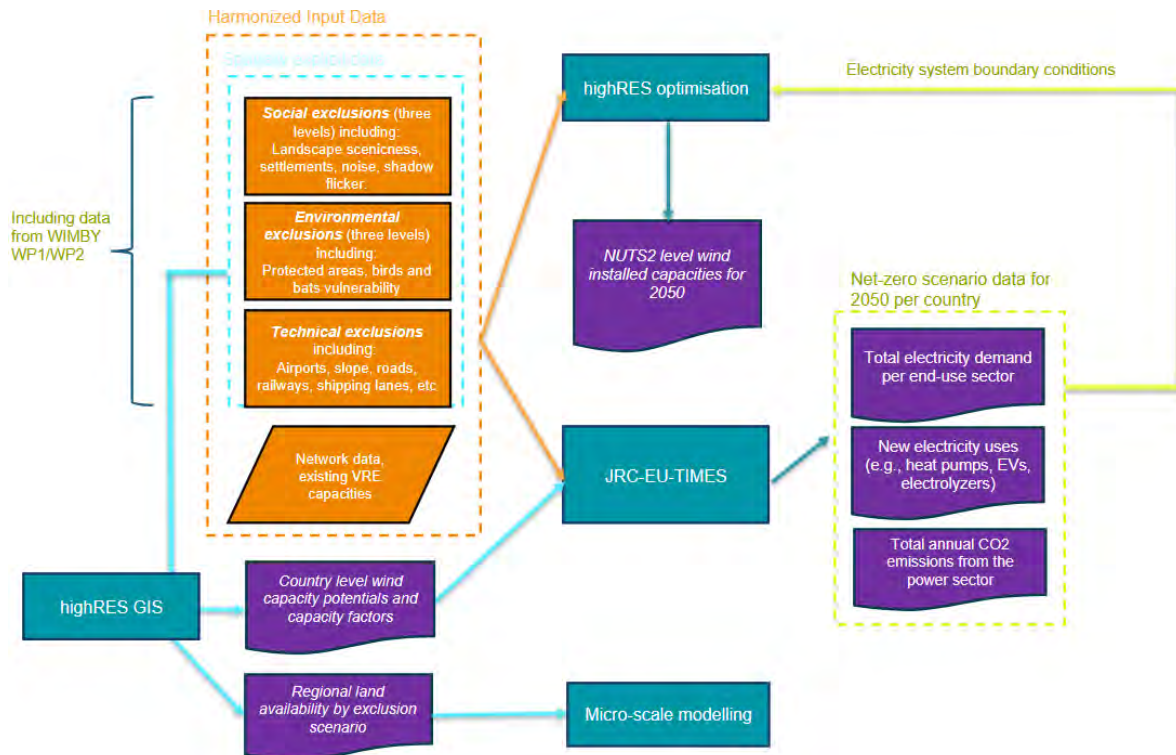


Figure 8: Schematic overview of the linkage between the models.

Secondly, the nine land availability scenarios (detailed in the next subsection) are ingested into JRC-EU-TIMES to act as constraints on onshore and offshore wind deployment at the country level during the transition of the whole energy system. The land area in km² is converted to capacity potentials assuming 3 MW/km² and 5 MW/km² for onshore and offshore, respectively [51]. The annual capacity factors coming from step one are used to harmonise the wind capacity factors in the two models. JRC-EU-TIMES then optimises the transition to net-zero and provides 2050 boundary conditions for highRES-Europe in terms of electricity demands and CO₂ emissions targets. As discussed in the next section, these are similar across the nine scenarios and are shown in Table 6.

Table 6: Electricity system boundary conditions for 2050. These boundaries are generated by JRC-EU-TIMES and input to highRES-Europe.

| Country | Annual electricity demand (TWh) | Annual electricity in 2050 | Annual emissions (kt) | CO ₂ budget |
|---------|---------------------------------|----------------------------|-----------------------|------------------------|
| AT | | 146 | | 0 |
| BE | | 179 | | -133 |
| BG | | 62 | | -5973 |

| | | |
|----|------|--------|
| CH | 83 | -2842 |
| CZ | 134 | -2282 |
| DE | 1151 | -12938 |
| DK | 114 | -2094 |
| EE | 13 | -849 |
| ES | 748 | -19703 |
| FI | 186 | 0 |
| FR | 818 | 0 |
| GR | 139 | -2772 |
| HR | 35 | -637 |
| HU | 92 | -1024 |
| IE | 61 | -2823 |
| IT | 793 | -9121 |
| LT | 23 | -498 |
| LU | 11 | -122 |
| LV | 23 | -563 |
| NL | 453 | -60 |
| NO | 262 | 0 |
| PL | 353 | -8368 |
| PT | 89 | -106 |
| RO | 118 | -4433 |
| SE | 226 | -1496 |
| SI | 24 | -302 |
| SK | 53 | -1298 |
| UK | 819 | 603 |

In the third and final step, highRES-Europe optimises the design and hourly operation of the European electricity system in 2050 for all nine of the exclusion scenarios. It does this subject to country level emissions targets for 2050 and models the need for minimum inertia to meet the maximum rate of change of frequency criteria (0.5 hz/s), as well as representing operating reserve and frequency response requirements (see Ref. [52] for further details). highRES-Europe determines the 2050 least cost spatial deployment pattern of wind and solar PV capacity at the NUTS2 level, together with insights on other generation, storage and network reinforcement at the country level. It also outputs the annualised total system cost, capturing investment in this infrastructure as well as the costs to operate it.

3.2 Land availability scenarios



To capture the implications of different prioritisation of the social and environmental factors shaping wind power deployment on where the technology can be sited, we have developed a set of land availability scenarios based on three broad categories of restrictions or exclusions. These exclusions serve to remove land from potential wind farm development, driven by a multitude of criteria that will be set out below. Two of the three exclusion dimensions, namely social and environmental, are further gradated over three levels, from low through medium to high. These levels can be interpreted as follows:

- Low: represents a permissive scenario where only the bare minimum land is excluded from wind farm development, implying a future where society does not prioritise this dimension.
- Medium: captures a more middle ground future based on central values for the range of each restriction, either internal to WIMBY or from the literature.
- High: represents a case where this dimension is prioritised at a local level and results in a very restrictive case, where the role of, particularly onshore, wind energy is largely diminished in a European context.

3.2.1 Technical exclusions

In addition to the environmental and social exclusions of the model scenarios, there are also technical exclusions that serve as a foundation across all scenario variations. These technical exclusions are closely harmonised with the hard constraints in the WIMBY Interactive Map and are described in WIMBY D2.2 [53]. We present the exclusions in full, below.

Table 7: Technical exclusion zones applied throughout all scenarios

| Category | Description | Buffer | Dataset (incl. code) |
|--------------------------------|----------------------------------|---------|--------------------------------------|
| <i>Onshore only exclusions</i> | | | |
| Hydrology | Exclude water bodies and rivers | 175 m | EU-Hydro River Network Database [54] |
| Airports | Exclude airports | 6,000 m | OSM + D2.10 |
| Slope | Exclude areas with a slope > 15° | None | Copernicus DEM GLO-90 [16] |
| Powerlines | Exclude powerlines | 175 m | OSM + D2.10 |
| Roads | Exclude roads | 175 m | OSM + D2.10 |

| | | | |
|---------------------------------|--|---------|--------------|
| Railways | Exclude railways | 175 m | OSM + D2.10 |
| Radar | Exclude radars | 7,000 m | OSM |
| Glaciers | Exclude glaciers | None | OSM |
| Ports | Exclude ports | 0.1 m | LUISA [55] |
| Onshore and offshore exclusions | | | |
| Military areas | Exclude military zones | 5,000 m | OSM + D2.10 |
| <i>Offshore only exclusions</i> | | | |
| O&G platforms | Exclude oil and gas platforms | 2000 m | [56], [57] |
| O&G pipelines | Exclude oil and gas pipelines | 150 m | |
| Shipping lanes | Exclude medium/heavily trafficked shipping lanes | None | eMODNET [58] |

In Table 7, we list the technical exclusions with their buffer distances and the dataset from which they were acquired. Some exclusions are only relevant for either onshore or offshore wind, whereas some are applicable for both.

The most impactful individual technical exclusion is the hydrology category, which excludes inland water bodies, rivers and canals from the EU-Hydro River Network database [54], including a 175 m (one turbine height) buffer around each polygon. Next is excluding airports from OSM (category: airport). Furthermore, we exclude areas with a slope steeper than 15°, generated from the Copernicus DEM GLO-90 [16]. This value is slightly lower than the lowest value (6 km) in the range provided by Ref. [37]. For the OSM categories of rail, power lines and roads, we use the minimum distance identified from the regulatory analysis in WIMBY D2.10 [23], but with a minimum of one turbine height (175 m). Glaciers (OSM) and ports (based on LUISA [55]) are excluded without any buffer.

The category Military areas from OSM is relevant for both onshore and offshore wind, and we apply a 5 km buffer, which was identified as the minimum regulatory exclusion in WIMBY D2.10 [23].



| Country | area (km ²) | share (%) |
|---------|-------------------------|-----------|
| AT | 34940.4 | 41.6 |
| BE | 13075.0 | 42.6 |
| BG | 66856.4 | 60.2 |
| CH | 8264.9 | 20.0 |
| CZ | 36724.9 | 46.6 |
| DE | 163383.5 | 45.7 |
| DK | 21387.8 | 49.5 |
| EE | 28563.5 | 63.0 |
| ES | 314355.2 | 63.1 |
| FI | 222584.4 | 65.9 |
| FR | 238552.2 | 43.5 |
| GR | 73021.6 | 55.4 |
| HR | 35264.7 | 62.4 |
| HU | 56315.0 | 60.5 |
| IE | 48460.1 | 69.3 |
| IT | 110309.2 | 36.7 |
| LT | 41922.9 | 64.6 |
| LU | 1163.6 | 44.8 |
| LV | 41795.0 | 64.7 |
| NL | 15520.7 | 41.5 |
| NO | 196296.3 | 60.7 |
| PL | 199251.0 | 63.9 |
| PT | 53961.9 | 60.8 |
| RO | 168269.8 | 70.6 |
| SE | 287859.2 | 64.0 |
| SI | 10657.6 | 52.6 |
| SK | 27609.0 | 56.3 |
| UK | 120409.1 | 49.2 |

Figure 9: Geospatial overview of eligible and excluded land areas for wind power deployment based on technical aspects only.

When considering the different layers in Table 7, almost half (44.2%) of the total land area of Europe is excluded, as illustrated in Figure 9.

Additionally, some exclusions are only relevant for offshore, such as oil and gas (O&G) platforms and gas pipelines. The location of O&G infrastructure is sourced from Martins et al. [56], [57], and we apply a 2 km buffer distance from platforms based on Moore et al. [59] and a 150 m buffer from pipelines based on the Netherlands Enterprise Agency [60]. Lastly, we exclude shipping lanes from the eMODNET Human Activities Vessel Density Map [58] for highly trafficked areas (>13.7 ships per day, which corresponds to the high and medium categories in D2.2 [53]). The right part of Figure 9 shows the remaining area and the share of area available for each modelled country.

3.2.2 Environmental exclusions

In terms of environmental restrictions for the deployment of wind power across Europe, we incorporate three main elements.

Firstly, we use the Common Database on Designed Areas (CDDA) for Europe from 2023 and the UK from 2020 to exclude wind deployment in IUCN categorised areas. We align the low and medium levels of this exclusion component with the WIMBY interactive map by excluding IUCN Ia-IV and

extending this to include Ia-VI with a 2000 m buffer at the highest setting. All CDDA data is represented as a 100 m resolution raster in our modelling.

Secondly, we also restrict the Natura 2000 protected sites, which are designated under the Birds and the Habitats Directives [61], [62], in the medium and high levels, with the latter additionally including a 2000 m buffer. The low case does not see these areas restricted to align with the WIMBY interactive map. The Natura 2000 dataset is ingested into our modelling as a 100 m resolution raster.

Thirdly, we leverage the insights on the number of bird and bat species that are vulnerable to collision with wind turbines developed in WIMBY D1.6. For birds, species richness rasters, which depict highly vulnerable and high latent risk, as shown in Figures 10a and b of WIMBY D1.6, are combined to produce a map of the number of bird species deemed highly vulnerable in each 10 km resolution grid cell. For bats, the status of 38 European bat species was obtained from the European Red List of Threatened species [63], with 10 species being classified as threatened (3 as endangered and 7 as vulnerable). Maps of threatened (and therefore vulnerable) species richness were then obtained from occurrence probability layers from Si-Moussi [64] at a 10 km resolution.



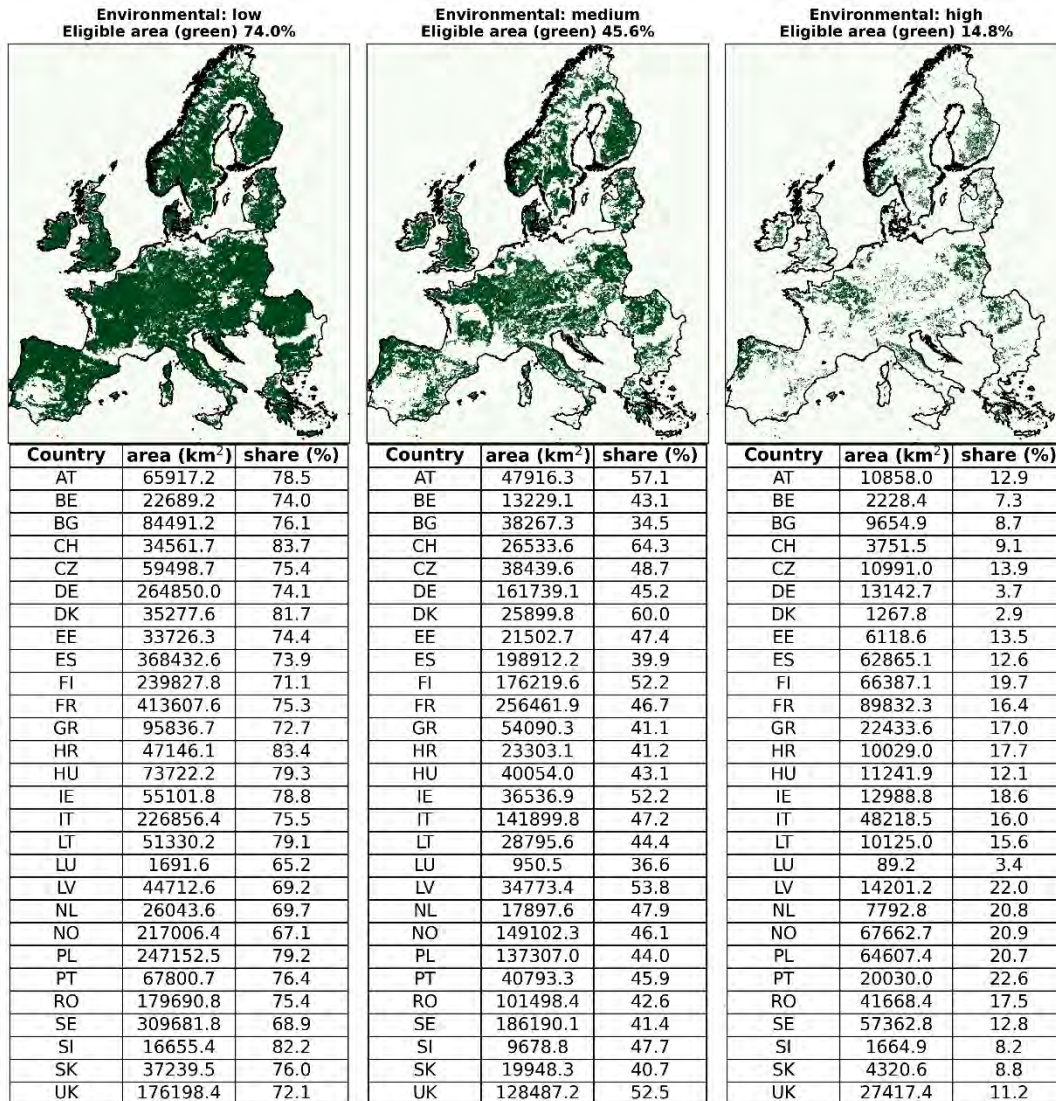


Figure 10: Geospatial overview of eligible areas for wind onshore deployment based on the three environmental scenarios.

Next, we sum the species richness rasters for birds and bats together to create a final dataset that contains the total number of species vulnerable to collisions with wind turbines within each grid cell. To convert this map into a set of exclusions, we take a quantile approach to identify three vulnerability thresholds. For each country, we take all grid cells in that country and compute the top 25, 50 and 75% quantiles. These thresholds are then used to mask all cells above that number from wind deployment to represent progressively more restrictive cases from low to high. For instance, low is to be interpreted as removing land areas (grid cells) where the upper quartile of the number of vulnerable species in each country is found. Thus, it is a more permissive case than medium (which blocks the upper 50%) or high (which blocks the upper 75%).



The three levels of our environmental exclusion dimension are shown in Figure 10, and Table 8 provides a summary of the data and assumptions involved.

Table 8: Environmental exclusions applied in each scenario.

| Name | Description | Buffer | Dataset |
|---|---|-----------------|--|
| IUCN protected areas | Low: Ia, Ib, II, III, IV Medium: Ia, Ib, II, III, IV High: Ia, Ib, II, III, IV, V, VI | High: 2000 m | Common Database on Designated Areas (CDDA) |
| Natura 2000 | Low: not included Medium: all sites included High: all sites included | High: 2000 m | Natura 2000 |
| Number of bird and bat species vulnerable to collision with wind turbines | Low: top 25% per country Medium: top 50% per country high: top 75% per country | | WIMBY D1.6 dataset |

3.2.3 Social exclusions

For social exclusion, we consider all impacts of onshore and offshore wind from a social perspective and define buffer distances to represent different levels of opposition. Within this dimension, we consider buffers around buildings and residential areas, identified in CORINE Land Cover Polygons 2018 [21] with categories: Continuous urban fabric (1.1.1), Discontinuous urban fabric (1.1.2), Industrial or commercial units (1.2.1), Construction sites (1.3.3), Green urban areas (1.4.1) and Sport and leisure facilities (1.4.2); visual impact on the landscape, defined in WIMBY D2.6 [65], and coastlines buffers.

Table 9: Social exclusions applied in each scenario.

| Category | Description | Buffer | Dataset (incl. code) |
|--------------------------|-------------|--------|----------------------|
| <i>Onshore exclusion</i> | | | |

| | | | |
|----------------------------|---|---|--|
| Settlement | Excluded area around residential areas due to regulations. | Low: 200 m Medium: 1,500 m High: 3,000 m | CORINE Land Cover Polygons, 2018 |
| Noise | Excluded area around residential areas due to noise. | Low: 400 m Medium: 600 m High: 1,500 m | CORINE Land Cover Polygons, 2018 |
| Shadow Flicker | Excluded area around residential areas due to shadow flicker. | Low: 84 m Medium: 1,250 m High: 2,500 m | CORINE Land Cover Polygons, 2018 |
| Landscape visual impact | Excluded areas based on scenicness categories (ternary map) | Low: No exclusion Medium: Category labelled 3 High: Categories labelled 2 and 3 | Landscape visual impact map - Ternary category map |
| <i>Offshore exclusions</i> | | | |
| Coastline | Excluded area based on a buffer around the coastline | Low: 6 nms Medium: 12 nms High: 12 nms | [51], [59] |

Table 9 lists all social exclusion categories, along with the corresponding buffer distances and dataset sources for the low, medium, and high scenarios. In this case, only one category is relevant for offshore wind, while all the others are used to exclude onshore wind. Figure 11 summarises the resulting eligible areas according to the different scenarios for onshore wind deployment.

The settlement category is one of the most relevant for onshore wind, as it shows the largest excluded areas in the medium and high scenarios due to the large buffers (1.5 km and 3 km). In this category, we defined the low and medium buffers around settlements based on the results of WIMBY D2.10 [23], where the distances correspond to the minimum and maximum values between the ten WIMBY countries studied (minimum distance to villages in Italy and maximum distance corresponding to 10 times the turbine tip height) in this report. For the high scenario, we considered the upper limit of 3 km from [37] for the distance to settlements criterion.

For the *noise* category, the buffers are defined based on the existing European regulations on wind turbines and noise, summarised in [66]. For the low scenario, a buffer of 400 m is considered, which is the minimum setback distance required by noise regulations. A similar buffer value is used

in other works, such as [13] for Germany, [7] for Portugal, and [14], where this value is theoretically calculated to maintain a noise level of 40 dB. For the medium scenario, we set a buffer value of 500 m, and for the high scenario, a value of 2000 m, corresponding to the modal and maximum values, respectively, in [66].

For the *shadow flicker* category, we have defined the three scenarios in conjunction with D2.4 [67]. In the low scenario, the buffer is set at 84 m, corresponding to one hub height. In the medium scenario, the buffer is set at 1250 m, corresponding to the average radius for having a threshold of 30 hours of shadow flicker per year over flat (50 turbines in the Netherlands have a radius of 1235 m) and mixed (50 turbines in Spain have a radius of 1221 m) terrain. This buffer is assumed for the width (east to west) and the height (north to south) of the shadows, although the latter can be smaller (half of the radius). For the high scenario, we define a buffer of 2.5 km to mitigate the effects of shadow flicker completely.

The *landscape visual impact* category takes into account the scenicness map developed in WIMBY D2.6 [65], which uses a machine learning model to predict the landscape scenicness across Europe. The resulting map from this model provides a binary and ternary classification of the landscape visual impact of onshore wind farms at a resolution of 1km×1km. To define the three scenarios in this category, we use the ternary classification prediction map with categories: unscenic to medium, scenic, and highly scenic. Thus, while no pixels are excluded for the low scenario, for the medium scenario, only pixels labelled as highly scenic are excluded, and for the high scenario, both scenic and highly scenic are excluded.

The coastline category is only relevant for offshore wind, where values are defined based on [51], [59]. For the low scenario, the buffer distance around coastlines is set to 6 nautical miles (11,112 m), and for the medium and high scenarios, it is set to 12 nautical miles (22,224 m).

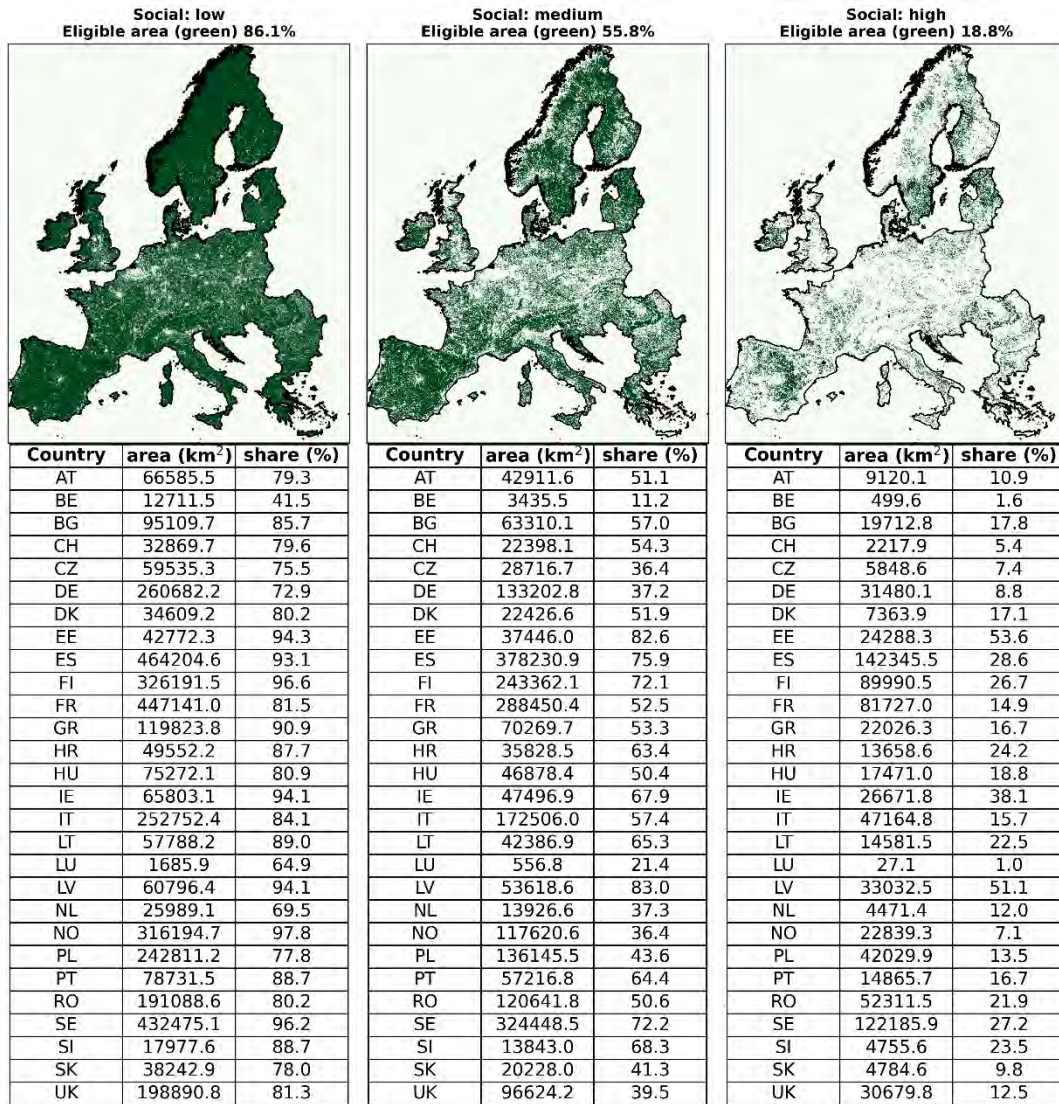


Figure 11: Geospatial overview of eligible areas for wind onshore deployment based on the three social scenarios.

3.2.4 Land availability in the spatial scenario combinations

The resulting land availability from the nine combinations of the social and environmental dimensions set out above, together with the technical dimension which is the same in all cases and are shown in Figure 12.

soc: low env: low
Eligible area (green) 37.51%



soc: medium env: low
Eligible area (green) 25.43%



soc: high env: low
Eligible area (green) 9.08%



soc: low env: medium
Eligible area (green) 23.04%



soc: medium env: medium
Eligible area (green) 15.27%



soc: high env: medium
Eligible area (green) 5.26%



soc: low env: high
Eligible area (green) 7.76%



soc: medium env: high
Eligible area (green) 5.00%



soc: high env: high
Eligible area (green) 1.71%



Figure 12: Overview of the resulting land availability and how large a share of the total area is available for onshore wind deployment for the nine scenarios.

3.3 Macro-scale scenario development

3.3.1 Whole energy system scenarios

JRC-EU-TIMES aligns with the land availability scenarios described in Section 3.2 in addition to the Climate change mitigation scenario (CLI) developed on the side of JRC-EU-TIMES. The CLI scenario aims to achieve net-zero GHG emissions in the EU and Switzerland by 2050. The scope of the GHG emissions

reduction target includes Energy (UNFCCC classification 1A-1B), Industrial Processes (2A-2H), Agriculture (3A-3J), LULUCF (4A-4H), Waste (5A-5E) and 50% of the emissions from international aviation and maritime. Details of these targets are summarized and listed in Table 10. The transition to net zero is to be achieved in this scenario solely with domestic mitigation measures in the EU. This scenario implements policies in the EU that are in the legislation up to 1.1.2024 or have been decided to be implemented in the near term. It assumes a continuation of the current energy supply and consumption trends and is used as a benchmark for the other two scenarios.

Table 10: The major EU directives included in the CLI scenario.

| Scenario | Directives |
|-----------------------------------|--|
| CLI (net-zero target scenario) | <ul style="list-style-type: none"> •EED energy efficiency (EU2023/1791) •EPBD buildings performance standards (EU2018/844) •ETS (all revisions up to EU2023/959) •EU RED III renewable targets (up to EU2023/2413) •GHG effort sharing (up to EU2023/857) •Vehicle emissions standards (EU2019/631, EU2023/851) •Heavy vehicle emissions standards (EU2019/1242) •Coal phase out 2030 in DE, DK, FI, GR, HU, IE, IT, NL, PT, SI, SK, ES •Intra-EEA aviation in EU-ETS •NTC electricity capacities as in ENTSO-E TYNDP 2022 plan •Reduction of nuclear share in France •New nuclear plants those under construction/advanced planning |
| | <ul style="list-style-type: none"> •GHG emissions from 1990: -55% in 2030, -90% in 2040 •Net-Zero GHG emissions in 2050 at the EU-level •Individual net-zero GHG emissions targets of the member states •GHG emissions reduction scope as in the EU Climate Law <ul style="list-style-type: none"> - includes LULUCF and 50% of the international transport •Refuel aviation SAF mandates •EU-ETS-2 from 2030 (although incl. in 2023 revision of EU-ETS) •+ 8GW new nuclear power (BG, CZ, RO, SI, SK, FI, FR) |

With the basis of CLI scenario, nine further scenarios are layered on top of the CLI scenario that are based on the three exclusion dimensions with three degrees (low, medium and high).

Table 11: Scenario name alignment between the two macro-models

| JRC-EU-TIMES abbreviations | Scenario | Corresponding highRES-Europe scenario titles |
|----------------------------|----------|--|
| CLILL | | soc:low env:low |



| | |
|-------|-----------------------|
| CLILM | soc:low env:medium |
| CLILH | soc:low env:high |
| CLIML | soc:medium env:low |
| CLIMM | soc:medium env:medium |
| CLIMH | soc:medium env:high |
| CLIHL | soc:high env:low |
| CLIHM | soc:high env:medium |
| CLIHH | soc:high env:high |

In quantifying the nine scenarios that are shown in Table 11 above with the JRC EU TIMES model, we therefore assumed that the EU Green Deal policy package is always active: this means that the nine wind deployment scenarios in JRC-EU-TIMES consider the identical emissions reductions targets, renewable deployment targets, energy efficiency targets, sustainable fuels blending targets, etc. that are also considered in the Directives forming the EU Green Deal. Therefore, the scenario exploration with JRC-EU-TIMES identifies which options can substitute or complement wind when the EU policy is implemented under the presence of varying levels of societal and environmental concerns.

3.3.1 Additional boundary conditions applied to highRES-Europe

In addition to the boundary conditions derived from the model coupling described above, a number of important assumptions are made in the highRES-Europe optimisation.

Firstly, following Millinger et al. [68], we assume that negative emission technologies, i.e. bioenergy with carbon capture and storage (BECCS) in this case, can only provide a limited amount of compensation for concurrent fossil fuel emissions. This assumption is taken here to be a maximum sequestration of 5 MtCO₂ beyond what is needed to achieve the emissions targets coming from the whole energy system model for the electricity system (which are ~ -80 MtCO₂). This choice is made to prioritise emissions reductions rather than offsetting via BECCS and also to reflect the substantial array of non-modelled factors surrounding speculative technology options like BECCS, such as risks and uncertainties around scale up and wider social, environmental and economic impacts [69], [70].

Secondly, biomass potentials, which provide fuel for both BECCS and biomass power plants, are taken from the medium scenario of JRC ENSPRESO [71]. Here we exclude: i) energy crops to minimise competition with

food production, ii) imports to ensure the highest standards for feedstock sustainability and iii) primary forest residues to mitigate concerns around the sustainability of that supply chain. This results in a total biomass potential for the 28 countries modelled in highRES-Europe of 1000 TWh/yr.

3.4 Micro-scale scenario development

To identify the micro-scale influence of wind turbine deployment in Europe, we used three scenarios reflecting varying levels of social and environmental constraints, as described in Section 3.2. These scenarios defined the feasible areas for wind farm deployment. Within these areas, potential wind farms were identified using our wind farm layout design and grid connection cost model.

For this deliverable, we have chosen Styria, Austria, as our case study from among the four pilot regions analysed in WIMBY due to the availability of multi-criteria satisfaction analysis (MUSA) indicators. More details on the applied MUSA indicators and methodology will be presented in WIMBY Deliverable 4.6. These indicators will be provided by WP4.1 and WP4.2 partners. These indicators are derived from surveys conducted within the study region and will inform the MCDA analysis that will be developed in Deliverable 4.6. Following the selection of the region, we obtained nine potential wind farm deployment scenarios from Section 3.2.4 and selected three representative ones for further analysis, as presented in Table 12.

Table 12: Scenarios considered in micro-level analysis.

| Scenario | Environmental level | Social level | Technical | Area available in Km ² - Styria |
|-----------|---------------------|--------------|-----------|--|
| High-high | High | High | Yes | 110.63 |
| Med-med | Medium | Medium | Yes | 2209.58 |
| Low-low | Low | Low | Yes | 5848.21 |

The potential deployment areas (polygons) vary across the different scenarios. To ensure consistency and comparability, the case study was narrowed down to a specific district. Styria comprises 13 political districts, as presented in Figure 13. Each district was evaluated for its presence in all scenarios, since some lack areas that are feasible under high environmental and social constraint levels.

To identify a consistent and technically viable case study region, we applied a combined spatial and technical filtering approach. First, all three scenario outputs were overlaid and clipped by district boundaries to evaluate the consistency in feasible wind deployment areas. Districts were then filtered based on a minimum wind speed threshold (≥ 4.5 m/s) and sufficient available land across all scenarios. Based on these criteria, the district of Leibnitz, located south of the city of Graz, was selected as a case study. It has a moderate average wind speed of ≈ 5 m/s at 100 m. The case study was conducted to demonstrate the effect of the developed scenarios on micro-level modelling.

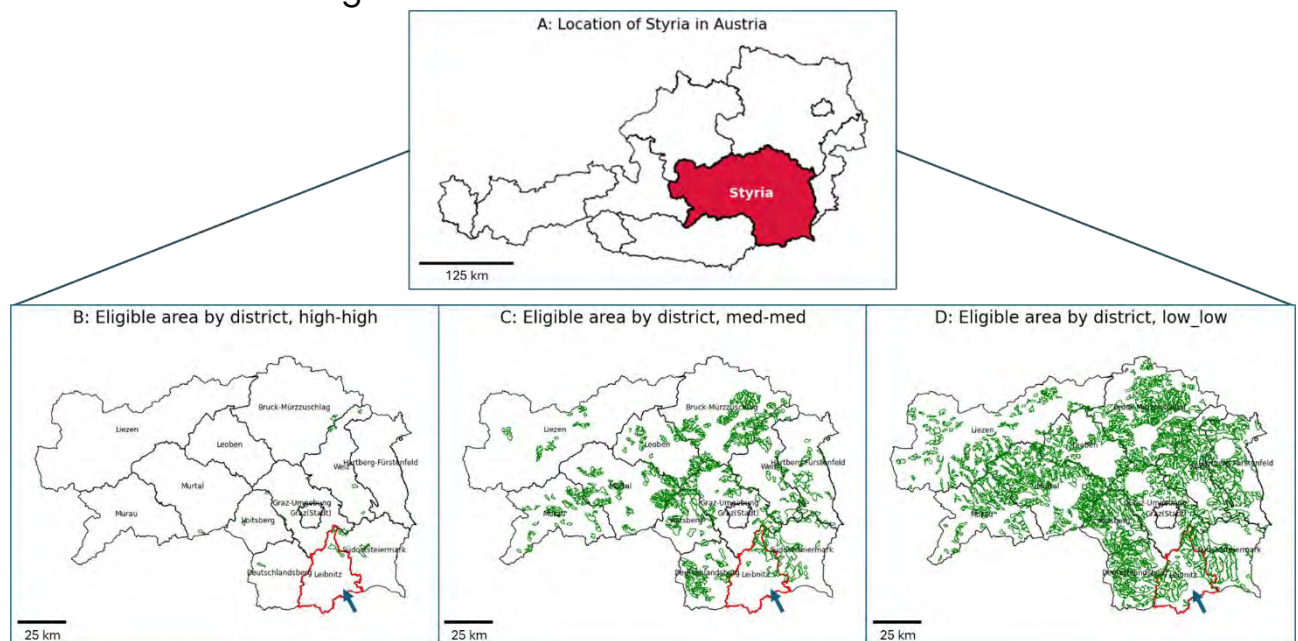


Figure 13: Feasible areas for wind energy deployment in Styria, Austria, across three land-use scenarios. Figure A represents the location of the Styria region in Austria, Figures B, C, and D show the three scenarios: high-high, med-med, and low-low, respectively. Blue arrows point to the Leibnitz district.

Once the district was defined, another filter criterion was applied based on typical onshore turbine density, which ranged from 6 to 7 turbines per Km^2 [72]. Given the scope of the project, the focus was placed on small to medium-sized wind farms. Figure 14 illustrates the resulting feasible areas (polygons) for wind farm development based on the scenarios presented in Table 12. The polygons were filtered according to two main criteria:

- The areas must be larger than the area required for three turbines.
- The maximum area was limited to 40 turbines. Larger polygons were split.

After applying the constraints:

- The high-high scenario yielded 3 potential polygons,
- The med-med scenario yielded 4 polygons, and
- The low-low scenario initially yielded 16 polygons, of which 5 exceeded the maximum size and were split, resulting in a total of 21 polygons.

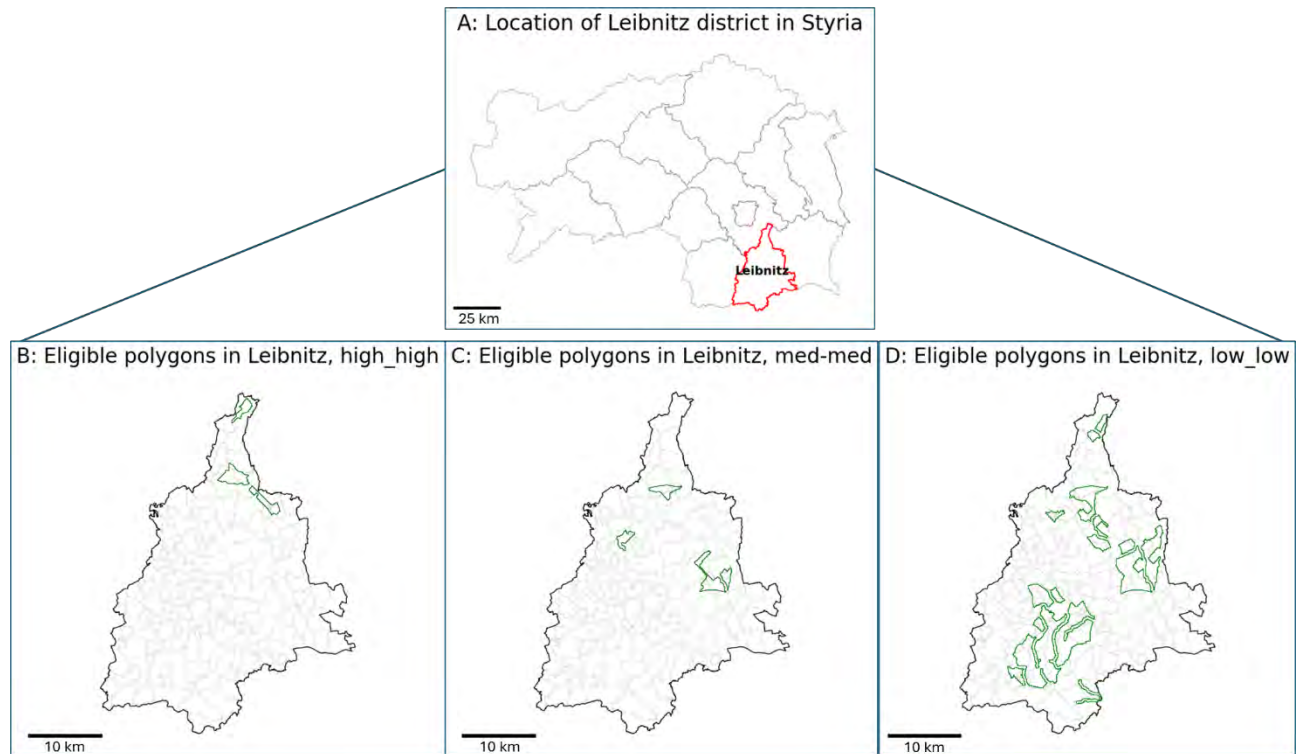


Figure 14: Feasible areas for wind energy deployment in Leibnitz, Styria, Austria, across three land-use scenarios. Figure A represents the location of the Leibnitz district in Styria, Figures B, C, and D show the three scenarios: high-high, med-med, and low-low, respectively.

4. RESULTS

4.1 Macro-scale modelling scenario results

4.1.1 JRC-EU-TIMES results serve as boundary conditions for highRES-Europe

JRC-EU-TIMES scenarios results are presented first as they set the boundary conditions for highRES-Europe in 2050. Greenhouse gas emissions among the scenarios also have no variation, as all CLI scenarios shown in Table 11 for the EU-27 plus UK, Norway and Switzerland, assume the achievement of

net-zero GHG emissions in 2050 with domestic measures only. Hence, we zoom in on the CLIMM scenario as shown on the right of Figure 15 in terms of sectoral emissions. In the following discussion, all results refer to the EU27, including the United Kingdom, Norway and Switzerland (called EU27+)

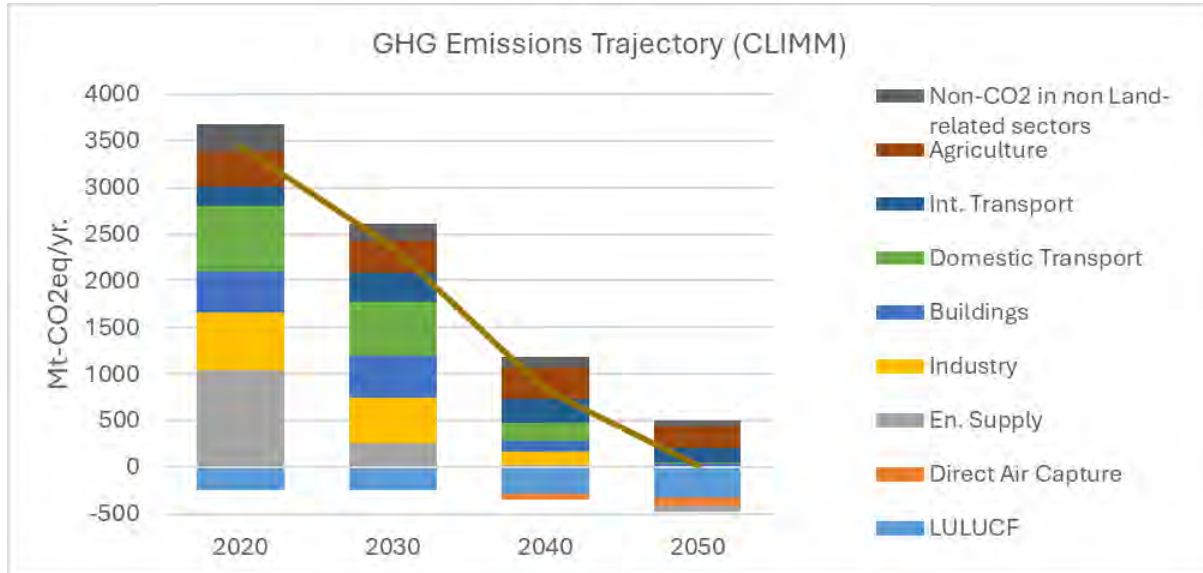


Figure 15: Total greenhouse gas emissions in CO₂ equivalent for CLIMM scenario.

Overall, energy supply emissions are reduced most, underlining the large potential for emissions cuts through renewable energy deployment in the power sector. From the demand side, the highest reductions can be observed in the building sector and transport. However, there is a more limited scope for transport in the near term than in the long term. The emissions trajectories in Figure 15 illustrate how crucial the next ten years are to develop and deploy new climate-neutral technologies at scale, decrease energy use, and phase out solid fossil fuels. In the EU-27+, buildings and the power sector show the highest emissions reductions until 2030, followed by transport. This is because the EU building stock is relatively old and inefficient, with many low-hanging fruits for emissions cuts compared to other sectors. In contrast, it can be claimed that electric vehicles are a proven technology that can deliver carbon reductions in the transport sector. The emissions reduction in the industry develops until 2030 at the annual rates observed over the last decade, which signals the high effort the sector has already put in place to reduce its carbon footprint as a result of the strengthening of the emissions trading system. The JRC-EU-TIMES model endogenously deploys mitigation options for the CO₂ emissions from fuel combustion and industrial processes. At the same time, the trajectory of the

non-CO₂ GHG towards net zero is an assumption of the model when formulating the emissions target constraints. Figure 15 shows that CO₂ emissions from combustion decrease faster than CO₂ process emissions in the industrial sectors, and it is likewise for non-CO₂ emissions from other sectors outside the energy system.

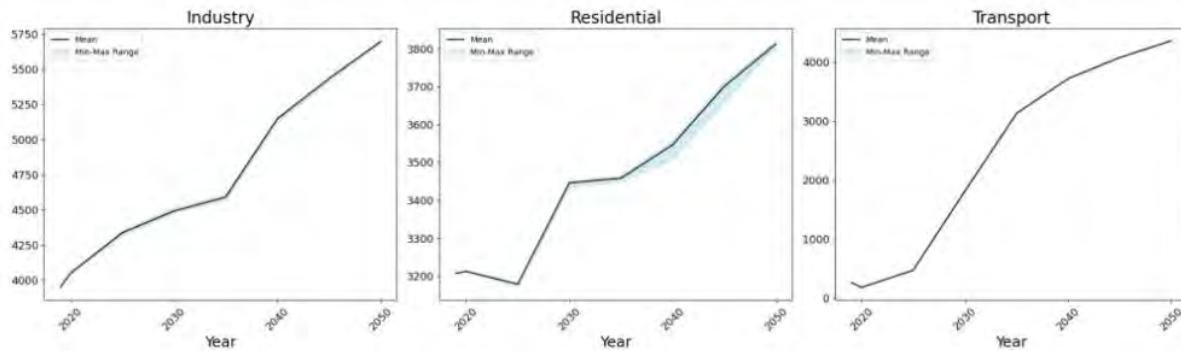


Figure 16: Electricity consumption for each end-use sector in JRC-EU-TIMES. Min-Max range refers to the difference between the scenario with the minimum and the one with the maximum.

The boundary conditions for the highRES modelling work include the total CO₂ emissions across all countries and electricity demand by end-use sector. These main boundary conditions have shown minimal variation among the scenarios, as seen in Figure 16. This is mainly led by the ETS and ETS2 implementations, which impose a cap on Greenhouse gas emissions in the industry, residential, and transport sectors. In addition, the implementation of the EPBD Directive for building energy performance standards, the new vehicle emissions standards, as well as the EED directive for energy efficiency, leave little space in the end-use sectors and constitute the electrification of the end-use sectors as the major option towards decarbonisation. As a result, all sectors experience drastic electrification, with transport being the most heavily electrified, consuming 4,367 PJ by 2050. The differences, however, among the scenarios are negligible except for the residential sector, implying some flexibility in the substitution of electricity for this sector.

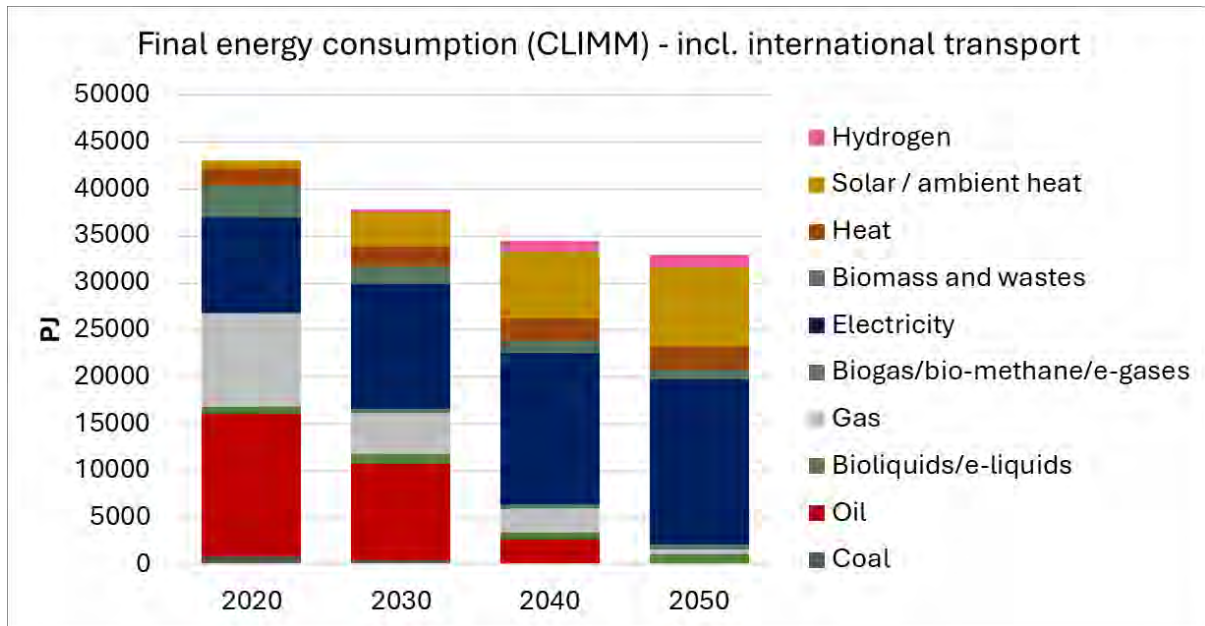


Figure 17: Final energy consumption in the CLIMM scenario for the EU-27+.

In the EU-27, coal becomes marginal in final energy consumption in 2030 (Figure 17), driven by reductions in industry and declared policies in several member states to reduce coal for heating purposes and increase renewable uptake. Oil remains a significant contributor to the final energy demand until 2030, but its consumption reduces to a fraction of the current level by 2050. Natural gas consumption decreases significantly by 2030, especially in the residential and services sectors. This is also driven by implementing the REPowerEU plan that foresees at least a 30% reduction in the use of natural gas in 2030 from today in the EU. In the long-run, natural gas consumption in the EU has a share in total final energy consumption of less than 5%.

4.1.2 Scenario Variations in energy supply and Power Conversion Sector

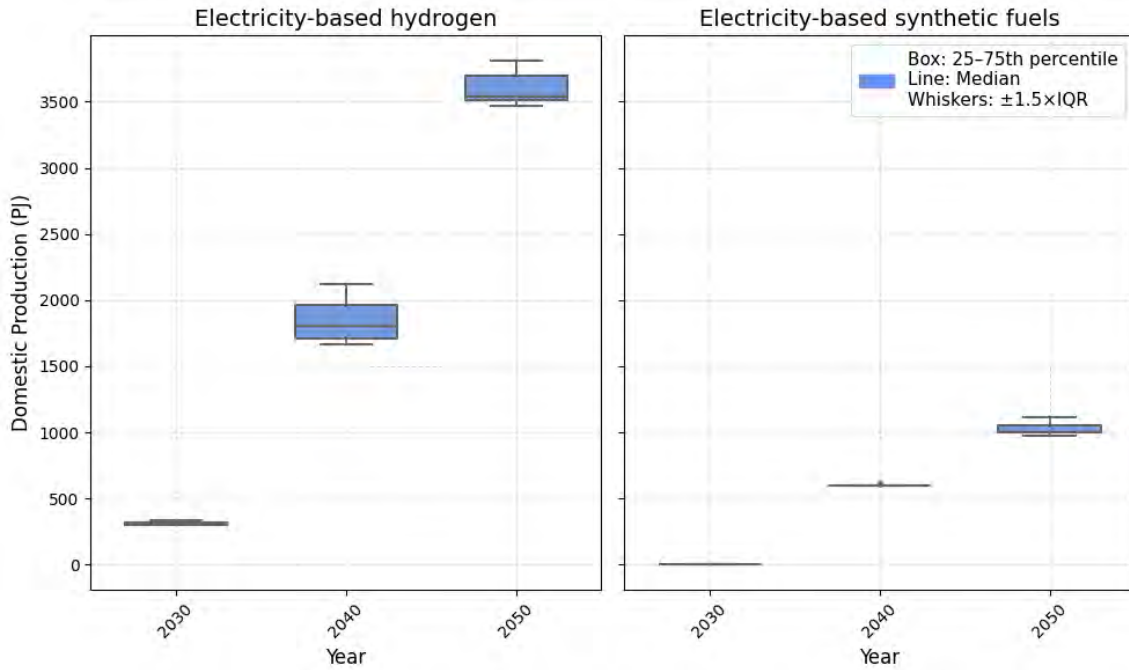


Figure 18: Changes in the hydrogen and synthetic fuels supply from JRC-EU-TIMES.

Electricity-based low-carbon fuels production takes off around 2030 and 2035 as seen in Figure 18 above. Synthetic fuel production has little variation among the scenarios as it is mainly driven by the needs for synthetic fuels in aviation, driven by the implementation of the ReFuelEU Directive in the scenarios. On the other hand, green hydrogen has a wider variation among the scenarios in 2040 which is enabled by the expansion of biomass and waste with CCS capacities to offset any limitations in the green electricity availability due to limited wind deployment in the highly constrained scenarios. Hydrogen production scales up after 2030s, from around 320 PJ/yr in 2030 to 3160 PJ in 2050 with an addition of 886 PJ of electricity-based synthetic fuels.

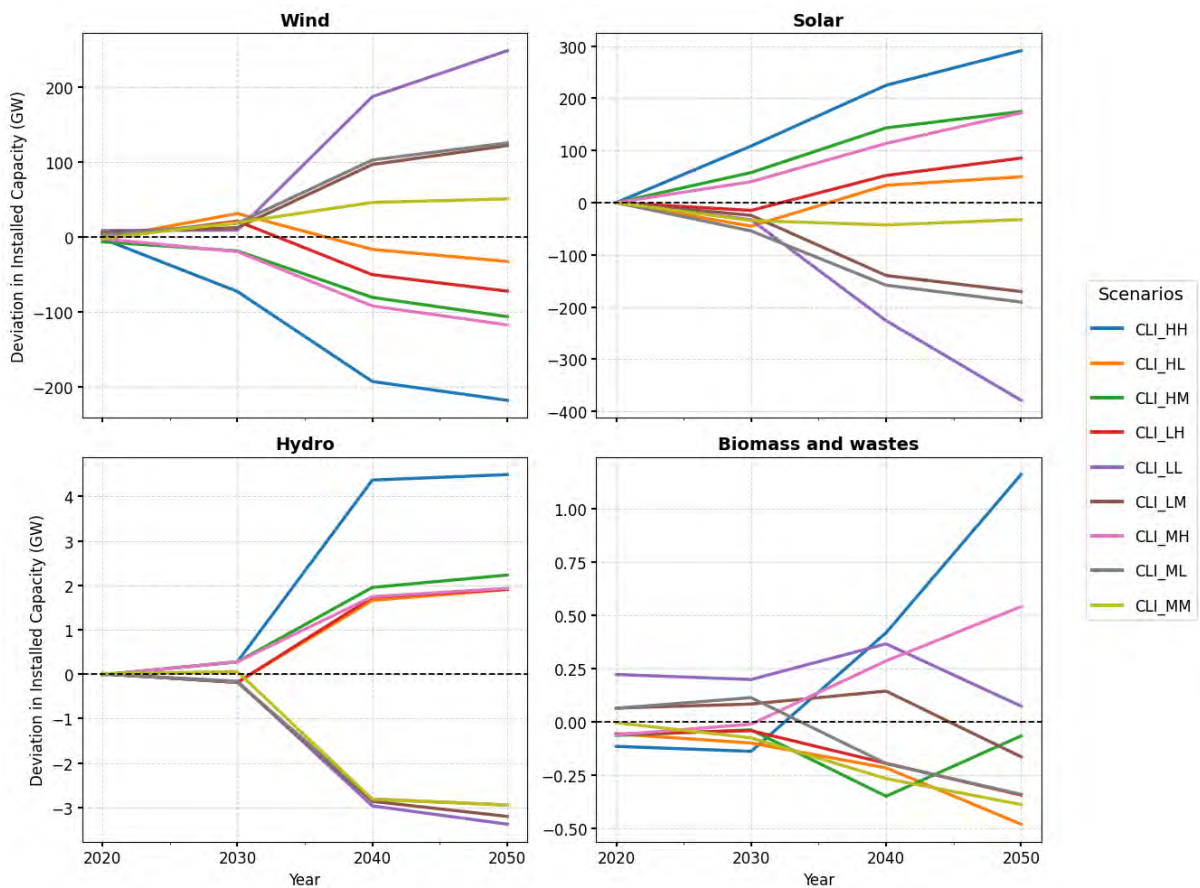


Figure 19: Scenario variations of renewable electricity deployment for total Europe deviating from the mean of all scenarios. The black dotted line is the arithmetic mean of the values from all 9 scenarios from JRC-EU-TIMES.

As highRES-Europe demonstrates in detail the electric system designs in 2050, Figure 19 above aims to show the trajectory of the variation in installed electric capacities of renewable technologies by considering the scenarios constraining wind capacity expansion based on social and environmental criteria. In particular, the figure shows the ways in which other renewables compensate for the reduction in wind installation to meet renewable targets and emissions targets (ETS) in the electricity sector by supplying the demand. Following the CLIHH case indicated by the blue line, we see the drastic compensation of electricity supply from solar and hydroelectric power. Though the compensation of the electricity supply reduction from wind via solar electricity scales more than hydro-electricity. While wind contributes to meeting electrification-driven demand, its potential appears to be overestimated. In contrast, the potential of hydro, as a near-perfect substitute, is already fully exploited. With the reduction of around more than 200 GW from wind in 2050 for the CLI_HH case, an addition of c.a. 300 GW of solar installations and merely 4 GW of hydro-electricity necessary. Biomass

and waste with CCS installations is minimally influenced by the reduction trajectory of wind and surges in capacity in 2040.

In the near-term period until 2030 the wind deployment remains relatively the same across all scenarios, with the exception of the very high constraint case. This is due directly to the capacity potential constraints introduced for 2050 from highRES. All the constraints are active in the optimization. The potential for the CLI_HH case is less than half of the potential given for the CLI_MM case. Due to the model's nature of perfect foresight and implemented extrapolation rules, the JRC-EU-TIMES pre-emptively reduces its capacity installation in the near term. This highlights the importance of wind deployment in meeting the climate and renewable energy deployment targets in the next 10-15 years. Figure 19 clearly shows that the trade-off in renewable electricity is mainly between solar and wind, as bioenergy and hydropower have limited potential for expansion due to resource constraints (bioenergy) or already high exploitation rate of sustainable potential (hydropower).

The JRC-EU-TIMES model has a perfect foresight optimisation with low intra-annual resolution, compared to the highRES-Europe model which is a snapshot model but with high spatial and temporal detail. Besides, JRC-EU-TIMES sees lead-in times for the infrastructure deployment, grids or energy supply assets including wind. This is particularly important for the deployment for the wind offshore, as good capacity factors are achieved in deep waters far from the coast with the need for extensive and costly grid connections. In this regard, and as discussed also in the next section, the results from the JRC-EU-TIMES are conservative in the deployment of wind offshore electricity.

4.1.3 National-level cumulative new wind capacities trajectories and near-term challenges

Figure 20 shows the total installed capacity per country for today and in 2035 (CLI_MM scenario case), as well as the cumulative new installations in wind for 2025 and 2035 in all scenarios examined. The numbers include both offshore and onshore wind.



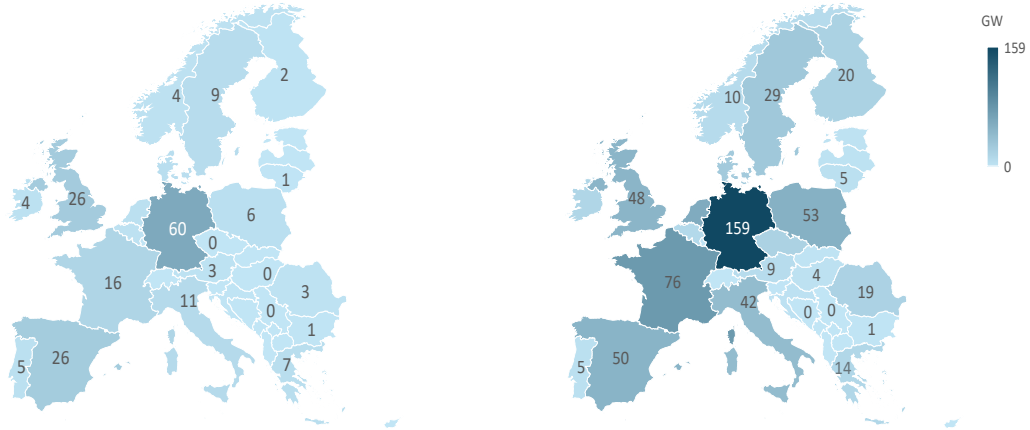
In the near-term horizon until 2035, and for the CLI_MM scenario, Europe is projected to add about 480 GW of wind, mostly onshore, while the offshore installations are ramping up. Germany is the onshore leader, due to the supportive legislation in recent years and continuing strong political backing and reform momentum; at the same time, offshore wind capacity in Germany sees a rapid expansion. The United Kingdom can be characterised as an offshore powerhouse, supported by supply-chain funding, the upcoming Crown Estate investments and the next offshore auction targets; however, the UK will need to proceed faster in the near term with the grid upgrades to support the expansion of offshore capacity by 2035. The Nordic countries (Sweden, Finland and Denmark) continue strong trajectories, leveraging supportive policies and community backing. Finally, a set of countries like France and Poland can be characterised as emerging markets, signalling the broadening of wind leadership beyond traditional players.

Based on Figure 20, Germany, United Kingdom, Ireland and Spain becomes the “first movers” in its expansion in wind installations. The potential restrictions in the scenarios play a bigger role in the early years, around the 2025 milestone years, as capacities vary more among the scenarios than in 2030. Germany remains the main the highest in wind capacity (ca. 145 GW) in 2035. On the other hand, France and Italy increase their new capacities in 2035 from ca. 1 GW to 55 and 48 respectively.

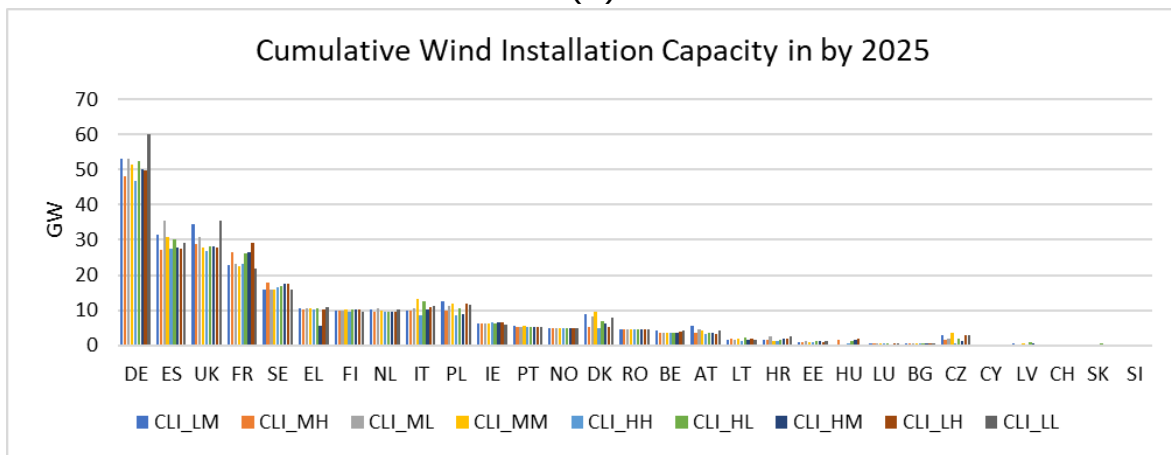
To realise the above geographical distribution of wind expansion in Europe between 2020 and 2035, concrete and persistent challenges need to be tackled. Even in countries which are first movers in wind expansion, like Germany and the UK, permitting for example remains an issue due to complex, decentralised processes and legal appeals. Supply chain constraints, including turbines, raw materials, vessels etc. need to be overcome too across Europe. Grid infrastructure upgrades will be needed to be completed in a rather short time, especially for offshore generation to keep pace with the new capacity ambitions of the UK and the Nordic countries. Finally, volatile auction designs and financing issues, seen for example in the UK’s failed AR5 round, underscore the need for stable, investment-friendly frameworks to de-risk deployment and accelerate wind uptake in the next 10 to 15 years across the European continent.



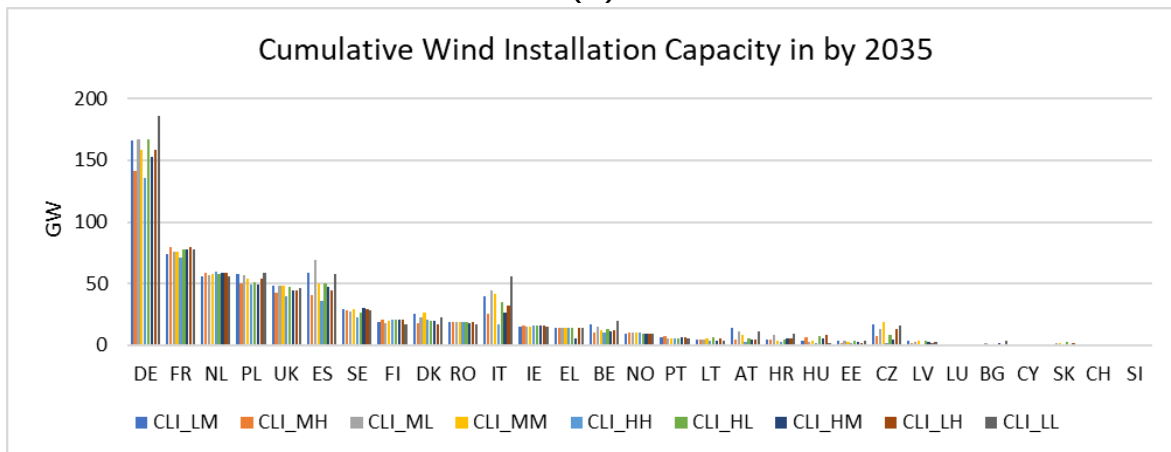
Installed wind capacity in GW in 2020 for the CLI_MM case Installed wind capacity in GW in 2035 for the CLI_MM case



(a)



(b)



(c)

Figure 20: (a) Installed wind capacity in 2020 and 2035; (b) cumulative wind capacity installation for 2025; (c) cumulative wind capacity for 2030 on a national European level. The ranking of the countries is based on the largest to smallest of wind capacity for scenario CLIHH. The figures (b) and (c) serve to observe the ranking.

4.1.4 Cost and design implications for Europe’s electricity system in 2050

In this section, we present an overview of the highRES-Europe modelling results, i.e. the design of the continental power system covering 28 European countries in 2050. Here, our aim is to showcase the implications of varying levels of social and environmental protections/restrictions on power system design and total annualised system costs.

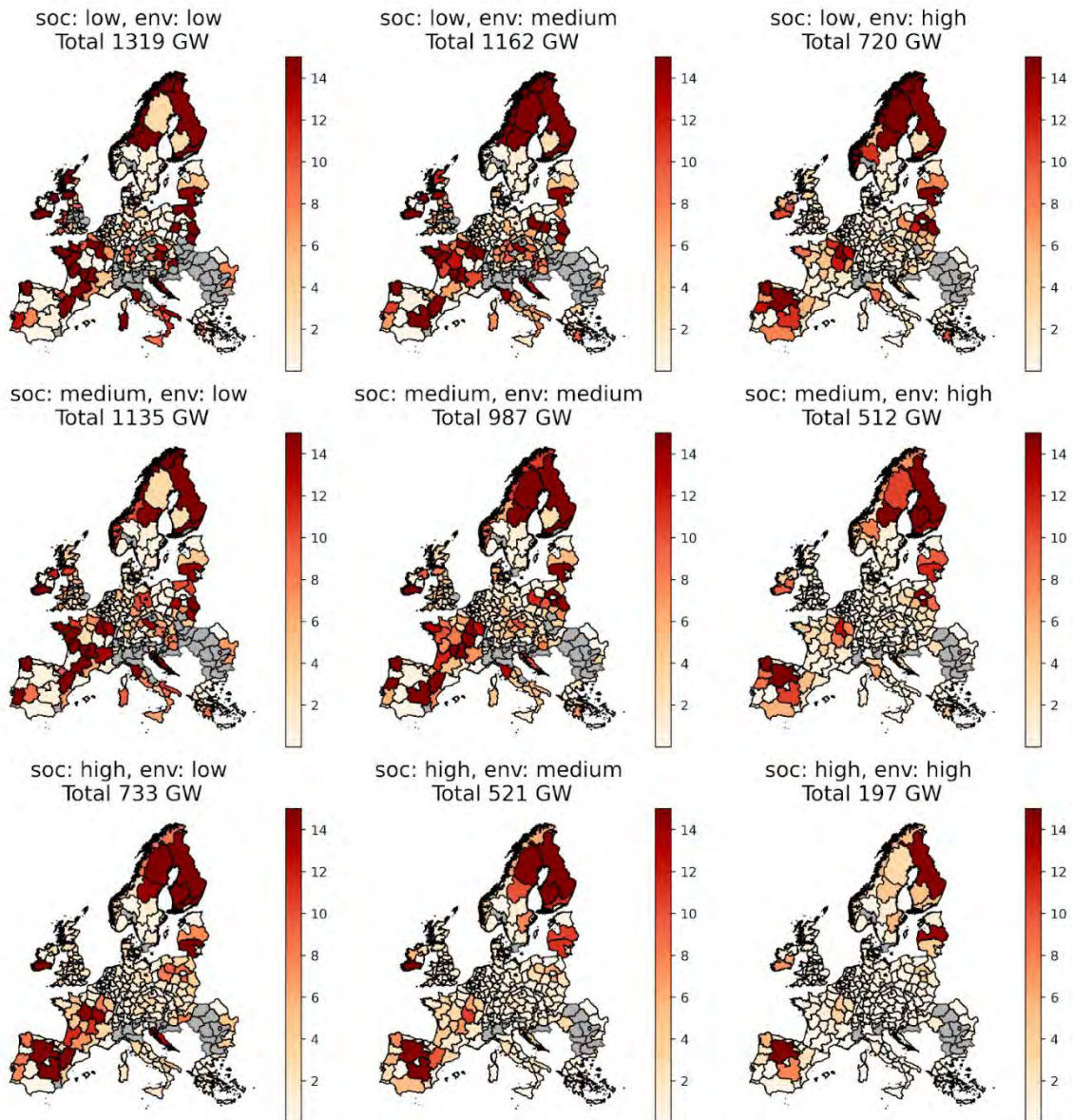


Figure 21: Spatial (NUTS2) distribution of onshore wind capacities for the nine scenarios from highRES-Europe modelling. The colorbar is capped at 15 GW to keep the lower end of the scale visible; some NUTS2 areas have installed capacity in excess of this limit.

Firstly, in Figure 21, we show the NUTS2 level capacity deployment of onshore wind across the nine land availability scenarios with their different levels of

prioritisation around social and environmental protections. It is clear that the deployment pattern changes substantially, both across Europe and within countries, from the low-low case to the high-high case. In the former, and a number of the other lower restriction cases, wind siting is concentrated in favourable (i.e. windy) NUTS2 regions. As one then moves to the higher restriction scenarios, and particularly high-high, installed wind capacity is both markedly less in absolute terms, but also more evenly distributed over a greater number of NUTS2 areas.

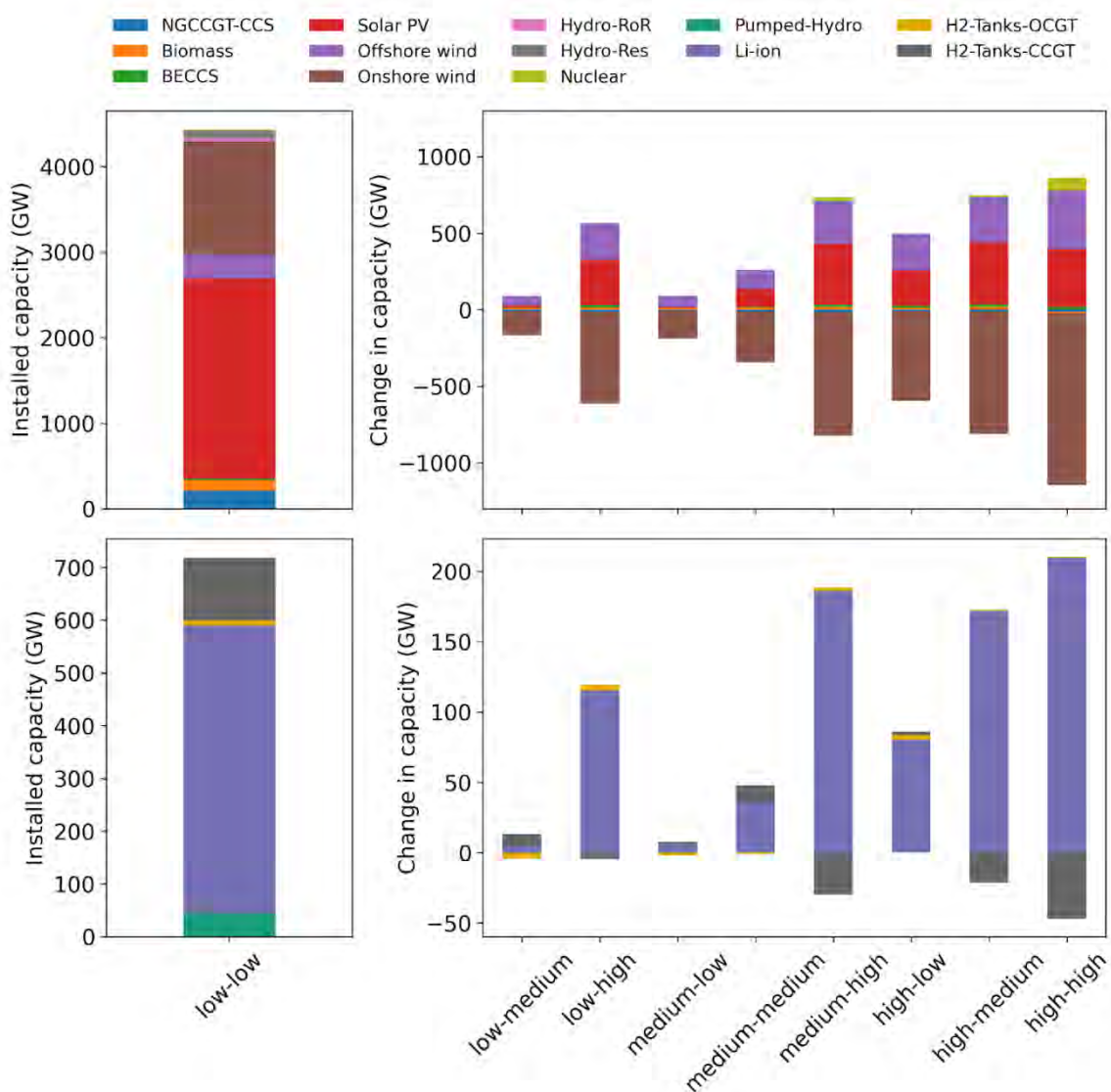


Figure 22: Installed electricity system capacities for the low-low (social-environmental) scenario (left) as well as the relative difference for the remaining eight scenarios, compared to the low-low scenario. The upper panel of the figure shows electricity generation technologies while the lower panel shows energy storage. All results from highRES-Europe modelling

Figure 22 plots the aggregated installed electricity system capacities, with generation in the top panels and storage in the bottom panels, of all 28 countries modelled in highRES-Europe in the low-low scenario (left panels). Here, we see a combined system dominated by variable renewables, with total wind power capacity of ~1300 GW onshore and ~300 GW offshore in the low-low case. The right panels then show that as the restriction/protection levels increase, this ratio changes such that by high-high there is just ~200 GW of onshore capacity and ~650 GW of offshore, i.e. the model responds in part to constraints on onshore by deploying more offshore wind.

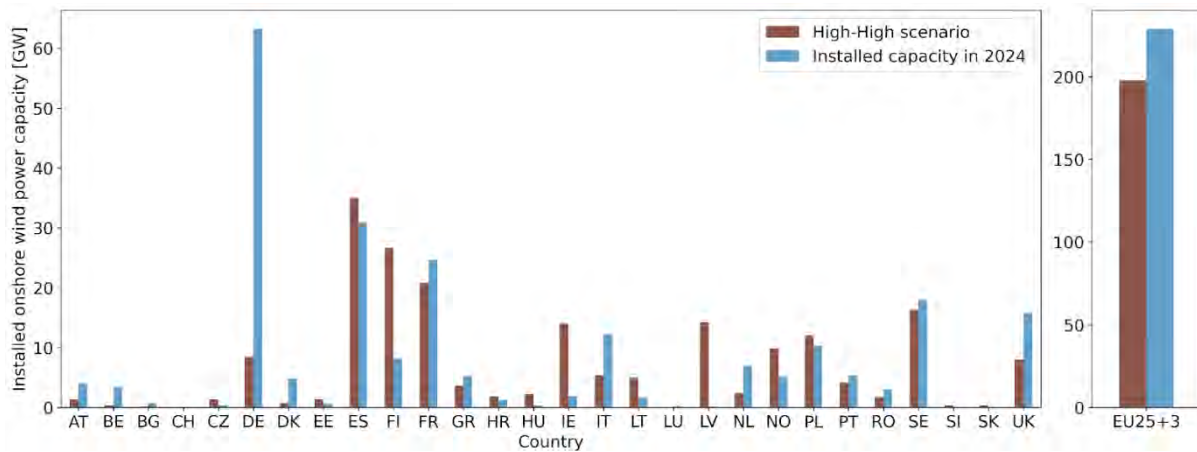


Figure 23: Comparison of installed onshore wind power capacity in the high-high scenario from highRES-Europe and 2024 levels, based on data from ENTSO-E [73] and U.K. Department for Energy Security and Net Zero [74].

For onshore, the deployed volume in the high-high scenario should be compared with today’s cumulative onshore capacity across these 28 countries of 229 GW [73], [74], indicating the pessimistic outlook this case has for this technology. The difference between today (2024) and the high-high scenario is particularly striking for Germany, which sees a reduction of 55 GW of onshore wind, as shown in Figure 23. Similar results are obtained for other large European countries, such as France, Italy, and the United Kingdom, although less dramatic than Germany. Some smaller countries (in terms of population) see an increase, even in the high-high scenario, such as Finland, Norway and Ireland. This is likely a combination of relatively large land area, low population density (making the high social scenario less impactful) and a lower existing capacity in 2024. Finally, it is also noteworthy that around 200 GW more battery capacity is installed in the high-high compared to the low-low cases. This is likely to be at least partially explained by the increase in installed solar PV between these two scenarios, given the typical synergy between batteries and solar.

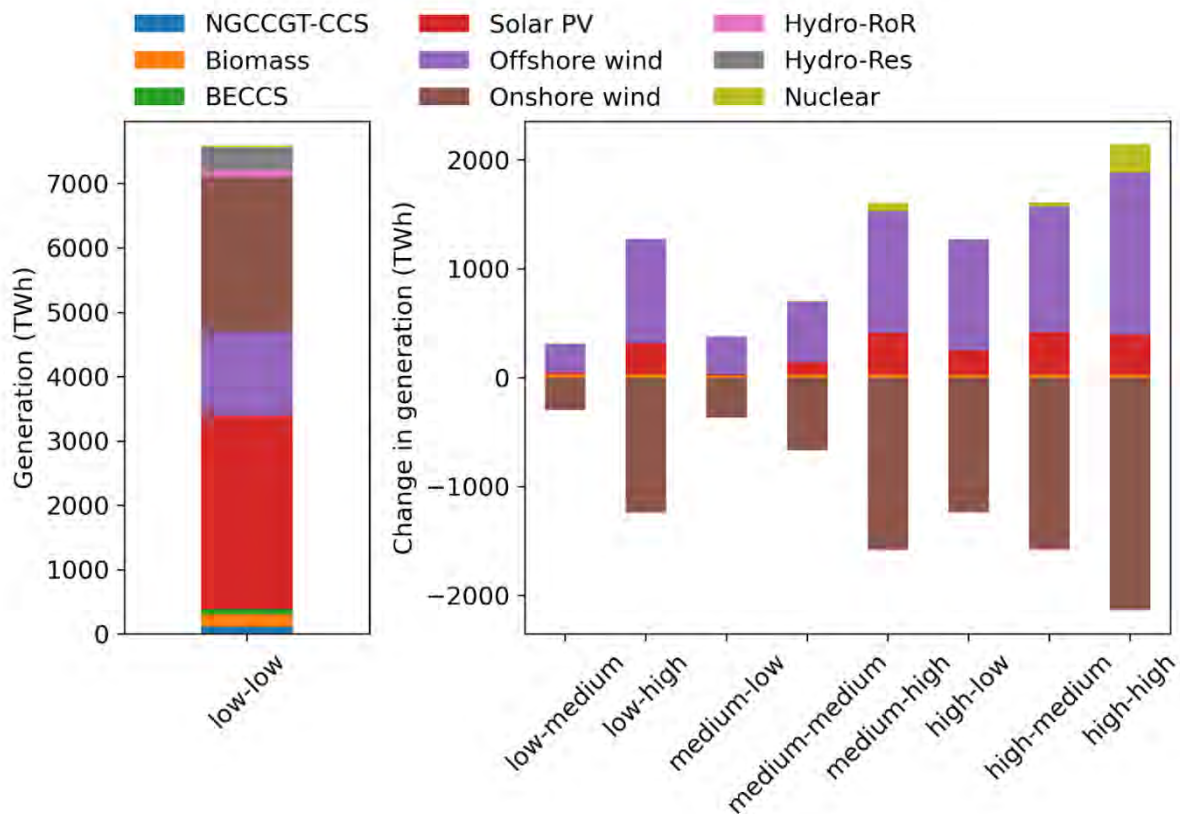


Figure 24: System-wide annual electricity generation for the low-low scenario (left), as well as the relative difference to the low-low scenario for the remaining eight scenarios (right) from highRES-Europe.

Finally, at the European level, in Figure 24, we show annual electricity generation in a similar manner to Figure 22, i.e. for the low-low case and then the change with respect to that across the other eight scenarios. This chart underscores the important role played by onshore wind in the lower restriction cases, with it providing ~2400 TWh or a third of electricity generation per year for the entire European system. It also highlights the pivotal role played by offshore wind in replacing electricity supplied by onshore wind as the prioritisation of social and environmental factors grows across the scenarios. While at the capacity level, offshore appears similar to solar PV, given its typically much higher capacity factor, it plays a much more significant role in generation terms. Ultimately, the vast majority of the ~2000 TWh of onshore generation lost in the high-high case is replaced by offshore wind, solar PV and nuclear.

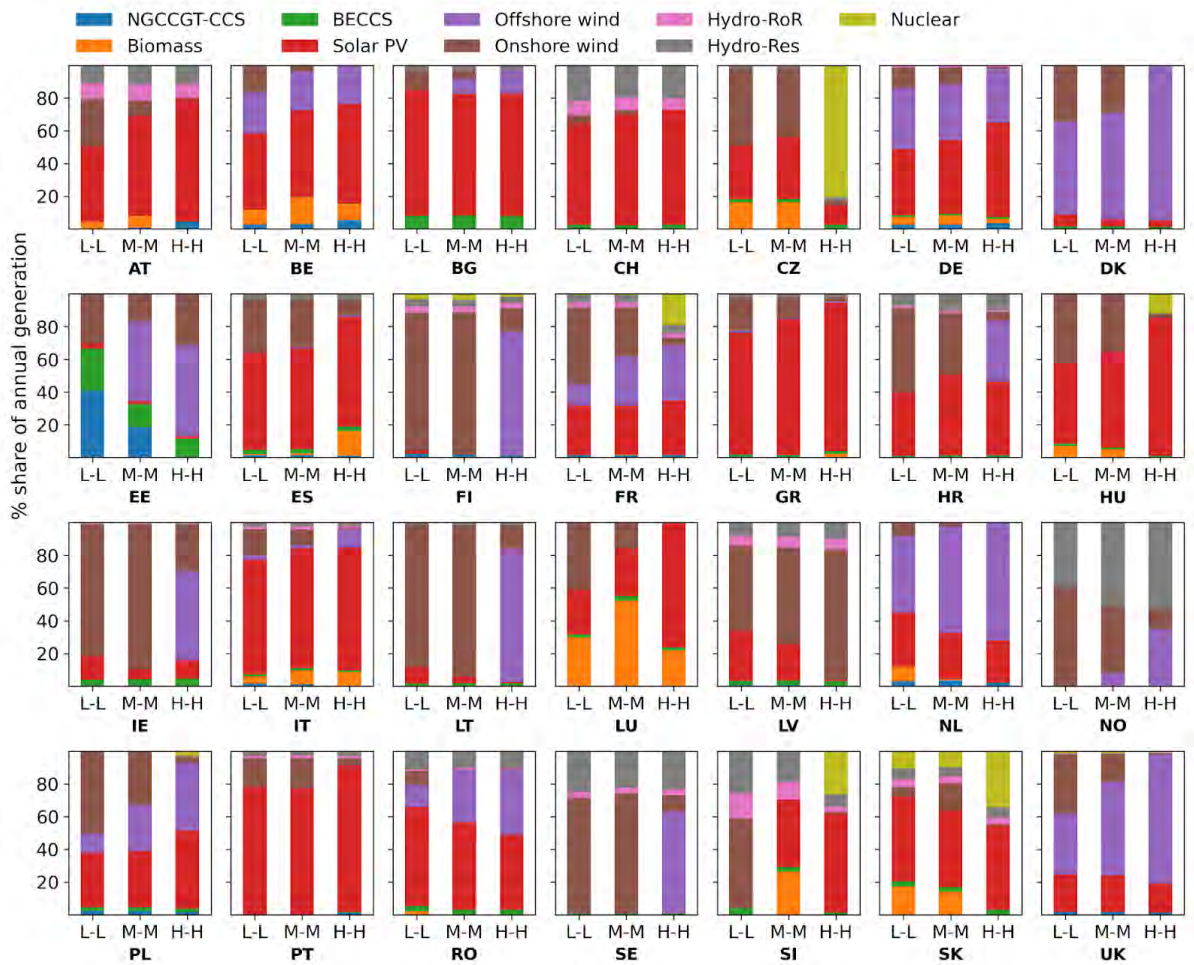


Figure 25: Share of annual generation across the 28 modelled countries for the diagonal scenarios of low-low (L-L), medium-medium (M-M) and high-high (H-H) from highRES-Europe modelling

Moving to the national level, Figure 25 shows the share of annual electricity generation by country across low-low, medium-medium and high-high scenarios. These panels demonstrate how, as the role of onshore wind is progressively reduced due to increasing social and environmental restrictions, national electricity systems are reorientated more toward offshore wind (where possible) and solar PV. Countries like France, the Czech Republic and Slovakia switch to deploying new nuclear power, despite it being a more costly choice than variable renewables. Nevertheless, most countries remain heavily reliant on a mix of wind and solar PV to meet their electricity generation needs, with small amounts of balancing power coming from biomass and natural gas (note that storage plays a key role in providing flexibility and is not shown in this figure).

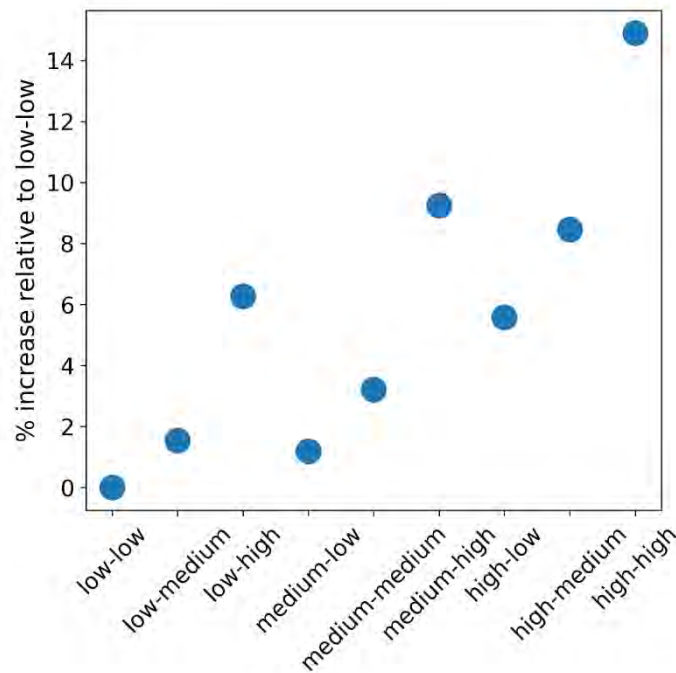


Figure 26: Total annualised system cost increase relative to the low–low scenario for the whole of Europe (all 28 countries modelled in highRES–Europe combined).

Next, we show the total annual system cost implications for the nine land availability scenarios relative to low–low in Figure 26. Here, we see that for restrictions involving a combination of low and medium, the system cost increases are at most ~4%. These increases are driven by the continent's electricity supply being re-orientated toward less reliance on onshore wind, one of the cheapest forms of electricity generation in our modelling, as land available for deployment progressively becomes less across the scenarios. Bringing the high prioritisation level of either dimension into play leads to cost increases of ~5% or more as the available space for onshore wind is further restricted. Indeed, the high–high case results in a ~15% increase in the total annualised cost of the system, equivalent to an extra ~104 €bn/yr (in 2024 euros) in expenditure on Europe's electricity system. Again, this is brought about by the high levels of protection assigned to social and environmental aspects in this potential future scenario, substantially restricting the land available for wind, particularly onshore wind. As a result, the optimal system moves towards a more expensive design that relies more on offshore wind, solar PV, batteries and particularly costly options like new nuclear.

4.2 Micro-scale modelling scenario results

This section presents the micro-scale modelling, focusing on the resulting wind farm layout and connection costs.

Figure 27 illustrates the spatial distribution of all eligible wind farm polygons across the three scenarios. The polygons highlighted with red arrows were selected for detailed analysis, as they were consistently identified as suitable across all three scenarios. The blue dots represent the existing MV/HV substations in the Leibnitz district [75]. In the low-low scenario, one of the selected polygons was subdivided due to its large size, following the constraints outlined in Section 3.4. The comparison across the scenarios illustrates how land-use assumptions influence both the spatial availability of suitable areas and their proximity to existing grid infrastructure.

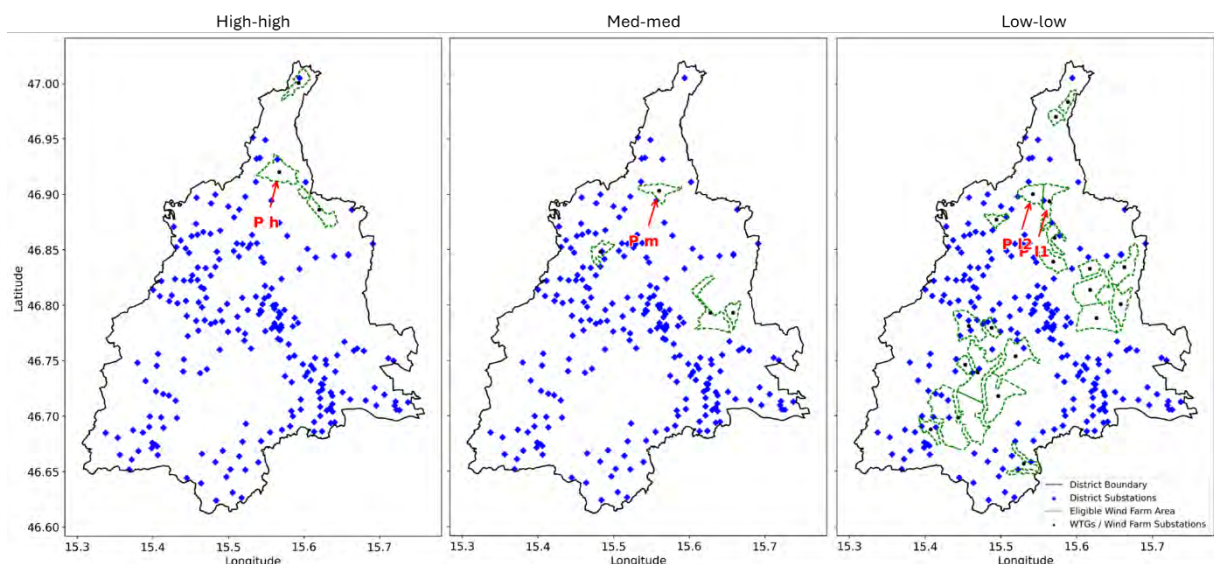


Figure 27: Spatial distribution of eligible wind farm areas and substation infrastructure under the three land-use scenarios in the selected district. Blue markers represent the location of existing MV/HV substations obtained from OpenStreetMap (OSM) [75]. Green dashed areas indicate regions eligible for wind farm deployment. Red arrows point at specific polygons selected for detailed analysis; each associated with an internal substation (black dot).

Figure 28 illustrates the internal wind farm layout for each scenario, including turbine placement, cable cross-sections, and substation location. The results clearly demonstrate the influence of the number of turbines and cable sizing on total internal costs. With a fixed turbine spacing of 4D, layout compactness varies with land availability, which in turn affects both energy

yield and infrastructure costs. This suggests that optimising turbine spacing is crucial not only for energy yield but also for minimising infrastructure costs. For instance, the low-low scenario, despite hosting more turbines, shows a less compact network and higher cable costs, highlighting how looser land constraints can increase internal infrastructure requirements.

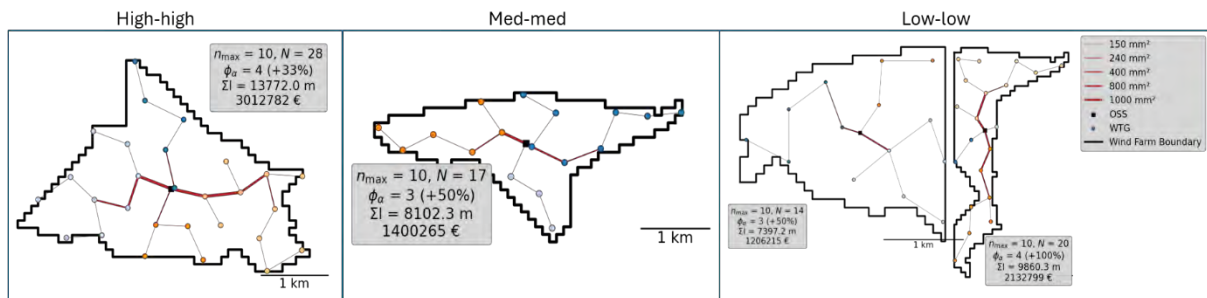


Figure 28: An illustrative example of the internal grid connection model output. The wind farm boundary is provided as a feasible area from Section 3. The location of wind turbine generators (WTG) is determined by the wind farm layout model described in Section 2.3.1. The figure shows n_{max} = Maximum number of cables that can be connected to the substation, N = Number of WTG, ϕ_{α} = Number of sharp cables turning angles along with the percentage increase, $\sum I$ = Total length in meters of all cables in the layout, € = Total estimated internal cabling cost in euros. The legend in the top-right corner indicates the cable cross-sections, OSS = Onshore substation, WTG, and wind farm boundary.

Figure 29 presents the optimised connection paths from the internal substation to the nearest external substation for three representative wind farm cases (high-high, med-med, and low-low). The routing varies significantly between scenarios, reflecting adaptations to the underlying terrain and land-use characteristics. This variation suggests the model effectively adapts to geographic constraints to reduce costs, even if it means longer or more circuitous routes. In the low-low case, the split polygon necessitates dual connections, which contributes to the higher external costs as presented in Table 13.

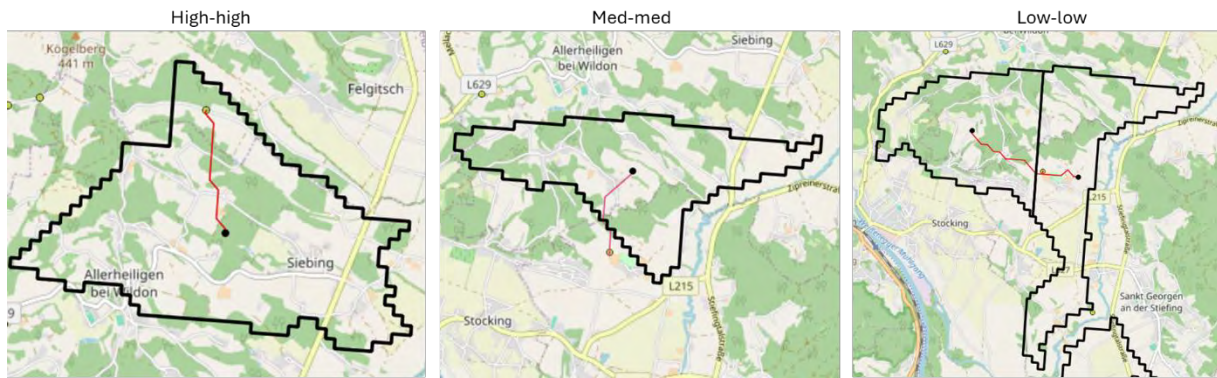


Figure 29: An illustrative example of the external grid connection model output.

Table 13 summarises the performance of each scenario in terms of turbine count, AEP, and the associated internal and external connection costs. While the low-low scenario leverages a significantly larger area, leading to the highest AEP, its external costs are nearly 80% higher than those of high-high. This is a disproportionate increase compared to its 64.5% gain in AEP. This highlights a clear trade-off between land availability and economic efficiency, where greater AEP may come at the expense of substantially higher infrastructure investment, depending on the scenario. This is particularly true when infrastructure costs rise non-linearly with spatial dispersion.

In contrast, the med-med scenario, though lower in both AEP and turbine count, achieves the lowest internal and external costs. It may offer a more cost-effective balance between yield and investment. These findings highlight the importance of integrating spatial, energy, and cost assessments in wind farm planning, where optimal solutions may not necessarily correspond to maximum energy output, but rather to strategic trade-offs among land availability, grid integration costs, and layout efficiency.

Table 13: Summary of results of the chosen polygon in each scenario.

| Scenario | N° Turbines | AEP (MWh) | Total Internal connection cost (k€) | External connection cost (k€) |
|-----------|-------------|-----------|-------------------------------------|-------------------------------|
| High-high | 28 | 100636.46 | 121.46 | 1002.51 |
| Med-med | 17 | 55954.49 | 62.05 | 888.66 |
| Low-low | 34 | 165537.78 | 141.41 | 1806.61 |

5. SUMMARY AND CONCLUSIONS

In this deliverable, we have used electricity and energy system modelling across a range of scales to understand the implications for these systems of varying levels of prioritisation of the social and environmental factors that can shape wind power deployment. To conclude, in this section we summarise our initial results, noting that a detailed trade-off analysis will follow in WIMBY Deliverable 4.6.

5.1 Macro-scale

5.1.1 *The pathway to a carbon-free Europe-wide energy system*

The JRC-EU-TIMES pathway scenario analysis underscores the urgent need to accelerate the deployment of renewable technologies and supporting infrastructure within this decade, particularly to enable the electrification of heating and transport. Given current construction and permitting lead times for wind in the EU and neighbouring countries, achieving the projected doubling of wind capacity from 2025 levels presents a major challenge. Most near-term additions are expected to be onshore wind, with offshore wind scaling up post-2035.

The shift toward a carbon-free energy system depends on rapid demand-side electrification. Electricity's share of final energy consumption rises from 24% in 2020 to at least 40% by 2035, and over 50% by 2050—including international transport. This shift is largely driven by regulatory mandates, such as the requirement for all new vehicles to be zero-emission from 2035 onwards. Some countries, like Sweden, have already enacted bans on fossil-fuelled cars.

Alongside electricity, hydrogen and synthetic fuels (advanced biofuels and e-fuels) gain importance, particularly in industry and international transport. Their combined share of final energy consumption grows from 5% in 2035 to 8% by 2050 under the net-zero scenario. This transition raises electricity demand from 450 TWh in 2035 to over 1200 TWh in 2050.



Meeting this demand is particularly challenging when wind deployment is constrained by non-cost barriers. As detailed in Section 5.1.2, limits on wind expansion create trade-offs, especially with solar PV. While JRC-EU-TIMES is somewhat more conservative than highRES-Europe in offshore wind deployment⁶, both models highlight the interdependence between wind and solar in the long run. An increased reliance on solar PV requires additional battery and seasonal storage—particularly in countries with pronounced seasonal imbalances—to ensure energy system resilience. In the near-term, until 2035, constrained wind deployment is also associated with increased gas imports (+200 PJ/yr in the high constraint case vs the low constraint case) and a deceleration of heating electrification, implying also an increase of the GHG emissions.

5.1.2 Cost and design implications for Europe's electricity system in 2050

To understand the cost and design implications for Europe's electricity system in 2050 and the role of wind power in delivering net-zero, the nine social and environmental land availability scenarios we developed were used to constrain wind deployment in highRES-Europe. We coupled the model with JRC-EU-TIMES to provide electricity system boundaries, thus ensuring the systems designed by highRES-Europe are compatible with a net-zero energy system. Initial insights from this modelling are as follows.

Firstly, varying the level of prioritisation given to social and environmental protections has substantial impacts on the role of onshore wind in Europe's 2050 electricity system. If a low restriction future is realised, the installed capacity of onshore wind reaches ~1300 GW in 2050. At the other end of the scale, if restrictions from social and environmental factors are pushed to the maximum we consider here, onshore wind drops to ~200 GW (around 15% of

⁶ The difference in the wind offshore deployment between JRC-EU-TIMES and highRES is partly due to investment lock ins that occur in the pathway analysis. Wind offshore is characterised by 1.5-2x the construction time of onshore, varying also by depth, while any additional underwater grid connections also require 2x the construction time of a landline. The longer the construction time is, the stronger is also the lock-in to alternative options to supply demand during these long construction periods, limiting further future deployment.

that installed in the low-low case), which is less total capacity than currently installed across these 28 countries.

As onshore wind is progressively constrained, the least cost European net-zero electricity system design is reorientated toward the installation of more capacity of the other key variable renewables, batteries and some new nuclear power. Indeed, offshore wind and solar PV increase by more than 400 GW and 350 GW, respectively. Therefore, despite the limitations placed on onshore wind, variable renewables continue to make up the bulk of Europe's electricity generation even in the highest restriction scenario.

The highest level of protections results in a pessimistic outlook for the role of onshore wind in a number of countries. For instance, installed capacity in Germany declines by ~55 GW compared with today (2024). However, other European countries, such as Spain, Norway and Finland, still see an increase in onshore wind capacity compared to today, even in this most challenging of scenarios.

Scenarios with greater levels of prioritisation for social and environmental factors lead to higher total system costs. Cases with some combination of low and medium level protections see total systems costs for Europe increasing by at most ~4%. However, the three highest restriction cases result in system costs growing by more than 8% per year with high-high reaching an almost 15% (~104 €bn/yr in 2024 euros) increase. This increase occurs because systems with greater restrictions are configured in a less spatially and technologically optimal manner compared to systems with less constraints. Put another way, due to social and environmental factors, total wind power deployment is restricted and, where possible, is no longer able to be sited in the most cost-effective locations, both in terms of access to the best capacity factors and to leverage spatial diversity.

5.2 *Micro-scale*

We have presented a comprehensive wind farm optimisation model that integrates wind resource assessment, turbine placement, wake effect modelling, internal cabling optimisation, and external grid connection cost estimation. The model operates at a high spatial resolution and accounts



for real-world constraints such as land use restrictions, terrain characteristics, and infrastructure availability.

The core strength of the model lies in its ability to balance multiple objectives: maximising the AEP, minimising internal cabling costs, and reducing external grid connection expenses. This is achieved by evaluating multiple scenarios that consider environmental and social constraints. Turbine layouts are optimised, while cabling follows a cost-efficient design based on Delaunay triangulation. External connection paths are further refined to avoid areas with high development constraints, demonstrating how routing is sensitive to land cover cost.

The scenarios with larger land availability, such as low-low, enable greater energy output by accommodating more turbines. However, this comes at a significant increase in total infrastructure cost—highlighting that more space does not automatically translate into better cost-performance. For instance, although the low-low scenario yields 64.5% more energy than high-high, its total connection cost is ~80% higher. This illustrates the trade-offs between land use type, energy potential, and capital expenditure. These findings emphasise the importance of integrated spatial and techno-economic modelling in wind energy planning. Rather than relying solely on wind potential or land availability, optimal site selection must consider a combination of energy yield, infrastructure costs, and land development constraints.

An MCDA of different wind farms aims to showcase the competition among technical, economic, environmental, and social criteria, using models and results from the micro-level modelling other work packages in WIMBY. The analysis will be presented in the final deliverable (D4.6).



REFERENCES

- [1] International Energy Agency (IEA), 'Europe – Countries & Regions', Europe. Accessed: May 19, 2025. [Online]. Available: <https://www.iea.org/regions/europe/electricity>
- [2] International Energy Agency (IEA), 'Denmark – Countries & Regions', Denmark. Accessed: May 19, 2025. [Online]. Available: <https://www.iea.org/countries/denmark/electricity>
- [3] International Energy Agency (IEA), 'United Kingdom – Countries & Regions', United Kingdom. Accessed: May 23, 2025. [Online]. Available: <https://www.iea.org/countries/united-kingdom/electricity>
- [4] International Energy Agency (IEA), 'Germany – Countries & Regions', Germany. Accessed: May 23, 2025. [Online]. Available: <https://www.iea.org/countries/germany/electricity>
- [5] R. McKenna *et al.*, 'System impacts of wind energy developments: Key research challenges and opportunities', *Joule*, vol. 9, no. 1, p. 101799, Jan. 2025, doi: 10.1016/j.joule.2024.11.016.
- [6] J. Price and M. Zeyringer, 'highRES–Europe: The high spatial and temporal Resolution Electricity System model for Europe', *SoftwareX*, vol. 17, p. 101003, Jan. 2022, doi: 10.1016/j.softx.2022.101003.
- [7] M. Zeyringer, J. Price, B. Fais, P.-H. Li, and E. Sharp, 'Designing low-carbon power systems for Great Britain in 2050 that are robust to the spatiotemporal and inter-annual variability of weather', *Nat. Energy*, vol. 3, no. 5, pp. 395–403, May 2018, doi: 10.1038/s41560-018-0128-x.
- [8] ENTSO-E, 'Opportunities for a more efficient European power system by 2050: Infrastructure Gaps Report', European Network of Transmission System Operators for Electricity, 2024. [Online]. Available: https://eepublicdownloads.blob.core.windows.net/public-cdn-container/tyndp-documents/TYNDP2024/foropinion/Infrastructure_Gaps_Report.pdf
- [9] Global Energy Monitor, 'Global Wind Power Tracker'. Feb. 2025. [Online]. Available: <https://globalenergymonitor.org/projects/global-wind-power-tracker/>
- [10] Global Energy Monitor, 'Global Nuclear Power Tracker'. Jul. 2024. [Online]. Available: <https://globalenergymonitor.org/projects/global-nuclear-power-tracker/>



- [11] Global Energy Monitor and TransitionZero, 'Global Solar Power Tracker'. Feb. 2025. [Online]. Available: <https://globalenergymonitor.org/projects/global-solar-power-tracker/>
- [12] H. Hersbach *et al.*, 'ERA5 hourly data on single levels from 1940 to present'. Copernicus Climate Change Service (C3S) Climate Data Store (CDS), 2018. doi: 10.24381/CDS.ADBB2D47.
- [13] M. Dörenkämper *et al.*, 'The Making of the New European Wind Atlas – Part 2: Production and evaluation', *Geosci. Model Dev.*, vol. 13, no. 10, pp. 5079–5102, Oct. 2020, doi: 10.5194/gmd-13-5079-2020.
- [14] A. N. Hahmann, N. N. Davis, and N. G. Alonso De Linaje, 'Wind Resource API', WIMBY Deliverable D1.1, 2023. [Online]. Available: <https://wimby.eu/resource/d1-1-wind-resources-api/>
- [15] N. N. Davis *et al.*, 'The Global Wind Atlas: A High-Resolution Dataset of Climatologies and Associated Web-Based Application', *Bull. Am. Meteorol. Soc.*, vol. 104, no. 8, pp. E1507–E1525, Aug. 2023, doi: 10.1175/BAMS-D-21-0075.1.
- [16] European Space Agency and Airbus, 'Copernicus DEM'. 2022. doi: 10.5270/ESA-c5d3d65.
- [17] D. Palmer, R. Gottschalg, and T. Betts, 'The future scope of large-scale solar in the UK: Site suitability and target analysis', *Renew. Energy*, vol. 133, pp. 1136–1146, Apr. 2019, doi: 10.1016/j.renene.2018.08.109.
- [18] European Environment Agency, 'Nationally designated areas for public access (vector data) - version 21, Jun. 2023'. Aug. 04, 2023. [Online]. Available: <https://sdi.eea.europa.eu/catalogue/srv/api/records/ef77dd7b-e5d0-4b93-81e1-f721b91ec9fe>
- [19] European Environment Agency, 'Nationally designated areas (CDDA) for public access - version 18, May 2020'. May 29, 2020. [Online]. Available: <https://sdi.eea.europa.eu/catalogue/srv/api/records/b07cd829-47da-416c-83f5-9dc952191bfc>
- [20] European Commission, 'Natura 2000 (vector) - version 2019, Apr. 2020'. Jun. 12, 2020. [Online]. Available: <https://sdi.eea.europa.eu/catalogue/srv/api/records/e40ca403-b81a-4ecb-b484-cade980e9a2f>
- [21] European Environment Agency, 'CORINE Land Cover 2018 (raster 100 m), Europe, 6-yearly - version 2020_20u1, May 2020'. European Environment Agency, 2019. doi: 10.2909/960998C1-1870-4E82-8051-6485205EBBAC.

- [22] E. Sandström, A. Namasivayam, S. Oostdijk, N. Scherpenhuijzen, N. Debonne, and P. Verburg, 'Preliminary land system map for Europe'. DataverseNL, 2023. doi: 10.34894/THARMK.
- [23] M. Bucha, A. del Villar, L. Ramirez Camargo, and J. Lowitzsch, 'Data on regulatory and socioeconomic conditions and impacts (b)', WIMBY Deliverable D2.10, 2025.
- [24] F. Mölder *et al.*, 'Sustainable data analysis with Snakemake', Apr. 19, 2021, *F1000Research*: 10:33. doi: 10.12688/f1000research.29032.2.
- [25] J. Price *et al.*, 'highRES-Europe: the high temporal and spatial Resolution Electricity System model for Europe'. Zenodo, doi.org/10.5281/zenodo.15735203
- [26] European Commission, 'Commission staff working document Impact Assessment Report Part I Accompanying the document Communication from the Commission to the European Parliament, The Council, The European Economic and Social Committee and the Committee of the Regions: Securing our future Europe's 2040 climate target and path to climate neutrality by 2050 building a sustainable, just and prosperous society', Strasbourg, COM/2024/63, 2024. [Online]. Available: <https://eur-lex.europa.eu/legal-content/EN/TXT/?uri=CELEX%3A52024SC0063>
- [27] P. Su-ungkavatin, L. Tiruta-Barna, and L. Hamelin, 'Biofuels, electrofuels, electric or hydrogen?: A review of current and emerging sustainable aviation systems', *Prog. Energy Combust. Sci.*, vol. 96, p. 101073, May 2023, doi: 10.1016/j.pecs.2023.101073.
- [28] K. Treyer, S. Romain, and C. Bauer, 'Life Cycle Assessment of synthetic hydrocarbons for use as jet fuel: "Power-to-Liquid" and "Sun-to-Liquid" processes', Paul Scherrer Institute (PSI), Villigen, Switzerland, 2022. [Online]. Available: <https://www.psi.ch/en/media/72878/download?attachment>
- [29] Fraunhofer IEE, 'Global PtX Atlas'. [Online]. Available: <https://maps.iee.fraunhofer.de/ptx-atlas/>
- [30] M. Pfennig *et al.*, 'Global GIS-based potential analysis and cost assessment of Power-to-X fuels in 2050', *Appl. Energy*, vol. 347, p. 121289, Oct. 2023, doi: 10.1016/j.apenergy.2023.121289.
- [31] European Commission, 'Commission sets out rules for renewable hydrogen', European Commission - European Commission. Accessed: Jun. 05, 2025. [Online]. Available: https://ec.europa.eu/commission/presscorner/api/files/document/print/en/ip_23_594/IP_23_594_EN.pdf



- [32] European Commission, 'National energy and climate plans'. Accessed: May 28, 2025. [Online]. Available: https://commission.europa.eu/energy-climate-change-environment/implementation-eu-countries/energy-and-climate-governance-and-reporting/national-energy-and-climate-plans_en
- [33] World Nuclear Association, 'Country Profiles - World Nuclear Association'. Accessed: May 28, 2025. [Online]. Available: <https://world-nuclear.org/information-library/country-profiles>
- [34] European Commission, Joint Research Centre, 'Joint Research Centre Data Catalogue - The JRC European TIMES Energy System Model - European Commission'. 2020. Accessed: Jun. 26, 2025. [Online]. Available: <https://data.jrc.ec.europa.eu/collection/id-00287>
- [35] 'Climate Data Store'. Accessed: Apr. 04, 2025. [Online]. Available: <https://cds.climate.copernicus.eu/>
- [36] E. Son, S. Lee, B. Hwang, and S. Lee, 'Characteristics of turbine spacing in a wind farm using an optimal design process', *Renew. Energy*, vol. 65, pp. 245–249, May 2014, doi: 10.1016/j.renene.2013.09.022.
- [37] R. McKenna *et al.*, 'High-resolution large-scale onshore wind energy assessments: A review of potential definitions, methodologies and future research needs', *Renew. Energy*, vol. 182, pp. 659–684, Jan. 2022, doi: 10.1016/j.renene.2021.10.027.
- [38] Y. Chen, H. Li, K. Jin, and Q. Song, 'Wind farm layout optimization using genetic algorithm with different hub height wind turbines', *Energy Convers. Manag.*, vol. 70, pp. 56–65, Jun. 2013, doi: 10.1016/j.enconman.2013.02.007.
- [39] M. Pierrot El, 'The Wind Power - Wind energy Market Intelligence'. Accessed: Apr. 06, 2025. [Online]. Available: https://www.thewindpower.net/about_en.php
- [40] R. Brogna, J. Feng, J. N. Sørensen, W. Z. Shen, and F. Porté-Agel, 'A new wake model and comparison of eight algorithms for layout optimization of wind farms in complex terrain', *Appl. Energy*, vol. 259, p. 114189, Feb. 2020, doi: 10.1016/j.apenergy.2019.114189.
- [41] R. Riva *et al.*, 'TOPFARM 2.5'. Accessed: Apr. 04, 2025. [Online]. Available: <https://topfarm.pages.windenergy.dtu.dk>
- [42] A. Cerveira, E. J. S. Pires, and J. Baptista, 'Wind Farm Cable Connection Layout Optimization with Several Substations', *Energies*, vol. 14, no. 12, Art. no. 12, Jan. 2021, doi: 10.3390/en14123615.

- [43] H. Smail, R. Alkama, and A. Medjdoub, 'Optimal design of the electric connection of a wind farm', *Energy*, vol. 165, pp. 972–983, Dec. 2018, doi: 10.1016/j.energy.2018.10.015.
- [44] L. Gonzalez-Sotres, C. Mateo Domingo, A. Sanchez-Miralles, and M. Alvar Miro, 'Large-Scale MV/LV Transformer Substation Planning Considering Network Costs and Flexible Area Decomposition', *IEEE Trans. Power Deliv.*, vol. 28, no. 4, pp. 2245–2253, Oct. 2013, doi: 10.1109/TPWRD.2013.2258944.
- [45] J. Li *et al.*, 'Cable Connection Optimization for Onshore Wind Farms Considering Restricted Area and Topography', *IEEE Syst. J.*, vol. 14, no. 3, pp. 3082–3092, Sep. 2020, doi: 10.1109/JSYST.2020.2982843.
- [46] 'DEAP documentation – DEAP 1.4.1'. Accessed: Apr. 04, 2025. [Online]. Available: <https://deap.readthedocs.io/en/master/>
- [47] Ministerio de Industria, Energía y Turismo, *Orden IET/2659/2015*, vol. BOE-A-2015-13487. 2015, pp. 117250–117269.
- [48] 'Transmission Cost Estimation Guide for MTEP24'. Midcontinent Independent System Operator (MISO), May 01, 2024.
- [49] Y. Yangyang and C. Yuning, *Road Planning for a Scenic Environment Based on the Dijkstra Algorithm: Case Study of Nanjing Niushou Mountain Scenic Spot in China*. DE: Wichmann Verlag, 2017. Accessed: Apr. 30, 2025. [Online]. Available: <https://doi.org/10.14627/537629017>
- [50] F. A. Medrano, 'Effects of raster terrain representation on GIS shortest path analysis', *PLOS ONE*, vol. 16, no. 4, p. e0250106, Apr. 2021, doi: 10.1371/journal.pone.0250106.
- [51] J. Price, M. Zeyringer, D. Konadu, Z. Sobral Mourão, A. Moore, and E. Sharp, 'Low carbon electricity systems for Great Britain in 2050: An energy-land-water perspective', *Appl. Energy*, vol. 228, pp. 928–941, Oct. 2018, doi: 10.1016/j.apenergy.2018.06.127.
- [52] J. Price, K. Mainzer, S. Petrovic, M. Zeyringer, and R. McKenna, 'The Implications of Landscape Visual Impact on Future Highly Renewable Power Systems: A Case Study for Great Britain', *IEEE Trans. Power Syst.*, vol. 37, no. 4, pp. 3311–3320, Jul. 2022, doi: 10.1109/TPWRS.2020.2992061.
- [53] A. N. Hahmann *et al.*, 'Wind Power Assessment Tool', WIMBY Deliverable D2.2, 2025.
- [54] European Environment Agency, 'EU-Hydro River Network Database 2006-2012 (vector), Europe - version 1.3, Nov. 2020'. European Environment Agency, 2019. doi: 10.2909/393359A7-7EBD-4A52-80AC-1A18D5F3DB9C.



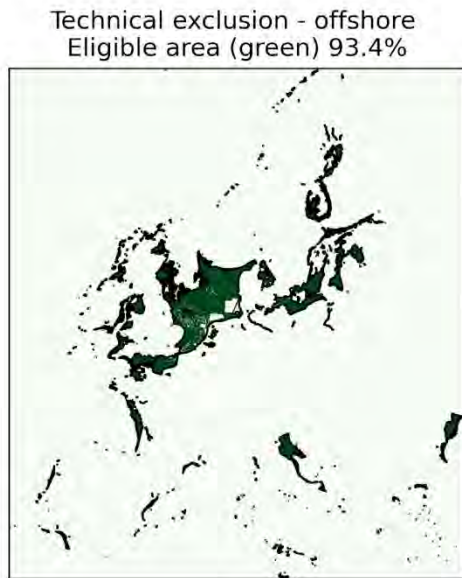
- [55] F. Batista and C. Pigaiani, 'LUISA Base Map 2018', Mar. 2021, Accessed: Feb. 25, 2025. [Online]. Available: <http://data.europa.eu/89h/51858b51-8f27-4006-bf82-53eba35a142c>
- [56] M. C. I. Martins, M. I. Carter, S. Rouse, and D. J. Russell, 'Offshore energy structures in the North Sea: Past, present and future', *Mar. Policy*, vol. 152, p. 105629, Jun. 2023, doi: 10.1016/j.marpol.2023.105629.
- [57] M. C. I. Martins, M. Carter, S. Rouse, and D. J. Russell, 'Offshore Energy Structures in the North Sea: Past, Present and Future-March 2023 version (dataset)'. University of St Andrews, p. 13MB, 2023. doi: 10.17630/338D5BA4-5E09-443F-9C08-013D24050C81.
- [58] European Marine Observation and Data Network, 'EMODnet Human Activities, Vessel Density Map'. <https://ows.emodnet-humanactivities.eu/geonetwork/srv/eng/catalog.search#/metadata/0f2f3ff1-30ef-49e1-96e7-8ca78d58a07c/formatters/xsl-view?root=div&view=advanced>, 2024. Accessed: Mar. 11, 2025. [Online]. Available: <https://ows.emodnet-humanactivities.eu/geonetwork/srv/eng/catalog.search#/metadata/0f2f3ff1-30ef-49e1-96e7-8ca78d58a07c>
- [59] A. Moore, J. Price, and M. Zeyringer, 'The role of floating offshore wind in a renewable focused electricity system for Great Britain in 2050', *Energy Strategy Rev.*, vol. 22, pp. 270–278, Nov. 2018, doi: 10.1016/j.esr.2018.10.002.
- [60] Netherlands Enterprise Agency, 'Hollandse Kust (west) Wind Farm Zone - Appendix A: Applicable Law for Offshore Wind Energy', 2022. Accessed: Mar. 11, 2025. [Online]. Available: https://offshorewind.rvo.nl/file/download/c85ef7b0-6229-4055-964b-9667164e4624/hkw_20220413_psd_appendix-a.pdf
- [61] *Directive 2009/147/EC of the European Parliament and of the Council of 30 November 2009 on the conservation of wild birds (Codified version)*, vol. 020. 2009. Accessed: May 12, 2025. [Online]. Available: <http://data.europa.eu/eli/dir/2009/147/oj/eng>
- [62] *Council Directive 92/43/EEC of 21 May 1992 on the conservation of natural habitats and of wild fauna and flora*. 2013. Accessed: May 12, 2025. [Online]. Available: <http://data.europa.eu/eli/dir/1992/43/2013-07-01/eng>
- [63] European Environment Agency, 'European Red Lists of species, 2009–2022'. European Environment Agency, 2025. doi: 10.2909/9A752C28-CB5F-4EAD-9922-2A8173E0306B.



- [64] S. Si-moussi and W. Thuiller, 'Species habitat suitability of European terrestrial vertebrates for contemporary climate and land use'. German Centre for Integrative Biodiversity Research, 2024. doi: 10.25829/WPFN43.
- [65] R. Chen, A. Lohrmann, and R. McKenna, 'Maps of landscape impact metrics (b)', WIMBY Deliverable D2.6, 2024.
- [66] European Commission. Joint Research Centre., *Wind potentials for EU and neighbouring countries: input datasets for the JRC EU TIMES model*. LU: Publications Office, 2018. Accessed: Mar. 26, 2025. [Online]. Available: <https://data.europa.eu/doi/10.2760/041705>
- [67] R. Sacchi, P. Burgherr, L. Ramirez Camargo, H.-H. Chen, R. Hueting, and A. G. Vicario, 'Maps of health and safety impact metrics (b)', WIMBY Deliverable D2.4, 2025.
- [68] M. Millinger, F. Hedenus, E. Zeyen, F. Neumann, L. Reichenberg, and G. Berndes, 'Diversity of biomass usage pathways to achieve emissions targets in the European energy system', *Nat. Energy*, pp. 1–17, Jan. 2025, doi: 10.1038/s41560-024-01693-6.
- [69] S. Fuss *et al.*, 'Betting on negative emissions', *Nat. Clim. Change*, vol. 4, no. 10, pp. 850–853, Oct. 2014, doi: 10.1038/nclimate2392.
- [70] A. Deprez *et al.*, 'Sustainability limits needed for CO₂ removal', *Science*, vol. 383, no. 6682, pp. 484–486, Feb. 2024, doi: 10.1126/science.adj6171.
- [71] P. Ruiz, 'ENSPRESO – BIOMASS'. European Commission, Joint Research Centre (JRC), May 07, 2019. Accessed: May 28, 2025. [Online]. Available: <http://data.europa.eu/89h/74ed5a04-7d74-4807-9eab-b94774309d9f>
- [72] P. Enevoldsen and M. Z. Jacobson, 'Data investigation of installed and output power densities of onshore and offshore wind turbines worldwide', *Energy Sustain. Dev.*, vol. 60, pp. 40–51, Feb. 2021, doi: 10.1016/j.esd.2020.11.004.
- [73] ENTSO-E, 'ENTSO-E Transparency Platform'. Accessed: Nov. 04, 2022. [Online]. Available: <https://transparency.entsoe.eu/dashboard/show>
- [74] Department for Energy Security and Net Zero, 'Energy Trends: UK renewables', GOV.UK. Accessed: May 29, 2025. [Online]. Available: <https://www.gov.uk/government/statistics/energy-trends-section-6-renewables>
- [75] 'OpenStreetMap Austria'. Accessed: Apr. 14, 2025. [Online]. Available: <https://www.openstreetmap.at/>



ANNEX



| Country | area (km ²) | share (%) |
|---------|-------------------------|-----------|
| BE | 2405.5 | 88.1 |
| BG | 3376.5 | 99.6 |
| DE | 29392.9 | 72.7 |
| DK | 60673.3 | 94.8 |
| EE | 9934.0 | 99.6 |
| ES | 4330.2 | 99.6 |
| FI | 20670.0 | 97.4 |
| FR | 32406.2 | 97.6 |
| GR | 1687.2 | 99.5 |
| HR | 8462.0 | 99.9 |
| IE | 8496.6 | 99.6 |
| IT | 16225.6 | 99.8 |
| LT | 4134.3 | 99.9 |
| LV | 12915.3 | 99.8 |
| NL | 44407.4 | 79.2 |
| NO | 24643.9 | 98.3 |
| PL | 13719.9 | 99.0 |
| PT | 2084.7 | 99.1 |
| RO | 12539.5 | 99.9 |
| SE | 42379.5 | 96.9 |
| SI | 0.0 | 70.6 |
| UK | 132806.9 | 96.5 |

Figure 30: Geospatial overview of eligible and excluded land areas for offshore wind power deployment based on technical aspects only.

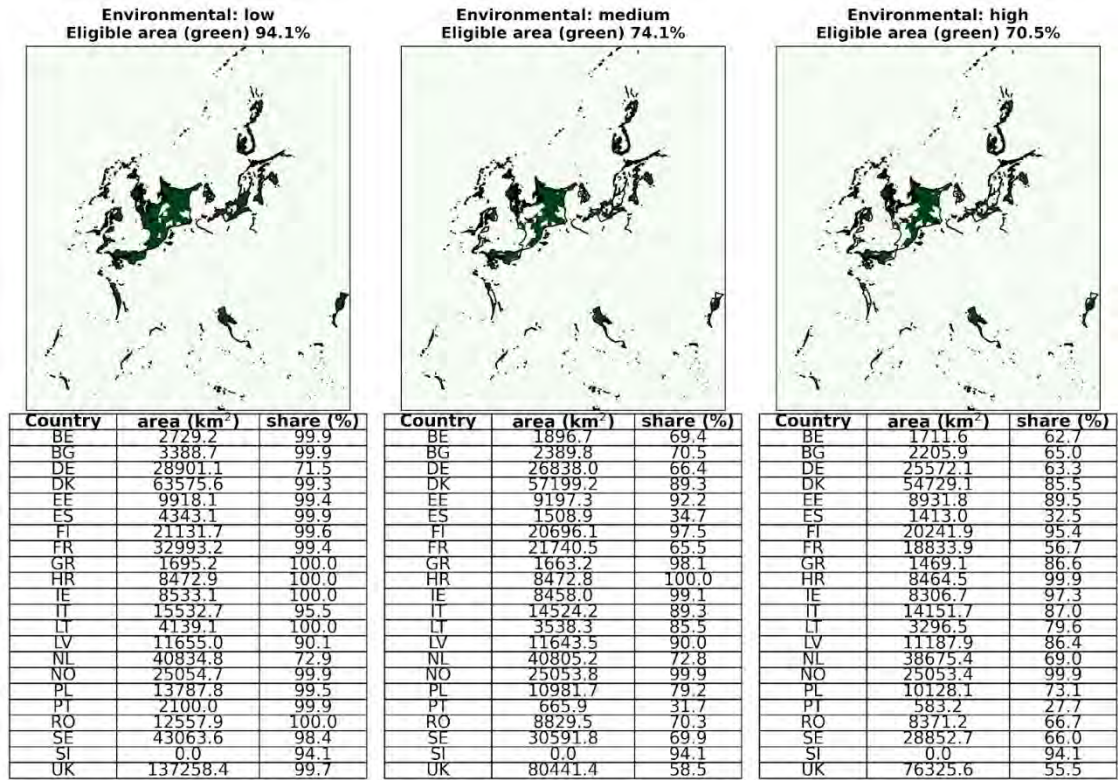


Figure 31: Geospatial overview of eligible areas for wind offshore deployment based on the three environmental scenarios.

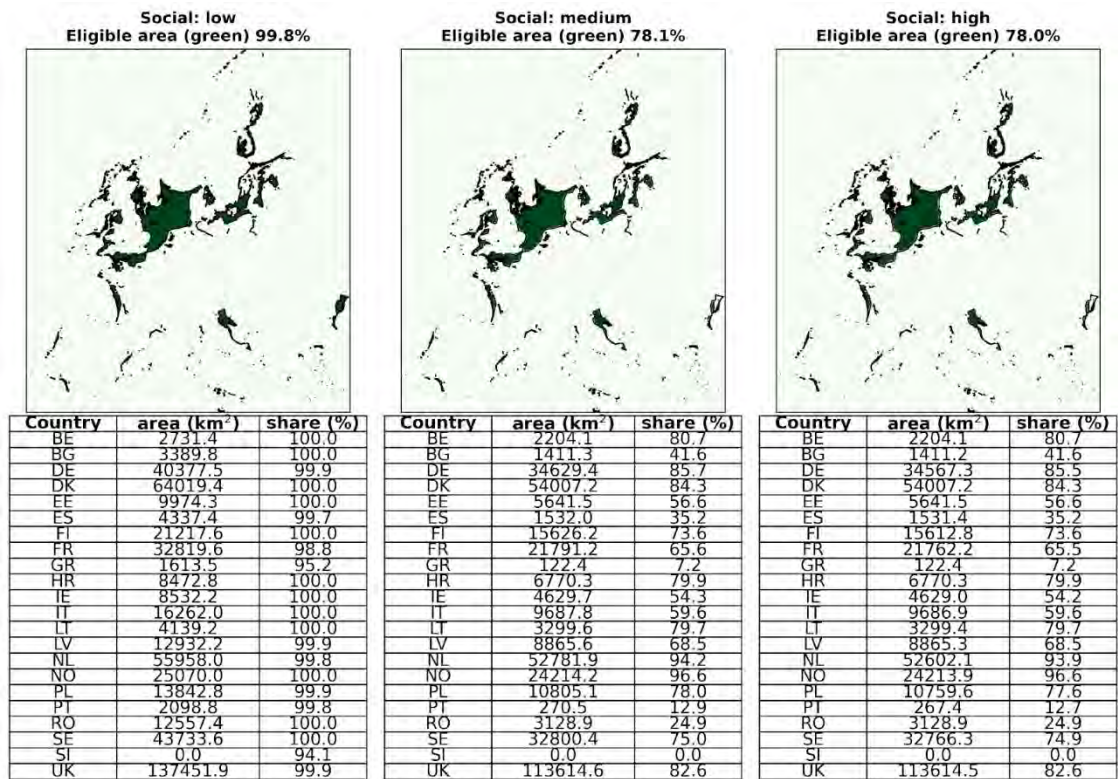


Figure 32: Geospatial overview of eligible areas for wind offshore deployment based on the three social scenarios.

Table 14: Major data sources used in the recalibration of the JRC-EU-TIMES model to the 2019 statistics

| Major data category | Major database(s) used |
|---|---|
| Macro-economic (GDP, Gross value added, Industrial production) | EUROSTAT national accounts (link) EUROSTAT industrial production (link) Swiss Federal Statistical Office - Gross domestic product: production approach (1995-2021) (link) Swiss Federal Statistical Office - Secondary sector Production, Orders and Turnover Statistics - yearly series 1999-2022 (link) |
| Demographic (population, households, building stock, floor area, urbanisation) | EUROSTAT population and demography (link) Federal Statistical Office - Demographic balance by Canton, 1971-2021 (link) Swiss Federal Statistical Office - Private households by Canton and household size (2010-2021) (link) SWEET CROSS database (link) |
| Energy balances, trade and cross-border infrastructure | EUROSTAT energy statistics (link) ENTSO-E (link) ENTSO-G (link) Swiss Federal Office of Energy - Energy Balances 2019 (link) Swiss Federal Office of Energy - Analysis of energy consumption by specific use (link) Swissgrid grid data production and consumption 2019 (link) Swissgas (link) |
| Power plants (capacities, production) | JRC IDEES database (link) EUROSTAT energy statistics (link) IEA WEO series 2019 and 2020 (link) EIA international statistics (link) Federal Office of Energy (link) Swiss Federal Office of Energy - Thermal production including CHP 2019 (link) Swiss Federal Office of Energy - Statistics of renewable energy sources 2021 (link) Swiss Federal Office of Energy - Statistics of hydroelectric installations in Switzerland 2022 (link) Swiss Federal Office of Energy - Statistics of solar photovoltaic and solar thermal installations 2021 (link) |

| | |
|---|---|
| | <p>Swiss Federal Office of Energy – Swiss Electricity statistics 2021 (link)</p> |
| <p>Mobility sector (vehicles, mileage, pkm, tkm)</p> | <p>JRC IDEES database (link)</p> <p>JRC POTENCIA Central Scenario database 2018 (link)</p> <p>EUROSTAT mobility statistics (link)</p> <p>EUROSTAT transport pocketbook (link)</p> <p>Swiss Federal Statistical Office – Vehicles stock (link)</p> <p>Swiss Federal Statistical Office – Passenger vehicles performance 2022 (link)</p> <p>Swiss Federal Statistical Office – Goods vehicle performance 2022 (link)</p> <p>Swiss Federal Office of Energy – Consumption in transport 2022 (link)</p> <p>SCCER JASM database car costs 2020 (link)</p> <p>SWEET CROSS database 2022 (link)</p> <p>EP2050+ 2021 (link)</p> |
| <p>Buildings sector (building stock, appliances, floor area, heating systems)</p> | <p>EU building stock observatory (link)</p> <p>JRC IDEES database (link)</p> <p>SCCER JASM database (link)</p> <p>SWEET CROSS database (link)</p> <p>Swiss Federal Statistical Office – General buildings overview by Canton 2019 (link)</p> <p>Swiss Federal Statistical Office – Buildings per heating system, construction period and category 2021 (link)</p> <p>Swiss Federal Office of Energy – Evolution of the heating floor area, annual updates, 2023 (link)</p> <p>Swiss Federal Office of Energy – Ex-post analysis of the energy consumption in households 2000 - 2021 (link)</p> <p>EP2050+ input assumptions on heating systems costs (link)</p> |
| <p>Industry and Services sectors (energy service demands and consumption by use)</p> | <p>JRC IDEES database (link)</p> <p>Swiss Federal Office of Energy – Energy consumption by NOGA activity 2021 (link)</p> <p>Swiss Federal Office of Energy – Energy consumption in Industry and Services sectors (link)</p> <p>SCCER JASM database (link)</p> <p>SWEET CROSS database (link)</p> <p>EP2050+ (link)</p> |

